PATHOMECHANISM AND THERAPEUTIC POSSIBILITIES OF ARTHRITIS

PhD Thesis

Edina Butt MD

Szeged

2021

PATHOMECHANISM AND THERAPEUTIC POSSIBILITIES OF ARTHRITIS

PhD Thesis

Edina Butt MD

Supervised by:

Endre Varga MD, PhD

Petra Hartmann MD, PhD

University of Szeged, Faculty of Medicine

Clinical Medical Sciences Doctoral School

PhD Program:

Clinical and Experimental Research for Reconstructive an Organ-sparing Surgery

Program Director: Prof. György Lázár MD, PhD

Szeged

2021

CONTENTS

List of abbreviations

α7-nAChR	alpha-7-nicotinic acetylcholine receptor
ACPA	anti-citrullinated-protein-antibody
ACR	American College of Rheumatology
ADP	adenosine diphosphate
Ama	antimycin A
ANOVA	analysis of variance
As	ascorbate
ATP	adenosine triphosphate
Azd	azide
BMI	body mass index
BRM	biologic response modifier
C/K	carrageenan-kaolin
CCR	coupling control ratio
CLSEM	confocal laser scanning endomicroscopy
CRP	c-reactive protein
CU	corrected uncoupling
CUI	corrected uncoupling index
Cyc	cytochrome c
D	diclofenac
DAS	Disease Activity Score
DIP	distal interphalangeal
EP	electroporation
ESR	erythrocyte sedimentation rates
ETC	electron transport chain
EU	European Union
EULAR	European League Against Rheumatism
FCCP	carbonyl cyanide-4-(trifluoromethoxy)phenylhydrazone
G	glutamate
HA	hydroxyapatite
HClO	hypochlorous acid
HPLC	high-performance liquid chromatography
HRR	high-resolution respirometry

HSS	Hospital for Special Surgery
H&E	hematoxylin and eosin
ICAM	intracellular adhesion molecule
ICD	International Statistical Classification of Diseases
IDDM	insulin-dependent diabetes mellitus
Il-6	interleukin-6
Il-1β	interleukin-1β
IVM	intravital videomicroscopy
kDa	kilodalton
KFS	knee functional score
KL	Kellgren-Lawrence
KSS	knee society score
M	malate
mtDNA	mitochondrial deoxyribonucleic acid
MPO	myeloperoxidase
MRI	magnetic resonance imaging
MTPM	maximum total point motion
NIDDM	non-insulin-dependent diabetes mellitus
NO	nitric oxide
NSAID	non-steroidal anti-inflammatory drug
NT	nitrotyrosine
OA	osteoarthritis
Omy	oligomycin
OxPhos	oxidative phosphorylation
O2	oxygen
O2k	oxygraph-2k
PBS	phosphate buffered saline
PMMA	polymethyl methacrylate
PMN	polymorphonuclear leukocytes
PRISMA	Preferred Reporting Items in Systematic Reviews and Meta-Analysis
RA	rheumatoid arthritis
RANKL	Receptor Activator of Nuclear factor-κB Ligand
RCR	respiratory control ratio
RCT	randomized controlled trial

RF	rheumatoid factor
ROS	reactive oxygen species
Rot	rotenone
RSA	radiostereometric analysis
S	succinate
SD	standard deviation
SMI	synovial mitochondrial integrity
TKA	total knee arthroplasty
TMPD	*N*,*N*,*N*,*N*-tetramethyl-*p*-phenylenediamine
TNF-α	tumor necrosis factor alfa
TP	total protein
URL	upper reference limit
VAS	Visual Analogue Scale
VCAM	vascular cell adhesion molecule
WBC	white blood cell count
WMD	weighted mean difference
XOR	xanthine oxidoreductase

List of original papers

List of full papers relating to the subject of the thesis

Hartmann P*, **Butt E*,** Feher A, Szilagyi AL, Jasz KD, Balazs B, Bakonyi M, Berko S, Eros G, Boros M, Horvath G, Varga E, Csanyi E, Electroporation-enhanced transdermal diclofenac sodium delivery into the knee joint in a rat model of acute arthritis. DRUG DESIGN, DEVELOPMENT AND THERAPY 12:1917-1930. doi: 10.2147/DDDT.S161703. (2018) **IF: 3.208**

*Shared co-first authorship

Horvath T**,** Hanak L, Hegyi P, **Butt E,** Solymar M, Szucs A, Varga O, Thien B., Szakacs Zs, Csonka E, Hartmann P, Hydroxyapatite-coated implants provide better fixation in total knee arthroplasthy. A meta-analysis of randomized controlled trials. PLOS ONE 12;15:e0232378. doi: 10.1371/journal.pone.0232378. (2020) **IF: 2.740**

Jávor P, Mácsai A, **Butt E,** Baráth Bá, Jász DK, Horváth T, Baráth Be, Csonka Á, Torok L, Varga E, Hartmann P, Mitochondrial dysfunction affects the synovium of patients with rheumatoid arthritis and osteoarthrosis differently (under review in PLOS ONE)

List of full papers not-relating to the subject of the thesis

Greksa F, **Butt E**, Csonka E, Jávor P**,** Tuboly E, Török L, Szabo A, Varga E, Hartmann P, Periosteal and endosteal microcirculatory injury following excessive osteosynthesis. INJURY 52 Suppl 1:S3-S6. doi: 10.1016/j.injury.2020.11.053. (2021) **IF: 2.106**

Jávor P, Csonka E, **Butt E,** Rárosi F, Babik B, Török L, Varga E, Hartmann P, Comparison of the previous and current trauma-related shock classifications – A retrospective cohort study from a level I trauma centre" European Surgical Research (accepted for publication) (2021) **IF: 2.351**

Cumulative IF: 10.405

1. INTRODUCTION

1.1. Background

Arthritis is a collective term encompassing many diseases with distinct etiologies but common symptoms, such as joint pain and inflammation. Osteoarthritis (OA) and rheumatoid arthritis (RA) are both common forms of arthritis despite of the substantial differences in their etiology and pathomechanism. The prevalence of OA in the population is approximately 10%, which makes it one of the most common chronic diseases. Although epidemiological studies have revealed both endogenous and exogenous risk factors for OA, it is basically a degenerative joint disease, initiated by an injury or repetitive joint stress of the joint [1]. The mechanical damage activates mechanosensitive intracellular signalling in cartilage, which involves the activation of inflammatory processes that may develope structural and symptomatic course of disease [1]. With regards to the etiology, RA is considered as a multifactorial, multigenic autoimmune disease with lower prevalence, affecting 1% of the world's population [2]. Although the exact pathomechanism is still unknown, the importance of genetic predisposition has been revealed, as polymorphisms of the HLA-DR4 and DR1 locus and cytokine genes have been associated with RA [3]. Additionally, the pathogenetic role of various bacteria and viruses has also been suggested. As a result, abnormal activation, adhesion and migration of T- and B-lymphocytes and macrophages occur, which is accompanied by increased proinflammatory cytokine production (TNF-α, IL-1). As a consequence of the chronic autoimmune inflammation, intensive angiogenesis and pannus formation in the synovium and cartilage damage may develop [3].

Owing to the high number of cases, arthritis is of significant public health and economic importance, yet therapeutic options are limited to pain relief, reduction of inflammation and finally, performing orthopedic surgery [4,5]. Today, the "gold standard" therapy for alleviating arthritis-related pain is diclofenac, a nonsteroidal anti-inflammatory drug (NSAID) of the phenylacetic acid class [6,7]. Unfortunately, the side effects of such an effective compound are also significant. Habitual use of diclofenac is associated with the NSAID category risk of dose-related gastrointestinal, cardiovascular, and renal adverse effects; consequently, topical preparations were developed to limit the potentially serious complications of systemic treatments.

After the exhaustion of conservative therapeutic options, destruction of articular cartilage, chronic pain, and limited mobility of patients can indicate surgical procedures. According to the severity of the condition, there are three types of surgical interventions that can also be

performed consecutively: arthroscopy, osteotomy or joint-replacement procedures, the latter may be unicompartmental or total arthroplasty of the knee [8]. Due to the need for early prosthesis in rheumatoid arthritis and post-traumatic osteoarthritis, implants with a lifespan of 10-15 years often have to be replaced multiple times. Although cementless prostheses offer a solution to this problem, the higher incidence of complications necessitated the elaboration of new techniques such as hydroxyapatite-coating [9,10].

1.1.2. Osteoarthritis

The degenerative cartilage damage in OA affects both large and small joints and characterized by continuous progression. Risk factors include female gender, advanced age, obesity, previous injury, repetitive sports activity, and family history of OA [11]. Interestingly, clinicians have recognized OA as a separate disease only in the late 18th century, since previously it was considered the same entity as rheumatoid arthritis. Typical symptoms include include activity-related pain, transient morning stiffness and crepitus on joint motion, that become more and more pronounced with the progrediation of the disease [12] [13]. With regards to the ethiology, we can differentiate between primary or idiopathic, and secondary OA. Obesity, mechanical stress, trauma, joint surgery, infection, metabolic or endocrin disorders, and congenital joint abnormalities are considered as secondary causes for OA [14]. Osteoarthritis affects articular cartilage, ligaments, synovial membranes and subchondral bone. Typical radiographic signs are ostophytes, subchondral cysts, and narrowing of the joint space [15].

1.1.3. Rheumatoid arthritis

The articular destruction in RA primarily occurs in small joints of the hands, but larger joints, knees and shoulders may also be affected. [3]. Furthermore, RA is often accompanied by extraarticular manifestations such as rheumatoid nodules, pulmonary fibrosis, vasculitis, secundary Sjögren syndrome, amyloidosis and Felty syndrome [16]. Rapidly or slowly developed symmetrical polyarthritis on the hands is considered as the most common first symptom [17]. Typically, remissions and exacerbations alternate in the course of the disease. Along with the slow destruction of joints, various bony and soft tissue deformities can occur. Ulnar drift, swan neck deformity and interosseus atrophy develop commonly in the joints of the hand [18], while flexure contracture appears typically in the elbow and knee joints. Additionally, joints may also dislocate due to chronic inflammation and altered morphology, most commonly in metatarsophalangeal joints. Moreover, rheumatiod arthritis can be fatal in

some cases and can have serious consequences, such as atlanto-axial subluxation [19]. Although RA can affect any joint, the thoracic and lumbar spine, as well as the distal interphalangeal joints (DIP) are typically spared. However, rare cases of DIP joint involvement have been described in the literature [20].

1.2. Biomarkers

1.2.1. Inflammation-related cellular and tissue changes

Both RA and OA are characterized by synovial inflammation and concomittant oxido-reductive stress resulting in tissue damage. Despite of these similarities, there are substantial differences in the cytokine profile, humoral and cellular immune responses involved in the pathogenesis of the diseases. Osteoarthritis can be considered as steril, antigen-independ inflammation, while growing evidence suggests that the development of RA is associated with an unknown antigen found in synovium [21]. T cell reactions causing tissue damage in RA include late-type hypersensitivity and direct cytotoxicity. In late-type hypersensitivity reactions, Th1-type CD4+ T cells attract other cells, mainly macrophages, through their cytokine production, which induces the production of tissue-damaging and fibrosis-inducing substances. In T cell-mediated cytotoxicity, antigen-specific CD8+ T-lymphocytes recognize and kill cells expressing the target antigen, resulting in tissue damage [22]. Disease-specific antibodies can be detected with serological tests. In RA, rheumatoid factor (RF) and anti-citrullinated-protein-antibody (ACPA) are present in the serum. The most well-known of these is RF, a non-specific IgM antibody, which is produced against the Fc portion of autologous IgG. In contrast to RF, ACPA has 95% specificity for RA, making it a more valuable biomarker in clinical practice [23]. With regards to laboratory tests, RA patients typically display increased C-reactive protein (CRP) and erythrocyte sedimentation rates (ESR) [24]. Setting the diagnosis of RA is often challenging and based on a multitude of morphological, radiographic, and serological changes. In case of symmetrical swelling of the metacarpophalangeal joints, banded osteoporosis and/or erosion in comparative hand or foot X-ray records, RF and/or ACPA seropositivity, the presence of RA can be presumed. In the absence of such typical symptoms, synovitis must be confirmed by ultrasound or MRI to set the diagnosis. Additionally, further investigation (abdominal ultrasound, chest X-ray) is needed to rule out other possible pathologies such as paraneoplasia.

The severity and progression of RA can be evaluated by using clinical scores. The DAS 28 test (Disease Activity Score for Rheumatoid Arthritis) is used to assess the effectiveness of

therapy in the course of the disease. It is validated for clinical trials and combinated with EULAR score criteria (European Alliance of Associations for Rheumatology). This combination is based on the number of tender and swollen joints, CRP and ESR values, and provides objective information for clinicians about patient activity. The clinical score ranges from 1 to 10 [25].

The articular cartilage is not covered by the synovial membrane; however, it receives nutritients by diffusion both from the synovial fluid ultrafiltrated from the synovial mebrane and the bone tissue under the cartilage. This synovial fluid contains viscous hyaluronic acid, mucinous lubricin, and phospholipids providing “lubrication” for joint movement. The joint capsule has two layers. The outer layer (stratum fibrosum) consists of a dense fibrous connective tissue. The inner layer is the synovial membrane, the cells covering the surface of which are mesenchymal, so called mast cells that are not true epithelial cells. These machrophages and fibrocytes produce and purify the synovial fluid. In arthrosis, cartilage degeneration consists in the depletion of matrix proteoglycans. The collagen skeleton of the matrix becomes bare and then breaks down, and the articular cartilage gradually wears off to the subchondral bone. In RA, *synovitis chronica villosa proliferativa* occurs, in which glove-finger inflammatory proliferation of the synovium can be seen. Fibrin is present on the synovial surface followed by lymphocytes, plasma cells, machrophages, and neutrophil granulocytes. This inflammatory tissue grows on the surface of the cartilage, leading ultimately to its destruction. It then turns into granulation tissue, calcifies, then the cartilage surfaces ossify and ankylosis develops, thereby stopping the joint from functioning [26].

1.2.2. Arthritis-related mitochondrial dysfunction

Mitochondria are responsible for the production of ATP and control the oxidative state of the cell [27], and regulate caspase-dependent and caspase-independent apoptotic pathways [28,29]. Beside these well-known functions of mitochondria, a growing body of evidence implicates the role of mitochondrial damage and dysfunction in synoviocytes and chondrocytes of OA [30] and RA patients. On the one hand, mitochondria are a major target of inflammation-associated injury in the synovial membrane and cartilages of patients with inflammatory arthritis. TNF-α induces mitochondrial damage through suppression of mitochondrial complexes I and IV [31]. Moreover, increased reactive oxygen species (ROS) production results in oxidation of mitochondrial lipids, sulfhydryl groups and iron sulfur complexes of mitochondrial respiratory enzymes that leads to the impairment of oxidative phosphorylation [32].

On the other hand, mitochondrial dysfunction has also been implicated in the pathogenesis of primary and post-traumatic OA [33]. Some haplogroups of mitochondrial respiratory genes are closely associated with higher prevalence of OA and RA meaning an increased genetic predisposition to the development of arthritis [34]. As a consequence of the altered mitochondrial genes, mitochondrial respiratory activity is impaired in arthritis. Electron transport through mitochondrial complexes II and III is decreased in chondrocytes of OA patients as compared with healthy patients that leads to higher ROS production and lower ATP levels [35].

1.2.3. Examination of mitochondrial functions with high-resolution respirometry

High-resolution respirometry is a suitable method for the investigation of mitochondrial functions such as oxidative phosphorylation (OxPhos) capacity and oxygen consumption [38]. In recent years, HRR played a central role in the development of mitochondrial research. Fo HRR, non-frozen, freshly prepared tissue samples are needed to be suspended in an appropriate medium and placed in two experimental chambers of the respirometer (Oxygraph-2k, Oroboros Instruments, Innsbruck, Austria). (Figure 1.) Based on the changes in the oxygen concentration in the chambers, the oxygen consumption of the mitochondria can be calculated, and each ventricle is equipped with an oxygen sensor. Such respirometric tests can be performed on 3 different samples: isolated mitochondria, permeabilized tissues and permeabilized cells (e. g. precisely cut synovial samples.). To facilitate the passage of chemicals across the membrane, the non-permeable tissues and cells are made permeable to the cell membrane. With sequential administration of substrates and inhibitors, the mitochondria undergo various “states” during respirometric measurements. (Figure 2.) Mitochondrial respirometry is an important method in studying mitochondrial dysfunction in various conditions and diseases, such as obesity [39], oxidative stress and ischemia-reperfusion injury [40], apoptosis, aging [41], cancer [42] and diabetes mellitus type 2 [43].

Figure 1. High-resolution respirometer (OROBOROS Oxygraph-2k (O2k). Measurements are performed by Clark-electrodes. Two chambers of the respirometer allows parallel investigations of mitochondrial functions.

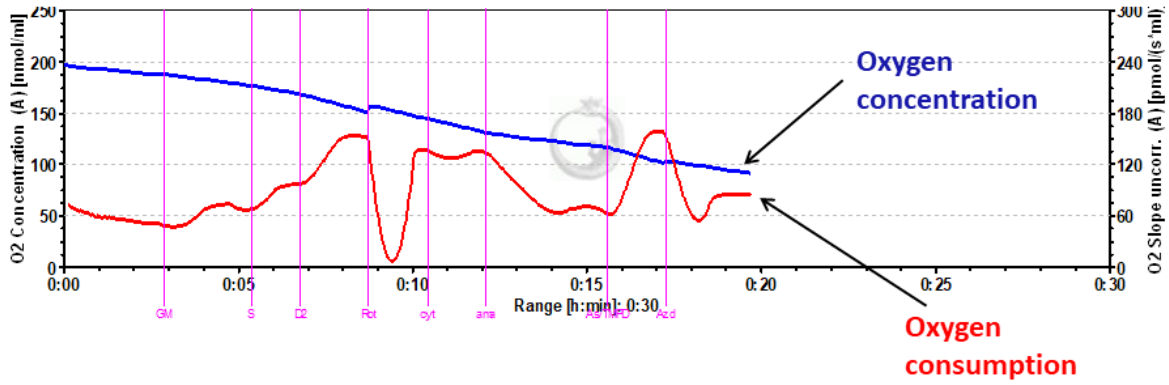

Figure 2. To measure the respiratory activity of the synovial mitochondria, tissue samples were homogenized in mitochondrial respiration medium and then subjected to high-resolution respirometry. Glutamate (G) (2 mM) and malate (M) (10 mM) were used in combination to induce complex-I-linked respiration, the complex II-linked state II respiration was determined with 10 mM succinate (S), saturating ADP (D2) (2.5 mM final concentration) was added in order to stimulate respiration to the level of OxPhos capacity. Complex-I was inhibited by rotenone (Rot) (0.5 µM). Cytochrome c (cyt) was added to test the membrane integrity, and complex-III was inhibited by antimycin A (ama) (2.5 µM). Finally, 2 mM ascorbate (As) and 20 µM *N,N,N,N*-tetramethyl-*p*-phenylenediamine (TMPD) were added for complex IV-linked respiration, which was inhibited by sodium azide (Azd) (50 mM).

1.3. Arthritis therapy

1.3.1. Conservative treatment

To date, therapeutic options for arthritis are limited mostly to pain relief and reduction of inflammation [5], therefore new approaches are needed. Pharmaceutical agents in the conservative treatment of RA include non-steroidal anti-inflammatory drugs,

immunosuppressive drugs such as corticosteroids, and biologic response modifiers (BRMs) such as TNF-α blockers. However, complete remission can hardly be achieved, and patients also suffer from the side-effects of drugs. Patients most commonly encounter gastro-intestinal side-effects such as abdominal pain, vomiting, ulcers, and bleeding; however hematological complications can also occur [44, 45]. Consequently, searching for new therapeutic approaches in the management of arthritic disorders is of high importance.

Lifestyle changes recommended by a physiotherapist and wearing orthoses may also decelerate the progression of the disease. The use of orthoses (splints) alleviates pain by stabilizing the joint, preventing and reducing the aggravation of deformities [46]. Complying with the principles of joint protection in the early stages of the disease reduces the rapid deterioration of the condition over time. According to these principles, patients are advised to find balance in rest and activity, exercise only in a pain free range, and avoid straining their joints during training [47]. Additionally, patients suffering from arthritis often manage to incorporate other favorable, joint protective habits such as balneotherapy into their daily routine [48]. Furthermore, nonthermal ultrasound, electrotherapy, cryotherapy, and low-level laser therapy may also be of high benefit as a part of conservative arthritis therapy [46].

1.3.2. Durg delivery with electroporation (EP)

Topical drugs have been developed to eliminate the potentially serious side effects of systematic treatments [44,45]. Diclofenac, used as a gold standard, is a lipophilic organic acid that is highly soluble in water, allowing the compound to enter the skin and synovial lining of the joints. However, the absorption of topically applied diclofenac is 3-5% of the oral medication, and it reaches the site of action ten times later than the oral dose [49,50]. Due to the slowness and ineffectivity of passive transdermal delivery, new dosing regimens are required to achieve adequate local drug concentrations directly at the site of application [51]. Different penetration techniques have been developed to increase bioavailability and transdermal drug delivery, including ultrasound and EP. Upon EP, the applications of short, high voltage pulses cause transitory structural perturbations in the lipid bilayer of the membranes. In this way, lipophylic or hydrophylic molecules, neutral or highly charged compounds can be transported across or into the membranes of bacteria or mammalian cells up to 40 kDa molecular weight. Common fields of indication for EP are biological and artificial membranes, but it can also be used on complex structures such as the synovium. [60]. (Figure 3.)

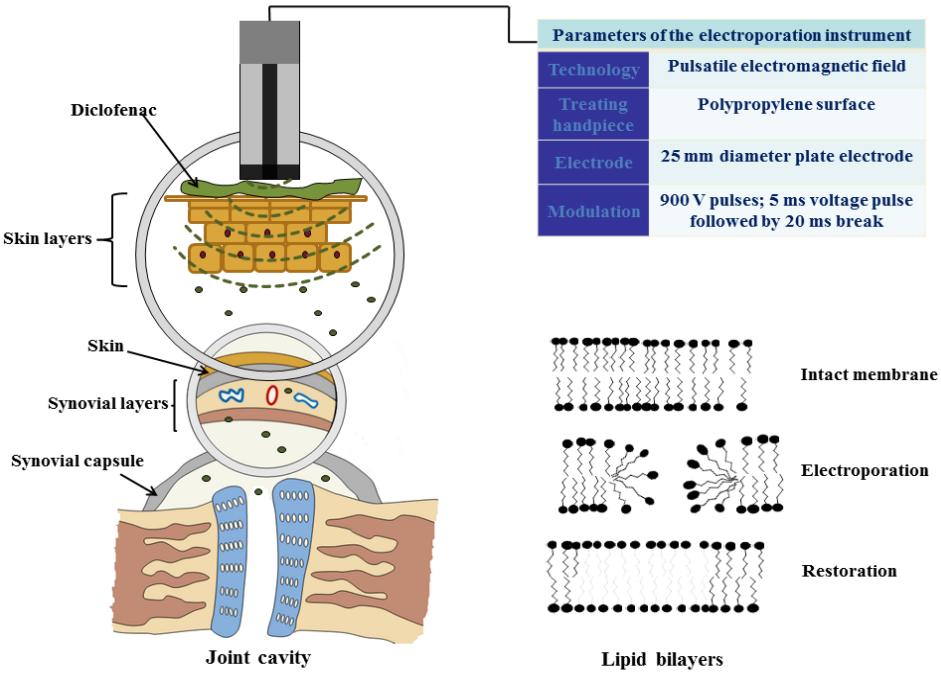

Figure 3. Drug delivery with EP over the joints. A pulsating electromagnetic field develops around the skin layers, which electrical pulse with an optimized voltage (1400Vpp-1800Vpp) lasting up to 5ms is discharged through the cell suspension, followed by a 20ms pause. This disrupts the phospholipid layer of the membrane and forms temporary pores. Upon completion of the EP, the phospholipid layer returns to its normal state.

1.3.3 Operative treatment

Prostheses for total knee arthroplasty (TKA) and resurfacing arthroplasty are recommended as treatment options for people with end-stage arthritis of the knee. Cemented fixation of prosthesis stems is widely used and considered as the gold standard for TKA [61]. The first knee replacement surgery was performed by Verneuil in 1986. He resected a piece of the joint sheath and placed it between the taste surfaces to prevent them from ossifying. Fascia lata was commonly used [62]. In 1860, Ferguson began resecting both taste surfaces to create movement between the tibia and femur. This resulted in reduced stability due to tendon laxity [63]. In the early 1950s, it was the first successful total knee joint uniaxial hinge prosthesis implantation. Both components of this continued into a long stem. These were incompatible with knee movements, eventually loosening [64]. MacIntosh introduced hemiarthroplasty in 1958 to treat varus-valgus deformity. The tibia was implanted in an acrylic plateau, which also reduced deformity and pain [65]. In 1971, the era of knee prostheses, which is still used today, began with Gunston. He made a polycentric prosthesis that replaced both surfaces, the components of which were not mechanically connected to each other (called “unconstrained”

prothesis). He replaced the tibial surface with high-density polyethylene and fixed the prosthesis with polymethyl methacrylate (PMMA) cement. Newer types of knee endoprostheses were based in the Gunston concept. The biomechanics of the knee were increasingly imitated [66].

Indeed, this kind of fixation has several potential advantages including immediate fixation, inaccurate-cut compensation, and the potential for local antibiotic delivery [67]. However, observed signs of osteolysis at the cement–bone interface has raised questions about the long-term durability of cemented TKAs. Due to concerns regarding late loosening caused by tension, shear or wear debris, cementless TKAs have been developed in an attempt to improve the longevity of implants, particularly in more active, younger patients. Considering an average of 10-15 years implant survival and the potential need for revision surgery, cementless fixation has an additional advantage in younger patients by preserving the bone stock.

Since the introduction of cementless prostheses, manufacturers came up with new materials such as titanium, cobalt-chromium alloys and tantulum, with better biocompatibility and with porotized, rough surface to increase prosthesis stability [68]. Among them, hydroxyapatite (HA)-coating was a promising coating material with the potential to achieve biological fixation of implants. HA is an osteoconductive calcium phosphate molecule, which is structurally and morphologically similar to human bone. Several studies have shown that these properties of HA stimulate the interaction between the bone and the implant, accelerating and inducing insertion, called osteointegration [69]. However, there are some disadvantages of HA-coating, such as stiffness, low extensibility, and brittleness [70]. Furthermore, its rough surface promotes bacterial adhesion and so, enhanced biofilm formation has been reported [71].

There are several studies comparing the outcomes of TKA using HA-coated and non-HA coated prosthesis stems. The results of these studies are conflicting with some indicating improved initial and late stability of stems, which are directly correlates with prosthetic life [69,72]. However, others showing neither clinical nor radiological benefits with the use of HA-coated implants [73]. As such, the signs of osteolysis also have been observed with cementless TKAs similarly to the cemented [74] together with early migration of the stem by radiostereometric analysis (RSA) studies [75]. The question remains whether cementless TKAs have an improved long-term survival. This can only be answered by a randomized trial comparing the two methods of fixation.

2. MAIN GOALS OF THE STUDIES

Our main goal in these studies was to characterize the pathomechanism of the main groups of arthritic disorders, namely the OA and RA, and to find optimal conservative and operative treatments.

- As a first step, in study I., we characterized the mitochondrial changes in the synovial membrane in OA and RA patients. For this purpose, we used intraoperative samples, that were subjected to HRR, biochemical analysis and histology.

- Then, in study II., we aimed to improve the efficacy of transdermal drug delivery in conservative treatment of arthritis. We hypothesized that EP can amplify the transport of topical diclofenac into the joints and thus the effectiveness of local administration increases. Our aims were to compare the penetration properties of diclofenac hydrogel into the synovial fluid after different administration routes, and to estimate the analgesic and anti-inflammatory reactions after oral and topical drug deliveries in a standardized rat model of carrageenan-kaolin (C/K)-induced knee joint monoarthritis.

- Our final aim was to investigate the current innovations of prosthesis implantation in the operative treatment of arthrosis. Therefore, we conducted a meta-analysis to compare the outcomes of TKA using HA-coated and non-HA coated prosthesis stems. The main purpose was to update current knowledge and compare data evidence on the quality of fixation of the tibial component evaluated with radiostereometric analysis (RSA) in TKA under two conditions: with HA-coated cementless prosthesis, or with non-coated cementless or cement fixation. RSA is able to accurately measure early migration of the stem and maximum total point motion (MTPM), which is the 3-dimensional vector of micromotions, has a predictive value of future loosening as primary outcome in our analysis. The secondary endpoints were clinical outcomes of TKAs including the Knee Society score (KSS) and the Knee Functional score (KFS), which are validated scoring systems for measuring the ability of the patient to function in everyday living and assessing the magnitude of tolerated pain. Other outcomes,

such as the Hospital for Special Surgery (HSS) score were also evaluated together with the characteristics of donors and recipients.

3. MATERIALS AND METHODS

The human study was conducted in accordance with the Declaration of Helsinki and has been approved by the local medical ethics committee at the University of Szeged under reference number 85/2019-SZTE.

Animal experiments were carried out on male Sprague-Dawley rats (average weight: 300±20 g) housed in an environmentally controlled room with a 12-h light-dark cycle and kept on commercial rat chow and tap water ad libitum. The experimental protocol was in accordance with EU directive 2010/63 for the protection of animals used for scientific purposes, and it was approved by the National Scientific Ethical Committee on Animal Experimentation (National Competent Authority) with the license number V./148/2013. This study also complied with the criteria of the US National Institutes of Health Guidelines for the Care and Use of Laboratory Animals.

3.1. Protocol in Study I.

3.1.1. Study design

Prospective clinical study was conducted at a single, level I trauma centre (Department of Traumatology at the University of Szeged) between 01 September 2019 and 30 November 2020. Data were collected from consecutive adult patients (age > 18 years) with signed informed consent undergoing open or arthroscopic knee or hip joint surgery. Pediatric patients and patients with multiple injuries, septic conditions, inadequate compliance, or incomplete dataset were excluded. Labor parameters (white blood cell count (WBC), C-reactive protein (CRP), total protein (TP)) and clinically relevant information (age, gender, height, weight, Body Mass Index (BMI), International Statistical Classification of Diseases and Related Health Problems (ICD) codes, comorbidities, previous joint injuries, medication, etiology and current activity of OA, operation type) were extracted from electronic database (MedSolution). Additional information regarding subjective life quality, the level of everyday joint pain (according to VAS) and the use of orthoses and walking aids were obtained from a detailed questionnaire.

3.1.2. Patient allocation

Participants were allocated into RA, OA and control groups based on their medical documentation, 2010 American College of Rheumatology/European League Against

Rheumatism (ACR/EULAR) rheumatoid arthritis classification criteria and Kellgren-Lawrence (KL) classification. Patients were allocated into the RA group if they have already been diagnosed with RA and fulfilled the 2010 ACR/EULAR score ≥6 criterion. For the diagnosis of OA, the KL classification is the most widely used radiographic clinical tool [76,77]. AP knee radiographs were graded from 0 to 4, according to KL-criteria, by two independent orthopedic trauma experts (Á.C., A.M.). A grade >1 entailed an allocation to the OA group, independently from the etiology of the disease (both primary and posttraumatic cases were included). The control group consisted of patients under the age of 40 with a KL grade ≤1.

3.1.3. Sampling

Synovial fluid and tissue samples from the knee joint synovium were taken with the permission and signed consent of the patients. Synovial fluid was aspirated prior to incision, with an 18 G needle, and placed into Eppendorf tubes. Synovium tissue samples of 1x1 cm in size were obtained from the suprapatellar pouch, sparing the Hoffa's fat pad. The samples were placed into 4% (v/v) neutral buffered formalin and phosphate buffered saline (PBS), and transported on ice directly to undergo biochemical measurements, histopathological evaluation and high-resolution respirometry respectively [78].

3.2. Protocol in Study II.

This study was performed in three experimental series. The goal of the first experimental series was to assess the serum and the synovial concentrations of diclofenac by high-performance liquid chromatography (HPLC). The animals were anaesthetized with ip sodium pentobarbital (45 mg kg-1) and placed in a supine position on a heating pad to maintain body temperature between 36 and 37°C. In the first group (n=16), diclofenac sodium gel (50 mg mL−1 in 230 µL volume) was applied topically above the knee joint. In the second group (n=16), after dispersion of the diclofenac gel over the knee joint, EP was applied for 8 min. Samples of blood from the inferior vena cava and of synovial washing fluid from the knee joint were collected at 10, 30, 60 and 120 min of the experiment. The samples were frozen at -80°C until the HPLC measurement. At the end of the last sampling point, the animals were sacrificed with a single overdose of anaesthetic (Figure 4.)

In the second series of experiments, inflammation-related changes to the synovial microcirculation were evaluated directly by intravital videomicroscopy (IVM). The animals

were anaesthetized with ip sodium pentobarbital (45 mg kg-1) and divided into four groups according to the administration route of diclofenac: The animals were treated with per os diclofenac (75 mg kg-1 diclofenac sodium, Novartis Hungaria Kft., Budapest, Hungary) in Group 1 (n=6), with topical diclofenac gel (50 mg mL−1 in 230 μL volume; n=6) in Group 2, and with EP-combined topical diclofenac gel (50 mg mL−1 in 230 μL volume; n=6) in Group 3. Group 4 served as a per os saline-treated control (n=6). The treatments were always applied 2 h before (t = -2 h) and 2 h after (t = 2 h) the arthritis induction (Figure 4.).

In the third experimental series, the effectiveness of different routes of diclofenac treatment on nociception and inflammatory oedema formation was compared in C/K-induced arthritis. The animals were divided into four groups (n=6) according to the administration route of diclofenac: (1) per os diclofenac sodium, (2) topical diclofenac gel, (3) EP-enhanced topical diclofenac gel and (4) sham (per os saline-treated). Treatments were applied twice daily (every 12 h). The nociceptive tests were performed 24 h after the C/K injection, while knee joint swelling was evaluated at the peak of oedema formation 48 h after arthritis induction. At the end of the experiments, the animals were anaesthetized with ip sodium pentobarbital (45 mg kg-1) for sample taking and thereafter sacrificed with a single overdose of anaesthetic. Synovial washing fluid samples and synovium tissue specimens were collected for biochemical measurements and histology. Tissue biopsies were stored at -20°C until the examinations (Figure 4.).

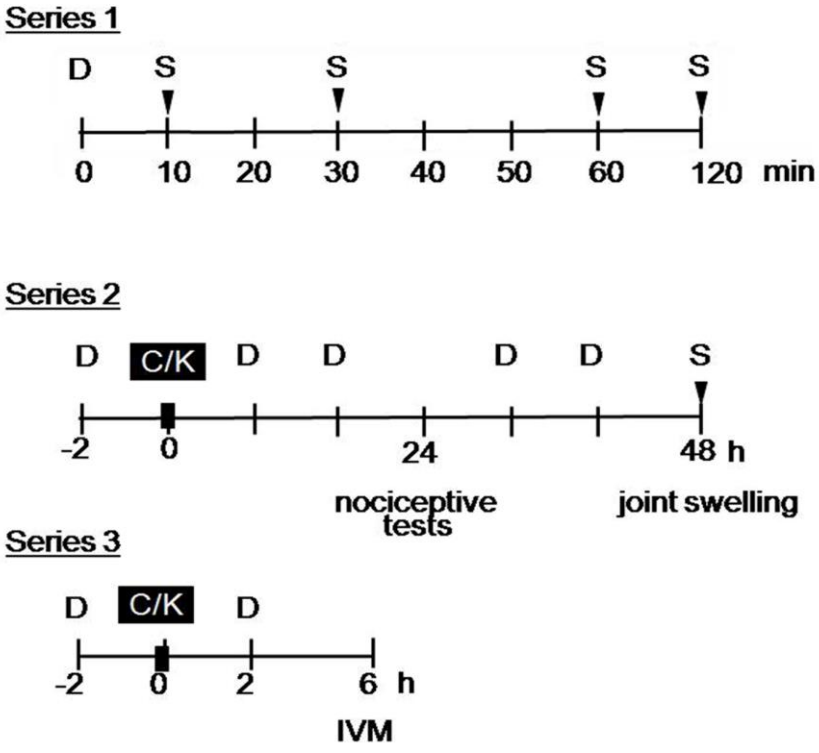

Figure 4. Time sequence of interventions.
Notes: In the first series, the diclofenac concentration in the serum and the synovial washing fluid was measured by HPLC. In the second experimental series, tests for secondary mechanical touch sensitivity and heat-provoked paw withdrawal were performed 24 h after arthritis induction with C/K and for knee joint swelling measurements 48 h after the challenge. In the third series, IVM examinations of the synovial membrane were performed 6h after the challenge.
Abbreviations: C/K, carrageenan/kaolin; D, diclofenac treatment; HPLC, high-performance liquid chromatography; IVM, intravital videomicroscopy; S, sample taken.

3.2.1. Arthritis induction

For arthritis induction, the animals were anaesthetized with intraperitoneal (ip) ketamine (50 mg kg-1) and xylazine (12 mg kg-1), and the skin over the knees was disinfected with povidone iodide. Then a single intra-articular injection of a 75 μL mixture of 2% λ-carrageenan (Sigma, St. Louis, MO, USA) and 4% kaolin in saline was administered to the right knee joint [79,80]. The contralateral knee was injected with saline.

3.2.2. Electroporation protocols

The non-invasive skin EP treatment was performed with a Mezoforte Duo Mez 120905-D instrument (Dr Derm Equipment Ltd., Budapest, Hungary). A polypropylene-covered treating handpiece with a 25 mm diameter plate electrode was used (modulation with 900 V pulses, a 5 ms voltage pulse was followed by a 20 ms break). 230 μL diclofenac hydrogel was used, and the EP treatment time was 8 min.

3.2.3. Diclofenac-containing hydrogel formulation

The hydrogel was prepared using the following procedure. 5 w/w% diclofenac sodium (Sigma-Aldrich, St Louis, MO, USA) was dissolved in a mixture of purified water and 30 w/w% ethanol (Sigma-Aldrich, St Louis, MO, USA). 2 w/w% hydroxypropyl methylcellulose (METHOCEL E4M Premium, Dow Chemical, Midland, MI, USA) was added to this solution. The pH value was adjusted for 8.0±0.1 to ensure the dissolution of the active substance by adding triethanolamine (2 w/w% solution, Hungaropharma Ltd., Hungary) if necessary.

3.3. Protocol in Study III.

This study was conducted in accordance with the PRISMA 2009 (Preferred Reporting Items in Systematic Reviews and Meta-Analysis) statement [81]. The review protocol was registered with the National Institute for Health Research PROSPERO system under

registration number CRD42019129619.

3.3.1. Search strategy

A systematic literature search was performed using EMBASE, MEDLINE PubMed, Scopus and CENTRAL. The query was designed based on MeSH terms combined with various free-text terms for hydroxyapatite and uncemented or cemented prosthesis and total knee arthroplasty. No language limitation was applied. The date of final literature search was May 31th, 2019.

3.3.2. Selection and eligibility criteria

Inclusion criteria specified any RCTs comparing the radiological and clinical outcomes of HA-coated tibial stem with uncemented or cemented stems for primary TKA. Reoperations (revision prostheses), hybrid fixation, unicompartment knee arthroplasty, non-clinical and uncontrolled studies were excluded. RCTs missing outcomes of our study were also excluded. Two authors (T.H. and E.B.) reviewed all studies upon the search strategy and controversies were resolved by discussion with a third author (P.H.). Full-text versions of potentially relevant studies were evaluated for inclusion using an eligibility pro forma screening document that was based on pre-specified criteria. At the end of literature search, 11 RCTs involving 902 patients were enrolled to analysis (Figure 5.).

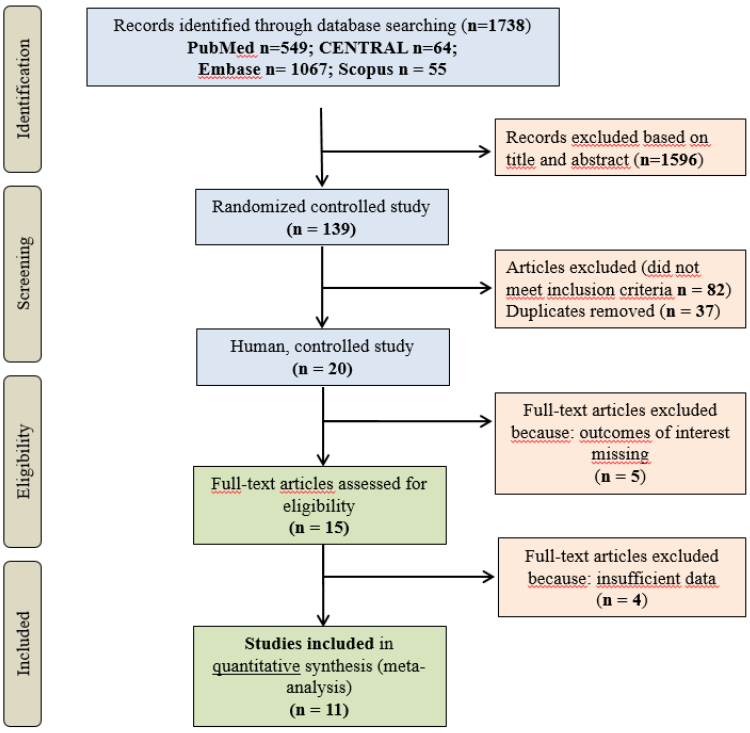

Figure 5. Flowchart of the meta-analysis.

3.3.3. Outcomes

The primary outcome was the MTPM of the tibial stem. MTPM is determined by RSA using the UMRSA software (RSA Biomedical, Umeå, Sweden) according to guideline [82] and were defined clearly in the articles as the total three-dimensional vector displacement of the marker to the greatest motion. When useful data were presented in graphic plots, we quantified them by using open source PlotDigitizer for Windows software (Version 2.6.8, Joseph A. Huwaldt). The median (range) was transformed to mean ± standard deviation (SD). Disagreements were resolved by discussion with a senior author or by contacting the corresponding author.

The secondary outcomes were validated scoring systems including KSS and KFS referring to the function of the implant in everyday life. The KSS evaluates the clinical profile with regards to pain intensity, range of motion and stability, flexion deformities, contractures and poor alignment. In contrast, KFS considers only walking distance and stair climbing with deduction for walking aids.

3.3.4. Data extraction and risk of bias assessment

We used the Cochrane Risk of Bias Tool to assess the risk of bias for each study (Figure 6.) [83]. Demographic, quality, and outcome data were extracted independently into Microsoft Excel by two authors (T.H. and E.B.). Data were taken from all articles describing the studies; Any questions in data extraction were settled by discussion with a third author.

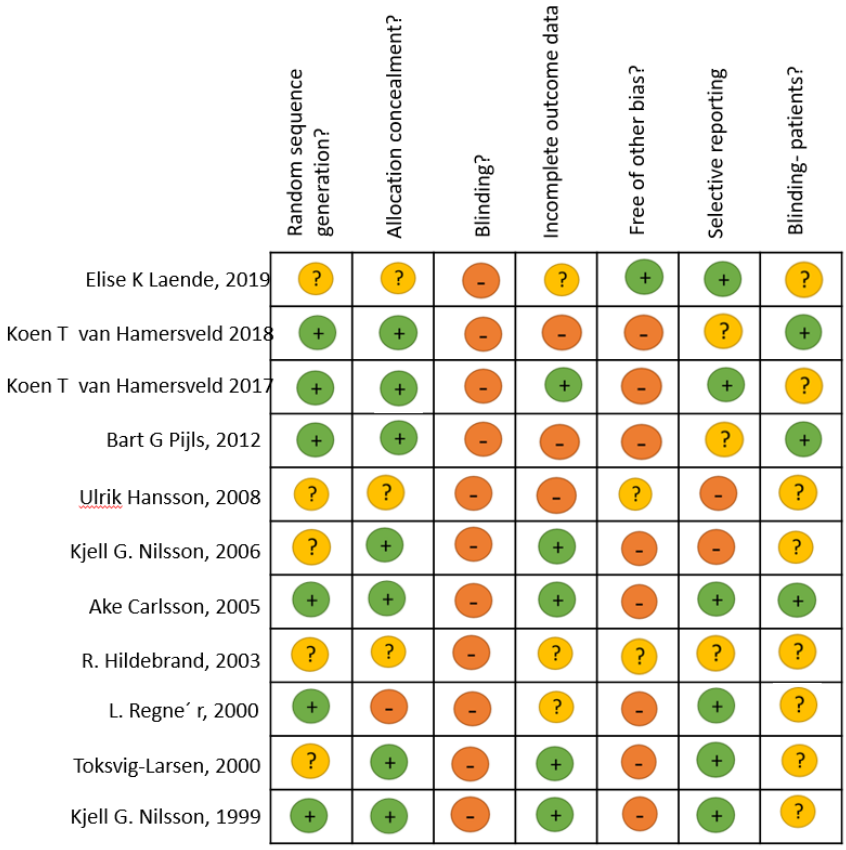

Figure 6. Risk of bias. Review of authors' judgments about each risk ofmbias item for each study included.

3.4. Biochemical analyses

3.4.1. Tissue xanthine oxidoreductase (XOR) activity

XOR is an important enzyme in purine catabolism. Besides converting xanthine to uric acid, XOR also catalyzes the reduction of nitrates and nitrites into nitric oxide (NO). This process is accompanied by the production of ROS, which can result in cellular disruption. Synovial membrane samples were homogenized in phosphate buffer (pH 7.4) containing 50 mM Tris-HCl, 0.1 mM EDTA, 0.5 mM dithiotreitol, 1 mM phenylmethylsulfonyl fluoride, 10 µg ml−1 soybean trypsin inhibitor, and 10 µg ml−1 leupeptin. The homogenate was centrifuged at 4 oC for 20 min at 24.000 g, and the supernatant was loaded into centrifugal concentrator tubes. The activity of XOR was determined in the ultrafiltered supernatant by a fluorometric kinetic assay based on the conversion of pterine to isoxanthopterine in the presence (total XOR) or absence (XO activity) of the electron acceptor methylene blue [84].

3.4.2. Tissue myeloperoxidase (MPO) activity

MPO plays a central role in the pathogenesis of autoimmune inflammation through initiating the production of hypochlorous acid (HClO) and other reactive agents causing tissue damage. According to the literature, elevated MPO levels are observed in a number of autoimmune diseases including multiple sclerosis and RA [85]. The MPO activity was measured in synovial tissue according to the method of Kuebler et al [86]. Briefly, the synovial tissue was homogenized with Tris-HCl buffer (0.1 M, pH 7.4) containing 0.1 M polymethylsulfonyl fluoride to block tissue proteases, and then centrifuged at 4 °C for 20 min. at 24.000 g. The MPO activity of the samples was measured at 450 nm (UV-1601 spectrophotometer; Shimadzu, Japan). The data was referred to the protein content.

3.4.3. Tissue nitrotyrosin levels

Free nitrotyrosine, as a marker of peroxynitrite generation, was measured by enzyme-linked immunosorbent assay (Cayman Chemical, Ann Arbor, MI). The synovial tissue was homogenized and centrifuged at 15,000g. The supernatants were collected and incubated overnight with antinitrotyrosine rabbit IgG and nitrotyrosine acetylcholinesterase tracer in precoated (mouse antirabbit IgG) microplates followed by development with Ellman's reagent. Nitrotyrosine content was normalized to the protein content of the homogenate and expressed in ng/mg-1.

3.4.4. Laboratory testing of synovial fluid

Pro-inflammatory cytokine (TNFα, RANKL) levels were measured in the synovial fluid samples using commercially available ELISA kit according to the manufacturer's instruction (Sigma-Aldrich, Budapest, Hungary).

3.4.5. Histology

Intraoperatively harvested synovium biopsies were assessed with light microscopy and confocal imaging. Confocal imaging with a laser scanning endomicroscope (CLSM, FIVE1 system, Optiscan, Victoria, Australia) was started immediately after retrieving the synovial sample. The rigid confocal probe (excitation wavelength 488 nm; emission detected at 505–585 nm) was mounted on a specially designed metal frame and gently pressed onto the inner surface of the joint capsule (1 scan/image, 1024 x 512 pixels and 475 x 475 μm per image). For the in vivo staining, 0.01% acriflavine (Sigma-Aldrich, Budapest, Hungary) was applied topically [87]. The analysis was performed twice separately by the same investigator (PH)

using a semiquantitative histology score (S0-S4) based on widening of synovial lining, neoangiogenesis, collagen fibre disorganization and fragmentation, as described previously [88]. For traditional light microscopy, the samples were fixed in buffered paraformaldehyde solution (4%) and embedded in paraffin. 5-μm thick sections were cut and then stained with haematoxylin and eosin (H&E).

3.4.6. Mitchondrial functional measurements

The efficacy of the mitochondrial respiration was assessed from synovium homogenates by high-resolution respirometry (Oxygraph-2k, Oroboros Instruments, Innsbruck, Austria). The tissue samples were homogenized in 200 μl of MiRO5 respiration medium [89] with a glass Potter homogenizer. Subsequently, the homogenates were weighed into the detection chambers, 50 μl in each, which were calibrated to 200 nmol/ml oxygen concentration in room air. Our protocol was used to explore the relative contribution of respiratory complexes to the electron transport chain (ETC) and the oxidative phosphorylation capacity (OxPhos) of mitochondria. First, the steady-state basal oxygen consumption of the homogenates (respiratory flux) was measured. Glutamate (10 mM) and malate (2 mM) were used in combination to induce C I-linked respiration. Complex II-linked baseline respiration (10 mM succinate-fuelled, in the presence of C I inhibitor 0.5 μM rotenone) was determined, then oxidative phosphorylation capacity was measured by adding saturating ADP (5 mM final concentration). The intactness of the inner mitochondrial membrane was assessed after adding cytochrome C (10 μM). Leak respiration (LEAK) was measured in the presence of C V inhibitor oligomycin (Omy) (1 mM). Thereafter, protonophore agent carbonyl cyanide p-trifluoromethoxy-phenyl-hydrazine (FCCP) (0.5 μM) was added to measure ETC coupling. Finally, residual oxygen consumption (ROX) was determined by adding 1 μM rotenone (Rot) and 1 μM antimycin-A (Ama).

3.4.7. Cytochrome c release

Cytochrome c serves as an electron shuttle in the respiratory chain, in the mitochondrial intermembrane space. It is well-known that proapoptotic stimuli promote the release of cytochrome c from the intermembrane space to the cytosol, where it facilitates apoptosis through initiating the proteolytic maturation of caspases [90,91]. Consequently, the elevated activity of cytochrome c oxidase enzyme indicates increased cytochrome c release suggesting the impairment in the inner membrane of mitochondria. The intactness of the inner mitochondrial membrane was assessed during respirometry after adding exogenous

cytochrome C (10 μM) to the homogenates.

3.4.8. HPLC measurements

The synovial washing fluid and plasma samples were analysed using an Agilent HPLC system (Agilent Technologies, Palo Alto, CA, USA) equipped with an automated solvent delivery system, which has an integrated degasser (1260 Infinity Quaternary Pump), an Agilent 1260 Infinity autosampler and a 1024-element diode array detector (1260 Infinity Diode Array Detector). The system control and data acquisition were performed with Agilent ChemStation B.04.03 software.

3.4.9. Nociceptive tests

Mechanical hyperalgesia was quantified using a plantar aesthesiometer (Dynamic Plantar Aesthesiometer mod-37450; UgoBasile, Comerio, Italy) and was expressed as paw withdrawal thresholds. Thermal hyperalgesia was detected with the paw withdrawal test using a Hargreaves apparatus [92]. Baseline measurements were performed before the induction of arthritis, while the development of inflammation was investigated at the peak of nociceptive sensitivity 24 h after C/K injection.

3.4.10. Knee joint swelling (morphological assessment)

Joint inflammation was characterized by the changes in the diameter of the joints 48 h after C/K injection. The anteroposterior and mediolateral diameters were measured with a caliper square, and the cross-sectional area was calculated.

3.4.11. Analysis of gastric effects

Gastric lesions potentially associated with diclofenac toxicity were assessed at 48 h. After retrieving and washing with saline, photographs were taken of the freshly prepared stomachs. The location (near the pylorus, lesser curvature of the fundus or diffuse) was recorded, and the extent of the lesions was evaluated by planimetric analysis using the Image J software.

3.4.12. IVM examinations

A detailed description of the surgical procedure can be found elsewhere. In brief, the animals were anaesthetized with ip sodium pentobarbital (45 mg kg-1) 6 h after the intra-articular C/K injection [93]. The jugular vein was cannulated for further supplementary doses of anaesthetic. Cannulation of the trachea maintained the patent airway, and the arterial pressure was monitored through a carotid artery cannule (Statham P23Db transducer, Budapest,

Hungary). The animals were placed on a specially designed heating pad in a supine position for the IVM examination, during which the slightly flexed knee joint of the hind limb was opened with a microsurgical technique. Surgical preparation included a longitudinal skin incision and the transverse cut of the quadriceps femoris tendon. After a circumferential cut on the joint capsule, the patella was turned aside, and the synovial membrane on the medial condyle of the tibia was visible. Synovial microcirculation was investigated by means of fluorescent IVM (Zeiss Axiotech Vario 100 HD microscope, 100W HBO mercury lamp, Acroplan 20x water immersion objective), while the synovial membrane was superfused with 37°C saline. Erythrocytes were labelled with fluorescent isothiocyanate (0.2 ml iv, Sigma-Aldrich Chemicals, St. Louis, MO, USA) and leukocytes were stained with rhodamine-6G (0.1 ml iv, Sigma, St. Louis, MO, USA). IVM records were analysed off-line and frame-to-frame using image analysis software (IVM, Pictron Ltd., Budapest, Hungary). PMN leukocytes were defined as adherent cells (stickers) to the endothelial lining within an observation period of 30 s. The number of adherent cells per mm2 of endothelial surface was counted in 5 postcapillary venules (diameter ranges from 11 to 15 μm) per animal.

3.4.13. Statistical analysis

In Study I, the statistical analysis was performed with SigmaStat 13.0 statistical software (Jandel Corporation, San Rafael, CA, USA). Normal distribution was tested with the Shapiro-Wilk test. In the case of a normal distribution, one-way ANOVA with Tukey's test was used and the data are expressed as mean ± SD. $P < 0.05$ was considered as statistically significant.
In Study II, data analysis was performed with the SPSS 17.0 software. Changes in variables within and between groups were analysed by two-way ANOVA, followed by the Holm–Sidak test. All data were expressed as means ± standard deviation of the mean (SD). P values <0.05 were considered statistically significant.
In Study III, the statistical analysis of this study was performed by a dedicated statistician (LH) using Stata 15 SE (Stata Corp) Pooled weighted mean difference (WMD) with 95% CI was calculated for continuous outcomes. Random effect model was applied at all analysis with DerSimonien-Laird estimation. Statistical heterogeneity was analysed using the I2 statistic and the chi-square to gain probability-values; I2 represents the magnitude of the heterogeneity (moderate: 30 – 60%, substantial: 50 – 90%, considerable, considerable: 75 - 100%). Publication bias was evaluated by visual inspection of the funnel plot, and the presence of this bias was considered in the case of an asymmetrical rather than a symmetrical graph. Due to the low number of included studies, we cannot perform Egger's test to detect

publication bias.

4. RESULTS

4.1. Study I.

4.1.1. Patient characteristics

A total of 528 patients underwent hip or knee joint surgery between 01 September l 2019 and 30 November 2020 at the Traumatology Department of the University of Szeged. Inclusion criteria were met in 71 cases, in which 17 patients suffered from RA and 31 from OA. The control group consisted of 23 patients under 40 years of age, without a history of OA and with a need for surgery due to trauma.

The mean age of all participants was 54 ± 18 years, 63 ± 10 years in the OA, 70 ± 5 and 29 ± 7 in the control group. The gender ratio was balanced. The members of the OA group had a higher mean Body Mass Index (BMI) compared to the control group. Furthermore, more than 65% of the OA patients had a BMI ≥30. As a well-known fact, a BMI ≥30 doubles the risk of knee OA compared to normal weight or underweight individuals [94]. Most patients in the OA group suffered from a moderate to severe (KL grade 3-4) joint degeneration. Despite of the advanced stages of the disease, only 28% of the OA patients reported a habitual, daily intake of NSADs. Prior to surgery, inflammatory markers (CRP, WBC) did not indicate an acute flare up of OA; however, a slightly elevated CRP (<25 mg/L) was measured by more than 50% of OA patients. The most common comorbidity of the study population was primary hypertension, affecting 40% of all participants. Samples were taken from the knee joint in 72% of the cases. The characteristics of the patients are shown in Table 1.

Demographics	All patients (n=71)	RA group (n=17)	OA group (n=31)	Control group (n=23)
Age (y) (mean ± SD)	51 ± 19	56 ± 14	66 ± 9	27 ± 4
Female n (%)	39 (55)	16 (94)	15 (48)	8 (35)
Male n (%)	32 (45)	1 (6)	16 (52)	15 (65)
OA risk factors				
Age >50 years n (%)	41 (58)	11 (65)	30 (97)	0 (0)
BMI (mean ± SD)	29 ± 5	28 ± 4	33 ± 6	26 ± 3
BMI ≥30 n (%)	29 (40)	2 (13)	23 (75)	4 (17)
Joint trauma in the anamnesis n (%)	39 (55)	1 (6)	15 (48)	23 (100)
Disease severity				
ACR/EULAR score (mean ± SD)		7 ± 1		
ACR/EULAR score (median [IQR])		7 [6-7]		
Kellgren-Lawrence Score (mean ± SD)			4 ± 1	
Kellgren-Lawrence Score (median [IQR])			4 [3-4]	
VAS (mean ± SD)		8 ± 2	5 ± 3	
Takes NSAIDs daily n (%)		11 (64)	12 (38)	
Needs walking aid n (%)		8 (47)	16 (52)	
Labor results				
WBC (G/L) (mean ± SD)	9.8 ± 3.6	10.8 ± 3.3	10.3 ± 3.8	8.3 ± 3.0
WBC (G/L) (median [IQR])	9.2 [7.5-12.0]	10.1 [8.8-13.2]	10.0 [7.9-12.1]	7.6 [6.1-10.0]
CRP (mg/L) (mean ± SD)	7.0 ± 7.0	11.2 ± 8.9	7.3 ± 6.1	3.5 ± 4.3
CRP (mg/L) (median [IQR])	5.5 [2.9-8.8]	6.9 [5.4-15.6]	5.6 [3.5-10.4]	2.8 [0.0-5.5]
TP (g/L) (mean ± SD)	70.1 ± 2.9	69.2 ± 2.5	70.5 ± 3.0	70.2 ± 2.7
TP (g/L) (median [IQR])	69.4 [68.5-71.0]	72.2 [67.5-69.8]	69.6 [69.2-71.0]	69.5 [68.5-71.6]
RF positive n (%)		11 (65)		
Comorbidities				
Presence of comorbidities n (%)	11 (44)	14 (82)	21 (68)	3 (13)
Primary hypertension	10 (40)	6 (35)	18 (58)	2 (7)
Diabetes	4 (16)	2 (11)	6 (19)	1 (6)
NIDDM	*3 (13)*	*2 (11)*	*5 (16)*	*1 (6)*
IDDM	*1 (4)*	*0 (0)*	*1 (3)*	*0 (0)*
Gout	2 (8)	1 (6)	2 (6)	0 (0)
Other	6 (24)	12 (70)	10 (32)	0 (0)
Operation type				
Arthroscopy n (%)	32 (45)	2 (12)	9 (29)	21 (91)
Open surgery n (%)	39 (55)	15 (88)	22 (71)	2 (9)

Table 1. Patient characteristics. RA patients were assessed based on ACR/EULAR criteria. OA patients were graded according to Kellgren-Lawrence classification. Scoring was performed by two independent orthopedic-trauma surgeons. VAS refers to the chronic pain in the joint affected by RA or OA. Acute pain due to acute trauma was not considered. Daily use of NSAIDs refers to habitual drug intake. Taking NSAIDs for a short period after trauma was not regarded as daily use. Crutches, rollators, and wheelchairs were categorized as walking aids. Labor parameters were measured prior to joint surgery. CRP levels were not measurable under 2 mg/L, thus a CRP<2 mg/L was considered as 0. OA=osteoarthritis;

SD=standard deviation; BMI=body mass index; IQR=interquartile range; VAS=visual analog scale; ACR/EULAR=American College of Rheumatology/European League Against Rheumatism; NSAID=non-steroidal anti-inflammatory drug; WBC=white blood cell; CRP=C-reactive protein; TP=total protein; RF=Rheumatoid Factor; NIDDM=non-insulin dependent diabetes mellitus; IDDM=insulin dependent diabetes mellitus

4.1.2. Mitochondrial functional measurements

Changes in mitochondrial respiratory functions were evaluated in the presence of glutamate and malate or succinate in order to differentiate between C I- and C II-based activity. Arthritis groups (92.3 ± 17.2 pmol/s/ml in OA, 61.9 ± 14.8 pmol/s/ml in RA) displayed significantly reduced C I OxPhos activity compared to the control group (115.2 ± 26.2 pmol/s/ml) in the presence of saturating amount of ADP. The decrease in C I-related OxPhos was significantly higher in the synovial samples of RA patients than in OA patients.

Respiratory acceptor control ratio (RCR) and coupling control ratio (CCR) were defined to quantify changes in the coupling of the ETC [24]. RCR is expressed as the OxPhos/LEAK ratio and is directly but non-linearly related to the OxPhos-coupling efficiency. CCR is a flux control ratio at a constant mitochondrial pathway-control state and ranges from 0-1. A reference rate is defined by taking maximum respiratory flux and flux in the electron transfer-state induced by complex-specific substrate, such that the lower and upper limits of the CCR. In comparison with the control group, C I-based RCR (4.4 ± 1.3 in the control group, 3.0 ± 0.8 in RA) and CCR (0.3 ± 0.1 in the control and OA group, 0.6 ± 0.2 in RA) both indicated a significant impairment of the ETC in the RA group. However, no significant difference was found in C II-related OxPhos, RCR and CCR between the study groups. (Figure 7.)

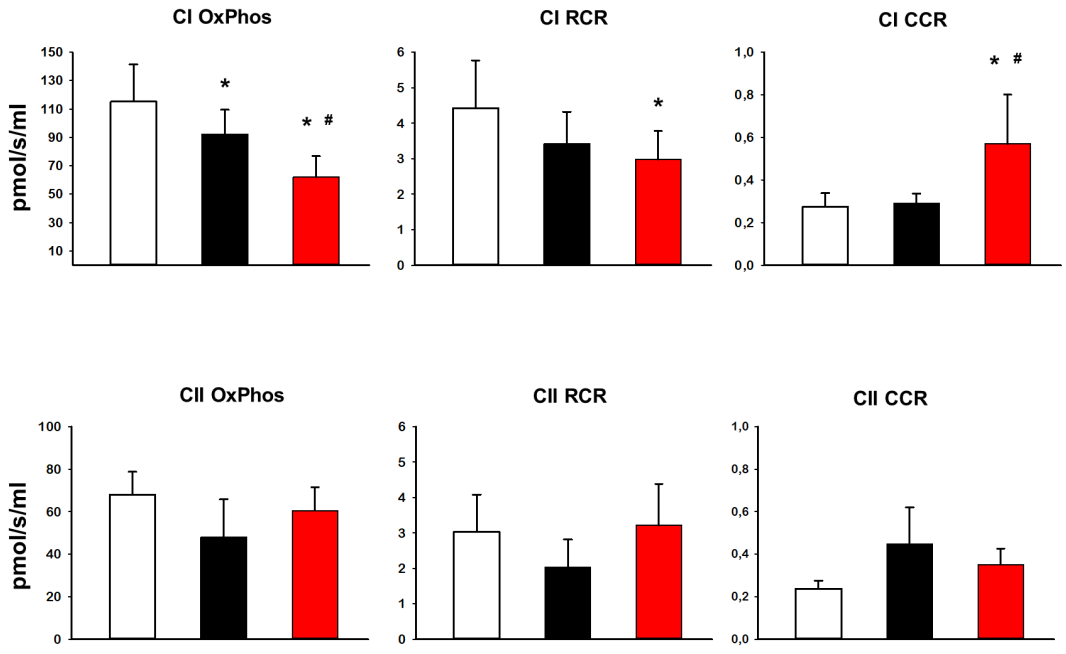

Figure 7. Mitochondrial functional measurements. Complex I (CI) and complex II (CII) related oxidative phosphorilation (OxPhos) capacity of synovial epithelial mitochondria is shown, together with the respiratory control ratio (RCR) and coulpling control ratio (CCR) of the complexes. Arthritis groups displayed significantly reduced C I activity compared to the control group. The C I-related respiratory control ratio (RCR) of the RA group was significantly lower compared to the control group. C I-related coupling control ratio (CCR) is significantly higher in the RA group. No significant difference was found in C II-related respiratory activity, RCR and CCR between the study groups. RA group is marked with red columns. Black columns represent the OA group. Control group is marked with white. Data are presented as means ± SD. *P<0.05 vs control; #P<0.05 vs OA (one-way ANOVA, Holm-Sidak test)

4.1.3. Cytochrome c release

Cytochrome C release was assessed by adding exogenous cytochrome C to the sample in the presence of glutamate and malate or succinate. OA (8.8 ± 2.4 pmol/s/ml) group exhibited significantly higher C I-based response in oxygen consumption compared to the control group (3.9 ± 1.4 pmol/s/ml), indicating lower initial levels of cytochrome C. Furthermore, a significant increase could be detected in the RA group compared with both the control and OA groups in both Complex I- (12.4 ± 2.6 pmol/s/ml) and Complex II-related (3.7 ± 1.1 pmol/s/ml in the control group, 4.6 ± 1.1 pmol/s/ml in OA, 10.5 ± 3.5 pmol/s/ml in RA) activity. (Figure 8.)

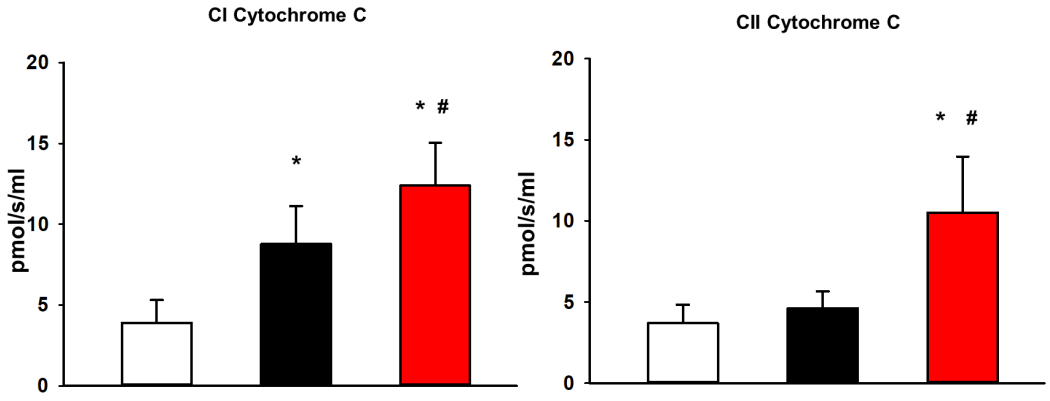

Figure 8. Cytochrome C induced respiration. RA and OA groups displayed significantly elevated O2-consumption in the presence of glutamate and malate (CI Cytochrome C) compared to the control group. In the presence of succinate (CII Cytochrome C), significantly increased O2-consumption occurred only in the RA group. RA group is marked with red color. Black color represents the OA group. Control group is marked with white. Data are presented as means ± SD. *P<0.05 vs control; #P<0.05 vs OA (one-way ANOVA, Holm-Sidak test). CI=Complex I, CII=Complex II

4.1.4. Pro-inflammatory cytokines in the synovial fluid

TNF-α and RANKL levels in the synovial fluid samples of the participants were measured using chemiluminescence assays. Concentration of RANKL was significantly increased in the RA group compared to the control group, while TNF-α levels in the RA group were significantly higher compared to not only the control group, but the OA group as well. (Figure 9.)

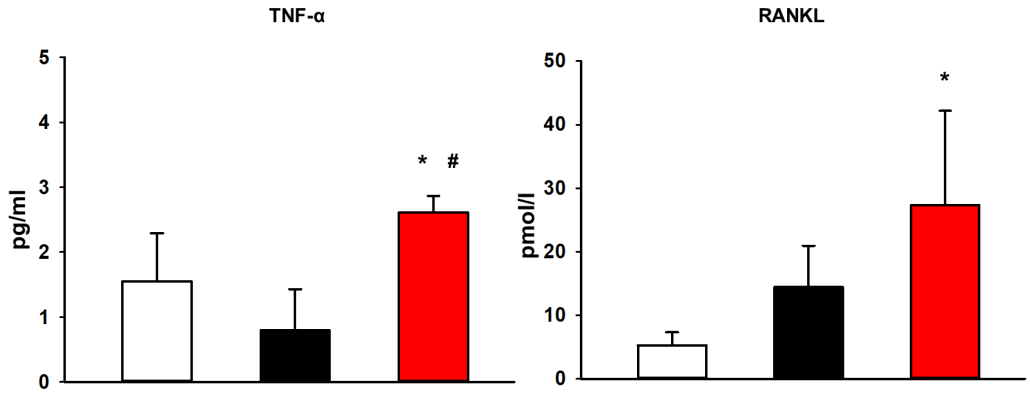

Figure 9. Inflammatory cytokines. Significantly elevated TNF-α and RANKL levels were measured in the RA groups compared to OA and control groups. This result confirms the presence of chronic synovitis in RA. RA group is marked with red color. Black color represents the OA group. Control group is marked with white. Data are presented as means ± SD. *P<0.05 vs control; #P<0.05 vs OA (one-way ANOVA, Holm-Sidak test). TNF-

α=Tumor Necrosis Factor-α, RANKL=Receptor Activator of Nuclear factor-κB Ligand.

4.1.5. Biochemical analyses

XOR and MPO activity were measured from synovial tissue, while NT levels were determined from synovial fluid as indicators of tissue damage. Significantly higher XOR activities were measured in the synovial membrane homogenates of RA and OA patients compared to the control group. The synovial tissues of RA patients displayed a significantly higher MPO activity compared to the synovial tissues of OA patients and healthy individuals. Significant difference in MPO activity occurred also between the OA and control groups. In the RA group, significant elevation of NT was present relative to both the OA and control groups. (Figure 10.)

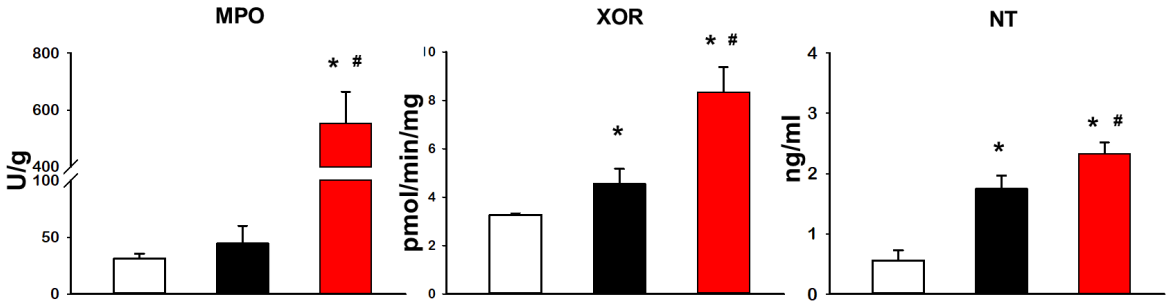

Figure 10. Biochemical analyses. Significantly higher MPO activity was detected in the RA group compared to OA and control groups. This result corresponds to the existing literature regarding the role of MPO in autoimmune inflammation. Elevated XOR activity was measured in tissue homogenates of RA and OA patients compared to the control group. Both RA and OA groups displayed significantly elevated NT levels in comparison with the control group. RA group is marked with red color. Black color represents the OA group. Control group is marked with white. Data are presented as means ± SD. *P<0.05 vs control; #P<0.05 vs OA (one-way ANOVA, Holm-Sidak test). MPO=Myeloperoxidase, XOR=Xanthine Oxidoreductase, NT=Nitrotyrosine.

4.1.6. Histopathology evaluation

CLSEM and H&E staining were used to validate the proper assignment of participants to study groups (Figure 11.). Histological assessment was performed independently and blindly on coded slides by two investigators (P.J. and P.H.) using a previously described 0–4-grade histological scoring system, representing a composite of the extent of angiogenesis and fibrosis. Additionally, on H&E stained sections, a thickened synovial membrane, increased

cellularity and mild lymphocytic infiltration occurred in samples from patients suffering from OA. (Figure 11.F) More prominent lymphocytic infiltration, fibrosis, and in some cases even extensive fibrosis could be observed in RA samples. (Figure 11.G)

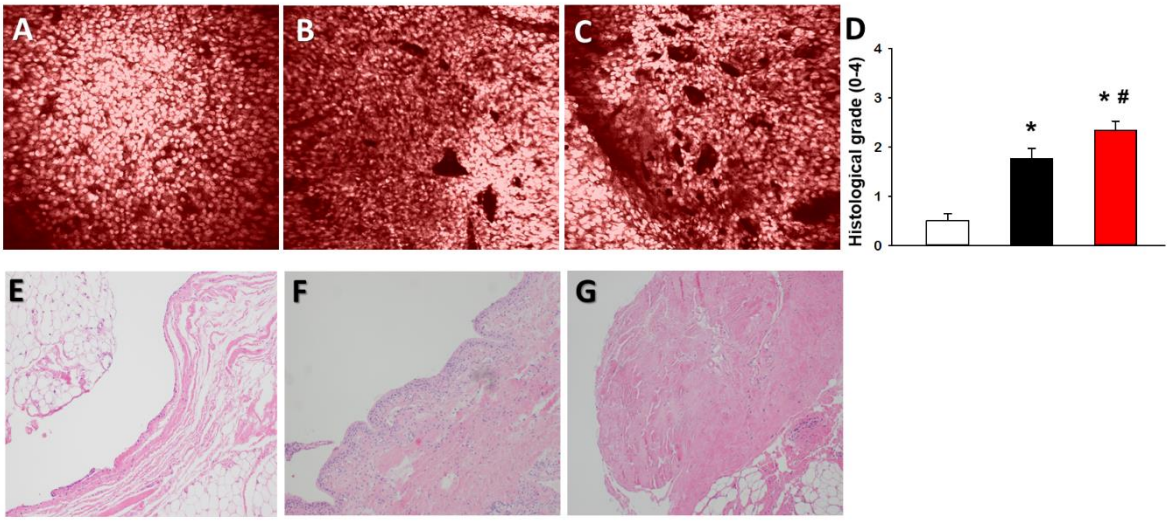

Figure 11. Histological changes in the synovium. A, B, C: Tissue sections show the results of in vivo confocal laser scanning endomicroscopy with acriflavine labeling. The bar represents 100 μm. D, E, F: Histological sections stained with hematoxylin and eosin. A: Healthy synovium with rounded synoviocytes. No signs of inflammation related angiogenesis and fibrosis can be seen. B: Osteoarthritic synovium with moderate angiogenesis due to low-grade chronic inflammation. C: Synovium of a patient suffering from RA. The large number of vascular cross-sections refers to inflammation-related angiogenesis. Scarring occurs as a result of chronic synovitis. E: Joint capsule section with synovial membrane from a healthy joint. Flattened mast cells constitute one, single cell layer. The lamina propria is poor in cells and rich in connective tissue fibers. Adipocytes and cross sections of capillaries can be observed in the deeper layers. F: Joint capsule sample from osteoarthritic joint. The synovial membrane is thickened, consists of 3-4 cell layers. Increased cellularity occurs partly due to the mild lymphocytic infiltration that can also be observed in the lamina propria. G: Joint capsule sample of a patient suffering from RA. As a result of the extensive scarring, the synovial membrane is unrecognizable. Fibrosis affects more than 50% of the stroma.

4.2. Study II.

4.2.1. Plasma and synovial diclofenac concentrations

The plasma and the serum concentrations of diclofenac were the highest 10 min after the EP treatment; they then decreased at 30 min and remained constant at 60 and 120 min. EP-enhanced diclofenac delivery exhibited a significantly higher plasma level of diclofenac as compared with the simple topical application 10 min after the application (Figure 12.). There were no significant differences in the diclofenac content of the synovial fluid and the plasma after the EP-combined application. However, simple topical application did not result in detectable diclofenac content in the synovial fluid at the same point in time (Figure 12.).

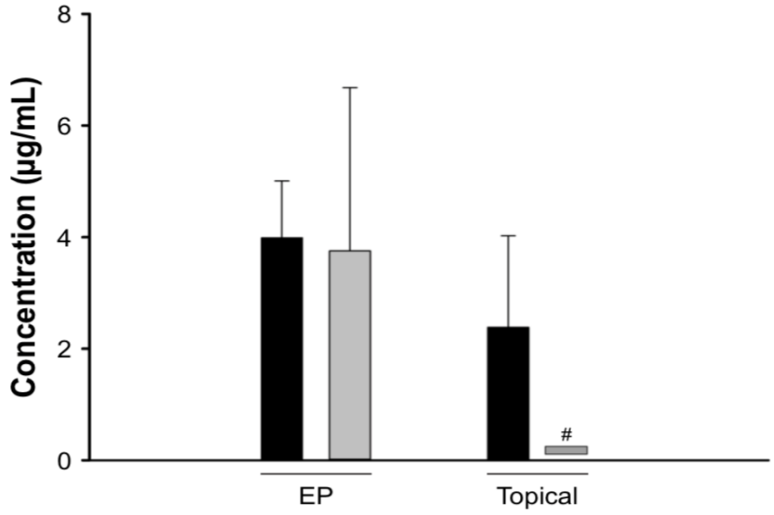

Figure 12. Diclofenac concentrations in the serum (black column) and the synovial washing fluid (grey columns) measured by high-performance liquid chromatography (Series 1). Diclofenac sodium gel was applied topically above the knee joint (Topical), or electroporation was applied for 8 min over the knee joint (EP) after the diclofenac gel dispersed. Samples of blood and synovial washing fluid were collected 10 min after application. Data are presented as means ± SD. # $p < 0.05$ vs serum level (two-way ANOVA and Holm–Sidak test). **Abbreviations:** EP, electroporation; HPLC, high- performance liquid chromatography; SD, standard deviation of the mean.

4.2.2. Leukocyte–endothelial interactions

In the second experimental series, the microcirculatory consequences of the joint inflammation were quantified via IVM, and the PMN–endothelial interactions (rolling and sticking) in the postcapillary venules of the synovial membrane were determined. The rolling fraction of the PMNs in the postcapillary synovial venules exhibited a large degree of dispersion, and no baseline differences were observed between the C/K- and saline-injected knees or between the groups which participated in the treatment protocols (data not shown).

However, the injection of C/K was accompanied by a statistically significant increase in PMN adherence (sticking) to the endothelial layer as compared to the control side (Figure 13.). This reaction was considerably reduced with the administration of oral diclofenac. However, it was only moderately ameliorated by the EP-enhanced diclofenac hydrogel, and there were no changes in response to the simple topical application of the hydrogel.

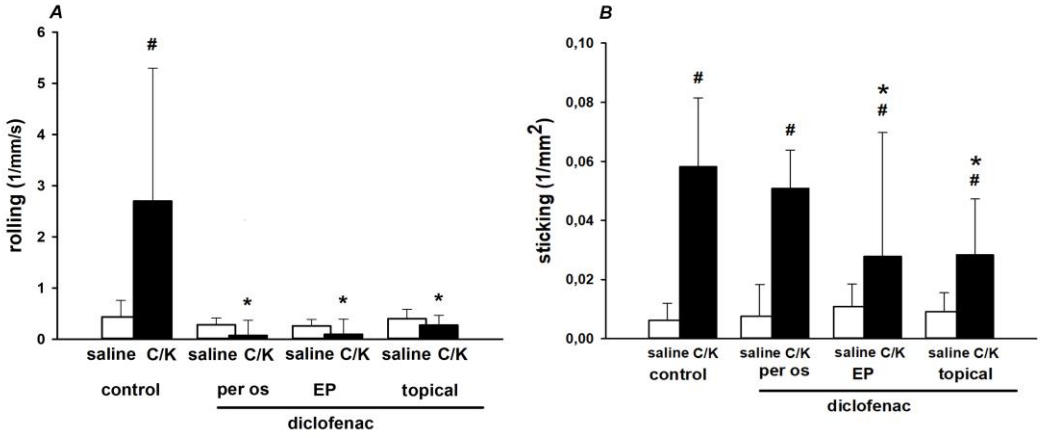

Figure 13. The effects of diclofenac treatments on the number of rolling (A) and sticking (B) leukocytes in the postcapillary venules of the synovial membrane (Series 3). Knees were injected with carrageenan/kaolin (black columns), or contralateral knees were treated with a saline vehicle (white columns). Data are presented as means ± SD. # $p < 0.05$ vs control limb; * $p < 0.05$ vs C/K + oral saline (two-way ANOVA and Holm–Sidak test).
Abbreviations: C/K, carrageenan/kaolin; SD, standard deviation of the mean.

4.2.3. Inflammatory enzyme activities and cytokine production

XOR activity was significantly increased in response to arthritis induction, in comparison with the saline-injected knee joint. These values were significantly decreased when diclofenac was applied orally or topically (Figure 14.A).

In the C/K-injected limbs, the MPO activity of the synovial tissue was significantly increased as compared with that of the saline-injected controls. In the oral diclofenac and EP-enhanced topical diclofenac-treated groups, MPO activity was significantly lower than in the non-treated animals. However, conventional topical treatment did not influence the increased MPO activity (Figure 14.B).

The C/K injection resulted in a significant increase in TNF-α concentration in the synovial lavage fluid, which was diminished by both the oral intake and EP-enhanced topical treatment (Figure 14.C).

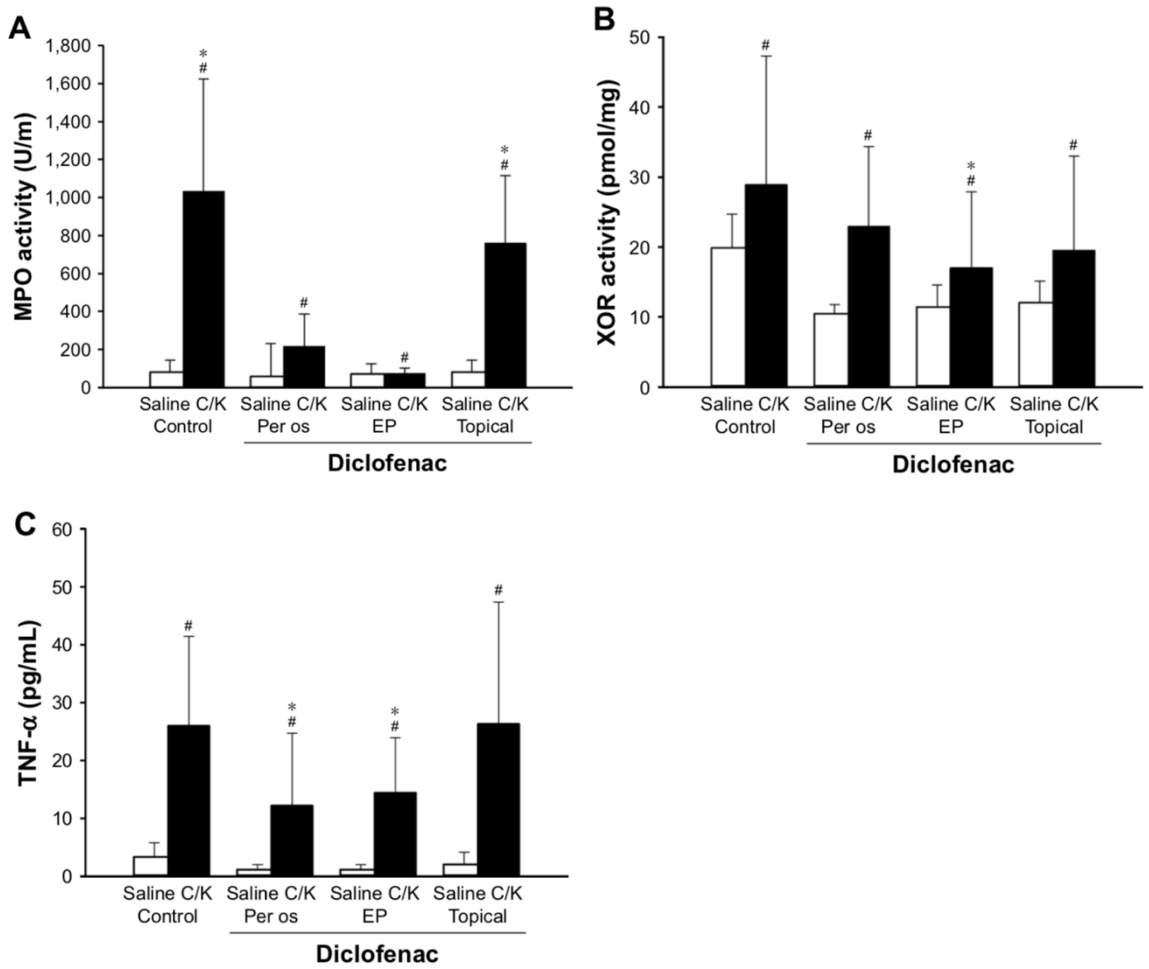

Figure 14. The effects of diclofenac treatments on the carrageenan/kaolin (C/K)-induced changes in myeloperoxidase (MPO) activity (A), xanthine oxidoreductase (XOR) activity (B) and tumour necrosis factor-alpha (TNF-α) levels (C) (Series 2). Knees were injected with carrageenan/kaolin (black columns), or contralateral knees were treated with a saline vehicle (white columns). Data are presented as means ± SD. # $p < 0.05$ vs control limb; * $p < 0.05$ vs C/K + oral saline (two-way ANOVA and Holm–Sidak test).
Abbreviations: C/K, carrageenan/kaolin; SD, standard deviation of the mean.

4.2.4. Nociception and inflammatory oedema

In the third series, the extent of inflammation was estimated with functional tests 24 h after arthritis induction. The mechanical touch sensitivity was considerably increased in response to arthritis as the C/K-injected limbs responded to a lower level of trigger than the saline-injected control limbs in animals receiving the saline vehicle (Figure 15.A). This parameter was significantly diminished in response to oral and EP-enhanced topical diclofenac treatments, albeit complete restoration was not achieved. The thermal nociceptive latency (Figure 15.B) was also significantly decreased in the injured leg in the saline-treated group, and oral and EP-enhanced topical diclofenac treatments exerted similar protective effects to

those seen with the von Frey test.

The changes in knee cross-section (Figure 15.C) furnish a direct and objective measure of joint inflammation. The cross-sectional area in the C/K-injected knees was significantly enlarged 48 h after the challenge but was significantly reduced by both the conventional topical and the EP-enhanced topical diclofenac treatments. In the case of oral diclofenac administration, complete restoration to the level for the saline-injected knees was achieved.

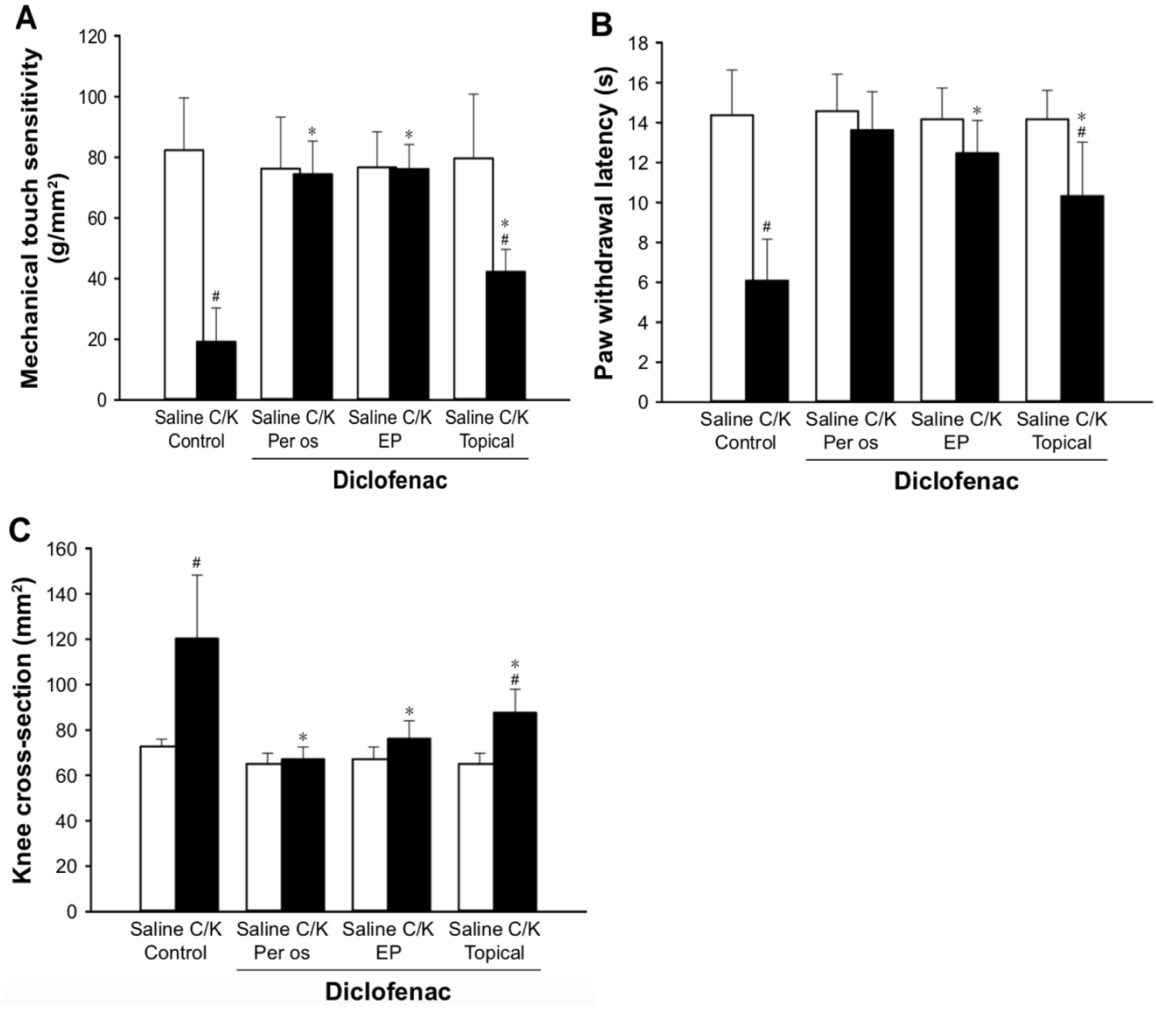

Figure 15. The effects of diclofenac treatments on the carrageenan/kaolin (C/K)-induced changes in mechanical touch sensitivity (A), heat-provoked paw withdrawal latency (B) and changes in knee joint swelling (C) (expressed as a knee cross-section) (Series 2). Knees were injected with carrageenan/kaolin (black columns), or contralateral knees were treated with a saline vehicle (white columns). Data are presented as means ± SD. # $p < 0.05$ vs control limb; * $p < 0.05$ vs C/K + oral saline (two-way ANOVA and Holm–Sidak test). **Abbreviations:** C/K, carrageenan/kaolin; SD, standard deviation of the mean.

4.2.5. Adverse effects of diclofenac intake

The gastric adverse effects of diclofenac intake were assessed by planimetric analysis of ulcers in the gastric mucosa. The topically-applied diclofenac sodium with or without EP had

no deleterious effect on gastric mucosa; however, an equivalent dose of oral diclofenac sodium resulted in ulcer formation in 70% of the animals. The location of gastric ulcerations in the rat stomach was variable and included only mild lesions such as oedema, irritation and petechia formation (Figure 16.).

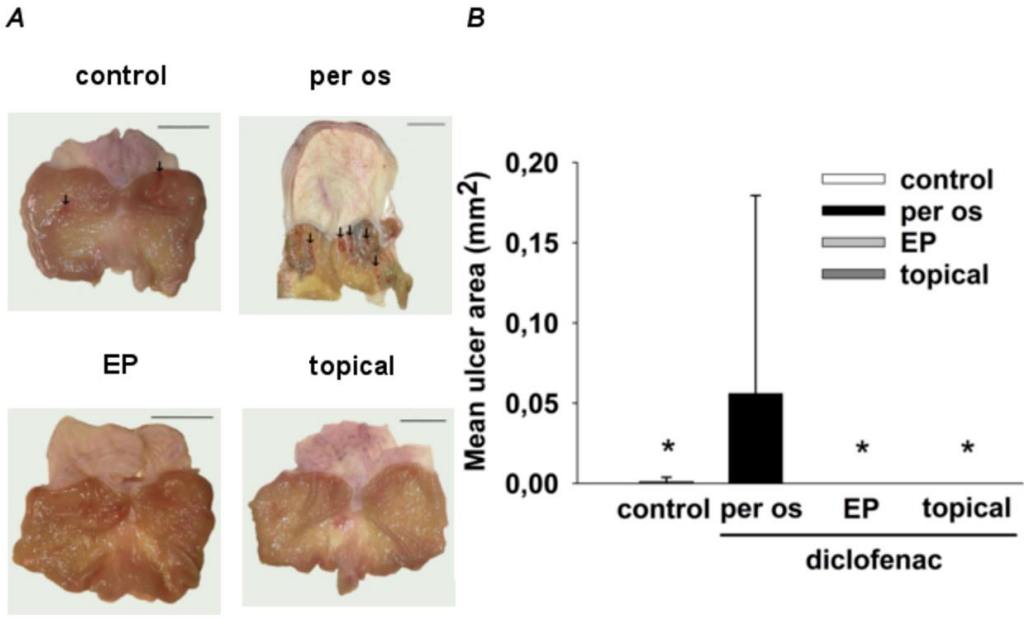

Figure 16. The effects of diclofenac treatment on the gastric mucosa. (A) Diclofenac treatment-induced gastric adverse effects. Bar represents 10mm. Black arrows show oedema, irritation and petechia formation. **(B)** Mean area of gastric lesions. The white column represents the control group (*per os* saline-treated), and the black column represents the *per os* diclofenac-treated group. The pale and dark columns represent the topical and EP-combined topical diclofenac-treated groups, respectively. Data are presented as means ± SD. * $p < 0.05$ vs *per os* diclofenac-treated group (Kruskal–Wallis one-way analysis and Dunnet test).

4.3. Study III.

Eleven RCTs were included in quantitative synthesis, in which TKA with a HA-coated tibial stem was compared to other tibial fixations (cemented and uncemented prosthesis). All trials were homogenous with respect to demographic characteristics (Table 2).

Author, Year	Design	Country	Recruitment period	Patients' characteristics					
				Patients	N⁰ of knees	Age (y)		Gender (male%)	BMI
						Mean	SD		Mean
Laende 2019 (95)	prospective randomized	Australia	2002-2015	ND	360	65	7,8	61	31,6
Hamersveld 2018 (96)	prospective randomized	Sweden	2007-2008	58	25	66	7,4	17,3	ND
Hamersveld 2017 (97)	prospective randomized	Sweden	2009-2010	60	60	66,2	7,2	16	28,3
Pijls 2012 (98)	prospective randomized	Sweden	ND	ND	68	62	ND	18,3	26,5
Hansson 2008 (99)	prospective randomized	Sweden	1997-1999	60	49	ND	ND	ND	ND
Nilsson 2006 (100)	prospective randomized	Sweden	1997-2003	85	69	55,7	ND	62	ND
Carlsson 2005 (101)	prospective randomized	Sweden	1992-1995	30	72	72,6	6	21,3	ND
Hildebrand 2003 (102)	prospective randomized	Germany	1992-1993	48	27	70,7	ND	ND	ND
Regne´ r 2000 (103)	prospective randomized	Sweden	ND	68	51	66,5	ND	16	ND
Toksvig 2000 (104)	prospective randomized	Sweden	ND	60	62	71	ND	ND	ND
Nilsson 1999 (105)	prospective randomized	Sweden	1991-1992	53	27	67	ND	17	ND

Table 2. Characteristics of the studies

4.3.1. Radiological outcome

The MTPM of the tibial stem is the primary outcome in this meta-analysis. We used 2 years follow up for the analysis of the MTPM. The higher MTPM is associated with lower stability of the implant with a 0,2 mm cut-off value. Accordingly, if the MTPM exceeds 0,2 mm, the prosthesis is classified as unstable, which greatly increases the likelihood of other complications such as aseptic loosening. If the MTPM is less than 0,2 mm the prosthesis can be considering as stable, in a long run [106]. Thirteen studies were enrolled to the MTPM analysis. The results showed that the MTPM values of the HA-coated cementless stems are significantly lower than that of the uncemented stems (WMD = 0.28, 95% CI: 0.01 - 0.56, P = 0.045) (Figure 17.A).

A

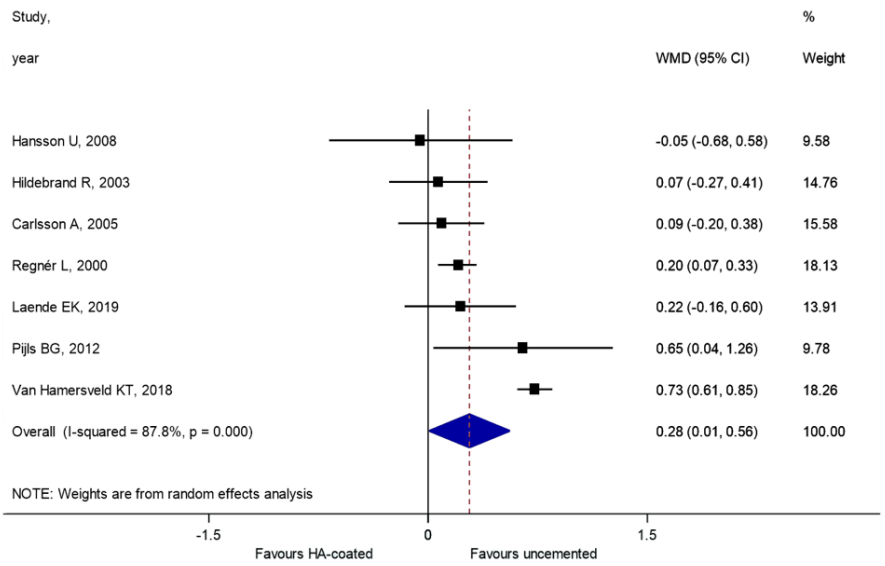

B

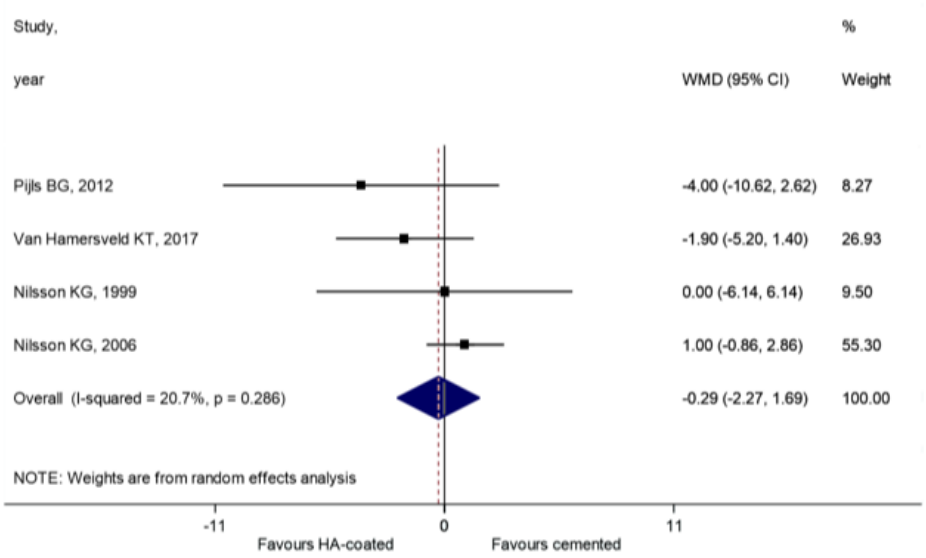

When HA-coated implants were compared to cemented prostheses, the letter displayed lower MTPM (WMD = -0.29, 95% CI: -0.41 to 0.16, P < 0.001) (Figure 17.B).

(Figure 17. C, D). In these two graphs show the funnel plot, but unfortunatelly we couldn't run Egger's test on it.

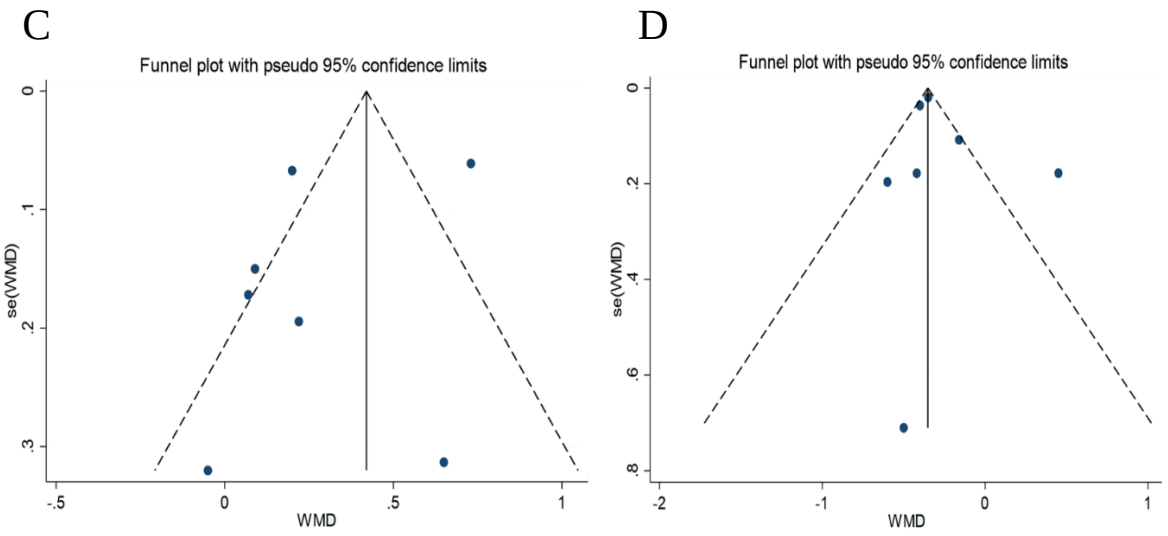

Figure 17. A MTPM analysis of the cemented and HA-coated cementless group. The value of cemented MTPM lesser than HA-coated cementless group. **B** MTPM analysis of uncemented vs. HA-coated cementless group. The MTPM values of uncemented prostheses are significantly higher than HA-coated. **C** Funnel plot 2 years follow-up; HA-coated cementless vs. uncemented group. **D** Funnel plot 2 years follow-up; HA-coated cementless vs. cemented group.

4.3.2. Clinical outcomes

The secondary outcomes were KSS and KFS. 4 RCTs were enrolled to the analysis of clinical outcomes. The result showed that KSS of HA-coated cementless prostheses is not significantly higher as compared to the uncemented group (WMD = -0.64, 95% CI: -3.02 – 1.73, P = 0.596) (Figure 18.A);

Of interest, there was no statistically significant difference in the KSS of HA-coated cementless and cemented prosthesis (WMD = -0.29, 95% CI: -2.27 to 1.69, P = 0.775) (Figure 18.B). Similar results could be obtained by the analysis of KFS of studies, however, have limited value due to the lack of the comparison between HA-coated and uncemented groups. As such, no difference could be observed between HA-coated cementless and cemented implants (WMD = -4.95, 95% CI: -13.59 to 3.69 P = 0.069); However, comparison between HA-coated and uncemented groups could not have been done due to the low number of studies in the uncemented group. (Figure 19.A). (Figure 18.C, D and 19.B) KSS data are shown on the funnel plot, but unfortunatelly we could not run Egger's test on it.

A

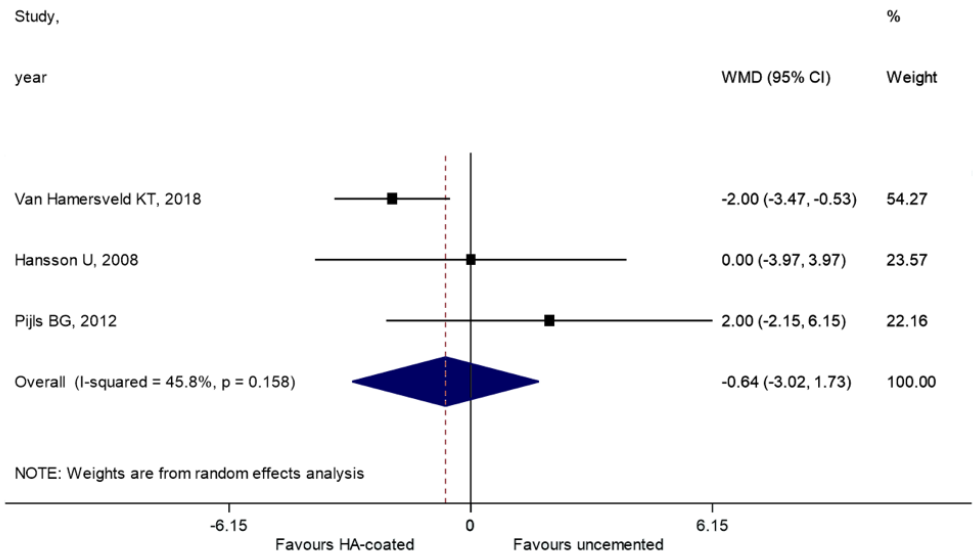
Study,
year
WMD (95% CI)
%
Weight
Van Hamersveld KT, 2018
-2.00 (-3.47, -0.53)
54.27
Hansson U, 2008
0.00 (-3.97, 3.97)
23.57
Pijls BG, 2012
2.00 (-2.15, 6.15)
22.16
Overall (I-squared = 45.8%, p = 0.158)
-0.64 (-3.02, 1.73)
100.00
NOTE: Weights are from random effects analysis
-6.15
0
6.15
Favours HA-coated
Favours uncemented

B

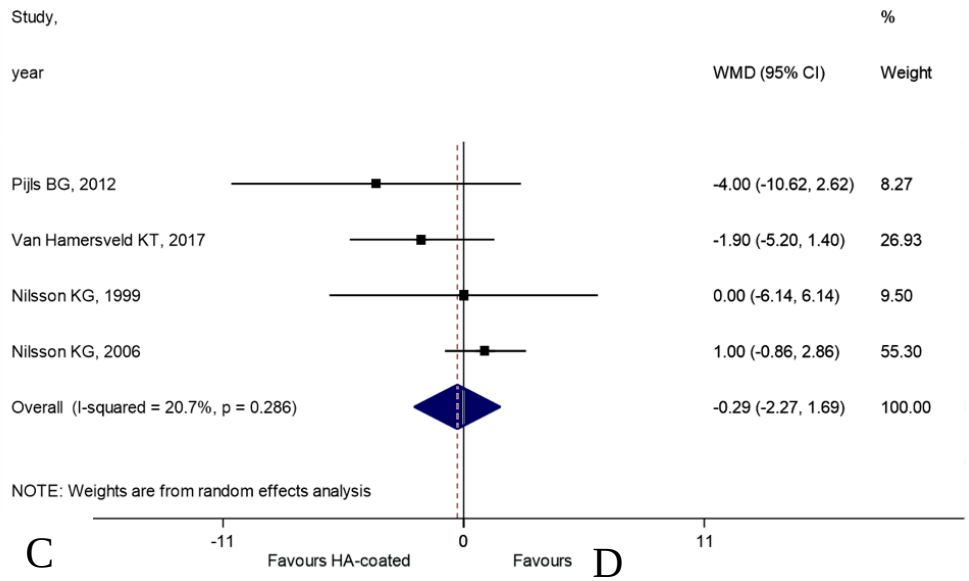
Study,
year
WMD (95% CI)
%
Weight
Pijls BG, 2012
-4.00 (-10.62, 2.62)
8.27
Van Hamersveld KT, 2017
-1.90 (-5.20, 1.40)
26.93
Nilsson KG, 1999
0.00 (-6.14, 6.14)
9.50
Nilsson KG, 2006
1.00 (-0.86, 2.86)
55.30
Overall (I-squared = 20.7%, p = 0.286)
-0.29 (-2.27, 1.69)
100.00
NOTE: Weights are from random effects analysis
-11
0
11
Favours HA-coated
Favours

C

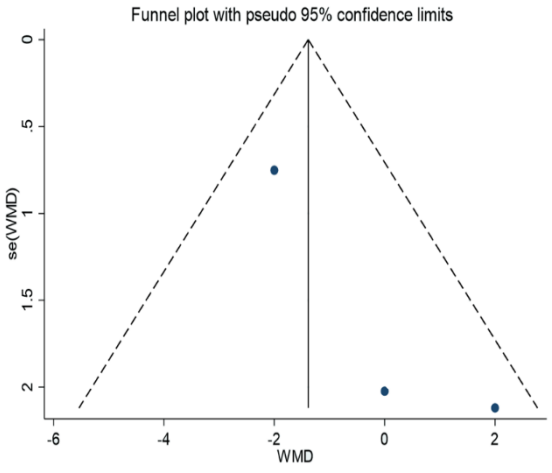
Funnel plot with pseudo 95% confidence limits
se(WMD)
0
.5
1
1.5
2
-6
-4
-2
0
2
WMD

D

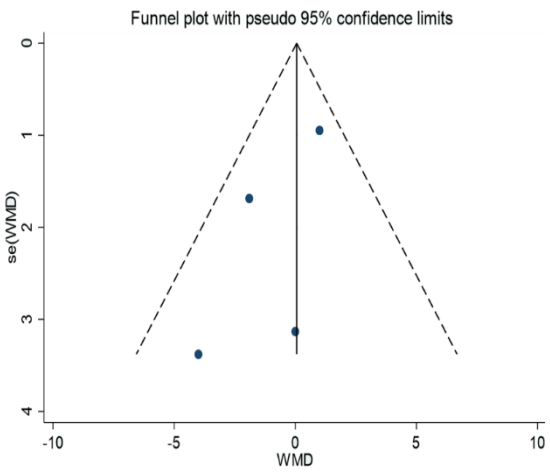
Funnel plot with pseudo 95% confidence limits
se(WMD)
0
1
2
3
4
-10
-5
0
5
10
WMD

Figure 18. A KSS analysis 2 years follow-up; HA-coated. cementless vs uncemented. The value of the uncemented is lesser than of HA-coated cementless group. **B** KSS of the HA-coated cementless vs. cemented group. The value of cemented KSS did not differ significantly from that of HA-coated. **C** Funnel plot 2 years follow-up; HA-coated cementless vs. uncemented group. **D** Funnel plot 2 years follow-up; HA-coated cementless vs. cemented group.

A

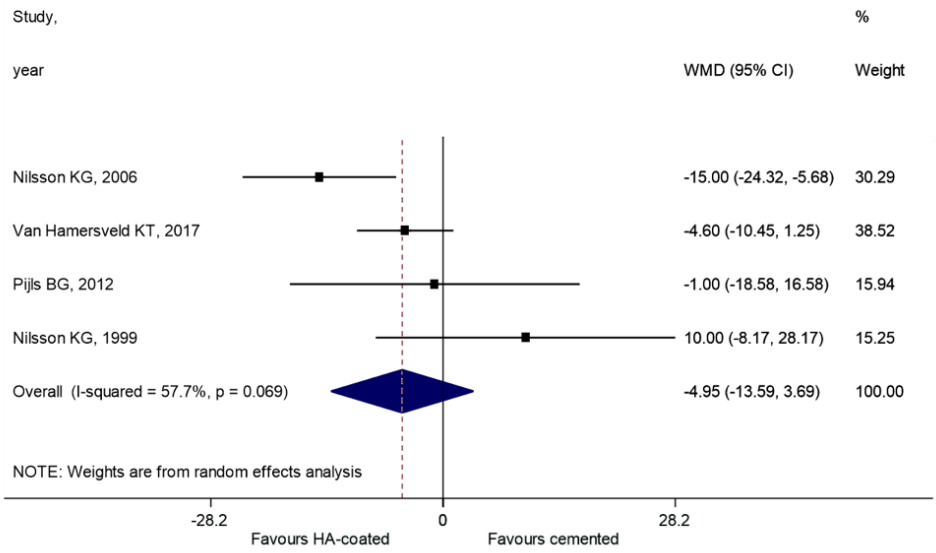

B

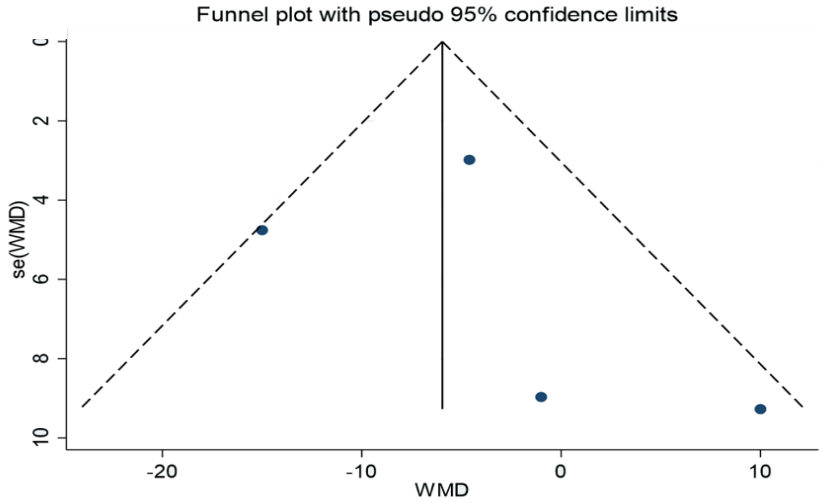

Figure 19. A KFS value of the cemented and the HA-coated cementless group. The value of cemented is not significantly different from the HA-coated cementless group. **B** Funnel plot 2 years follow-up; HA-coated cementless vs. uncemented group.

5. DISCUSSION

5.1. Different mitochondrial functions in the synovia of RA and OA patients

Our present study provides quantitative clinical data on mitochondrial derangements in RA and OA. Systemic disease activity was evaluated by CRP serum concentrations, proinflammatory cytokines in the synovial fluid samples and clinical scores (KL, ACR/EULAR) of our patients. Additionally, histopathological evaluation and in vivo histology with CLSEM were also performed on tissue samples to detect the histological characteristics of RA and OA. Our results complied with the literature as RA patients had significantly higher levels of proinflammatory cytokines and hyperactive pathways of ROS production. Additionally, histopathology revealed signs of chronic inflammation such as neoangiogenesis, increased mean lining thickness and fibrosis in both OA and RA patients; however, with a much higher extent in the latter.

The capacities of the ETC complexes in the study groups were tested with high resolution respirometry. Interestingly, C I activity was strongly diminished in the RA group, while there was no significant difference in C II activity between the groups. This result highlights the central role of C I in mitochondrial dysfunction in RA, setting it as the main target of future RA therapies. C I is the first, largest, and most complicated component of the respiratory chain. Furthermore, as the major entry point for electrons to the respiratory chain, C I is considered as the rate-limiting factor in overall respiration [107]. Additionally, it generates significant levels of ROS, especially during reverse electron transport [108,109]. As a consequence, C I has already stood in the focus of researchers investigating potential mitochondrial protective drugs. According to this, a recent study demonstrated the C I specific ROS-production inhibiting effect of OP2113 (5-(4-Methoxyphenyl)-3H-1,2-dithiole-3-thione, CAS 532-11-6) and raised its role in the therapies for Parkinson’s and Alzheimer's diseases [110]. Additional to aging-related diseases, based on our findings, we emphasize the importance of C I related ROS blockers in autoimmune diseases including RA. Compared to patients suffering from RA, members of the OA group displayed a milder, but still notable decrease in C I activity compared to healthy individuals in the control group. Again, a significant deficit in C II activity did not occur. This result complies with literature data accentuating the importance of C I in aging related diseases. Based on our findings, we suggest putting the focus on C I specific pharmaceutical agents in the research for novel therapeutic options for OA. Beyond highly effective conservative treatment options, prognostic biomarkers for disease progression and early-stage osteoarthritis are also lacking

[111]. A recent study suggested that certain mitochondrial DNA (mtDNA) haplogroups may be suitable to aid the recognition of early-stage OA and also have a prognostic potential for disease progression [112]. Further studies investigating other mitochondrial parameters such as C I activity or cytochrome c release as prognostic markers for disease progression are warranted.

5.2. Beneficial effects of EP delivery of diclofenac into the knee joint

This study has demonstrated the added value of EP to the transdermal delivery of diclofenac into the knee joint in experimental arthritis. The analgesic effect of EP-enhanced delivery was comparable to that of the oral administration and manifested in decreased nociceptive sensitivity, reduced joint swelling and lower cytokine concentration in the synovial fluid and lower inflammatory enzyme activities in the synovial tissue. The EP treatment also influenced the number of PMN–endothelial interactions at the level of the synovial microcirculation.

Following oral administration, diclofenac absorbs rapidly absorption through the gastrointestinal tract. However, due to first-pass metabolism, only 60% of the dose reaches the systemic circulation, where it bonds extensively to plasma proteins, mainly albumin [113]. Substantial concentrations of the drug are attained in synovial fluid, which may be one of the sites of action of diclofenac. It has been shown that the anti-nociceptive and anti-inflammatory action of diclofenac is directly proportional to its concentration in the synovial fluid [114]. Diclofenac has a short biological half-life (approx. 2h) and is eliminated following biotransformation to glucuroconjugated and sulfate metabolites, which are excreted in urine [115]. The pharmacological action of oral drugs depends on the absorption into the circulation and subsequent distribution to the peripheral tissues; in contrast, efficacy of topical drugs relies on penetration through the skin.

EP is promising among skin penetration enhancement techniques; apart from transdermal delivery, application of EP has been widely investigated in cell biology, biotechnology and electrochemotherapy [116-118]. EP applies high-voltage pulses to the biological membranes and results in conformation changes in their stereo structures. Transdermal drug penetration into the joint cavity is mostly limited by the low permeability of the stratum corneum of the skin, the thickness of the surrounding tissue layer and the special physico-chemical barrier function of the synovial membrane, which is commonly referred to as the “blood-joint barrier” [119]. However, EP is capable of opening transitory pores on complex structures, such as the multilamellar lipid bilayer of the stratum corneum and the synovial membrane [120,121]. Macromolecules of up to 40 kDa can thus be transported through and/or into the

skin [122,123].

Electroporation is now widely used as an alternative to small interfering RNA or naked DNA delivery for targeted suppression of therapeutic genes into the knee joint in arthritis [124,125]. However, electrotransfer of painkiller drugs into the knee joint is less widespread [126]. According to a recent review, plasma levels of diclofenac after topical administration decrease from 0.2% to 8% of those after oral administration [127]. Unfortunately, the resultant synovial concentration is also decreased, as compared to an equivalent oral dose. Effective concentrations in target tissues can be augmented with EP [127]. In accordance with literature data, our results revealed that EP causes higher concentration values in the serum as compared with the topical administration. The diclofenac concentration in the synovia was equal to the serum concentrations; however, conventional topical treatment did not result in a detectable amount of diclofenac sodium in the synovial fluid.

Intra-articular injection of C/K is a well-established model of an acute onset monoarthritis resembling osteoarthritis. In this model, arthritis is probably initiated by mechanical damage to the inner surface of the synovium resulting in an inflammatory response indirectly to the activation of the endothelial side of the synovial barrier. It is characterized by an initial non-phagocytic oedema and rapid uptake of the late phagocytic inflammatory phase, where PMNs accumulate in the affected area [128,129]. It has been demonstrated that PMNs are primed within 1 h and are in the majority up to 12 h after the arthritis induction; subsequently, they are replaced by predominating macrophages until the resolution of the inflammation at 48 h. [119]. It has also been found that the rate of PMN infiltration is directly related to severity of inflammation in the synovial membrane [78,130]. Based on the pivotal role of PMNs in the initiation and maintenance of joint disorders, we employed the PMN-derived experimental model of inflammatory arthritis in these studies.

Adhesive cell-to-cell interactions are regulated by beta2 integrins (CD11/CD18) expressed on PMN leukocytes and their associated endothelial ligands (intercelluar adhesion molecules, ICAMs and VCAMs) [131]. The presence of adhesion molecules on postcapillary endothelial cells in the inflammatory synovial microenvironment has previously been shown and proven to be appropriate markers for estimating inflammation [93,132,133]. These reactions can be quantitatively assessed by IVM, and the efficacy of various therapeutic interventions can also be judged objectively. PMN accumulation peaks very early, usually at 6–8 h in this model, and (at approx. 24 h) macrophages predominate in the exudates thereafter [134]. Like other non-selective cyclooxygenase inhibitors, diclofenac diminishes the number of PMN–endothelial interactions [135,136]. Sticking in the synovial vessels was considerably reduced

with the oral administration of diclofenac. However, it was only moderately ameliorated by the EP-enhanced diclofenac hydrogel, and there were no changes in response to the simple topical application of the hydrogel.

Administration of C/K injection into the knee joint results in primary and secondary hyperalgesia in the inflammatory monoarthritis [137]. Secondary hyperalgesia develops at the paw to heat and mechanical stimuli, and primary hyperalgesia is present over the inflamed knee joint [138,139]. Secondary hyperalgesia develops as a result of the sensitization of the dorsal horn neurons neighbouring the spinal representation of the injured tissue [140]. Secondary hyperalgesia reactions were investigated at the peak of the joint inflammation and both demonstrated a significant amelioration as a consequence of diclofenac treatment [141]. Like the oral diclofenac treatment, EP completely restored thermal nociceptive sensitivity and increased mechanical touch sensitivity, but to a lesser extent. Knee swelling, which is an objective parameter of joint inflammation, was significantly reduced with both the oral and the EP-enhanced diclofenac treatment [142]. Again, this increased volume was significantly reduced by both oral and EP-enhanced diclofenac treatments 48 h after arthritis induction.

The C/K-induced arthritis is also an appropriate model for the evaluation of the analgesic and anti-inflammatory properties of diclofenac. The TNF-α response is an early marker in carrageenan-induced inflammation, and thus the changes were measured in the synovial fluid 48 h after intra-articular C/K or saline injections. Free radical formation has been demonstrated in the synovial fluid and synovial membrane under clinical conditions and proposed as a causative factor in joint disorders [143,144]. Specifically, oxidoreductive stress has been shown to play a fundamental role in the pathogenesis of osteoarthrosis as a result of increased pressure in the synovial cavity, reduced capillary density and vascular changes, and due to the increased metabolic rate of synovial tissue in joint inflammation [145-147]. Being a source of the oxygen free radical formation located in synovial cells, XOR activity has been shown to increase in joint inflammation [78,148]. Moreover, joint inflammation was also associated with enhanced XOR activity in the synovial fluid [149]. Our present findings demonstrated increases in XOR activity in response to arthritis attenuated by diclofenac treatment applied either in oral or simple topical routes of administration the latter being more accentuated in the case of EP. PMNs are also important sources of free radicals through their NADPH oxidase 2 activities [150]. As for microcirculatory inflammatory reactions induced by inflammation, the increase in both the primary and secondary forms of PMN–endothelial interactions (rolling and firm adherence) were confined to the periosteal postcapillary venules. In this model, C/K-induced monoarthritis was the positive control. This aggressive

arthritis model, which is associated with severe tissue destruction, is also known to be mediated by infiltrating PMNs [80,93]. Data regarding the final step of PMN–endothelial interactions (i.e. sticking) were well correlated with the tissue accumulation of PMNs, as determined by MPO activity. Diclofenac treatment attenuated the MPO activity in the inflamed synovial tissue, applied either in oral or EP-enhanced topical routes of administration.

5.3. HA implants provide better fixation in TKA

This study reviews the current evidence and updates knowledge on the use of HA-coated tibial stem for primary TKA. The treatment groups were homogenous in terms of characteristics of patients, thus the prediction of primary and secondary outcomes (i.e. MTPM and KSS and KFS) was likely independent from individual risk variables, patient selection or the overall severity of osteoporosis at prosthesis implantation. Direct meta-analysis comparison was made, and the sample size of included trials was large enough to provide good evidence that HA-coating yields better stability than other, uncemented prostheses; However, cement fixation of prostheses stems still performs greater anchorage against migration. More importantly, the HA-coating is not outperformed by cemented prosthesis in providing good functional outcome with regards to pain intensity, range of motion and walking distance.

The survival probability of the stems is often cited in the literature as predictor of prosthesis outcome. However, the TKA outcomes are generally good with a mean survivorship rate (or projected rates) of 95% or more at 10 years. Hence, this parameter is less sensitive to evaluate the quality of stem fixation, than radiological results [151]. The migration analysis with RSA is a standardized and objective method with low susceptibility to different interpretations [152]. This technique allows movements between the implant and host bone measured with an accuracy of 0.2 mm [106,153]. As a primary outcome of our study, the migration pattern of the prosthesis stems was determined as the maximum total point motion (MTPM) of the tibial stem measured by RSA. The MTPM value is the unit of measurement for the largest 3D migration of any point on the prosthesis surface. The migration pattern was defined as at least 2 postoperative follow-up moments within the first 2 years of follow-up [106]. MTPM mainly depends on mechanical factors such as the bone-implant interface or different biological reactions at the implant-bone interface therefore is a reliable parameter to assess the added value of HA-coating in implant surface.

RCTs in our meta-analysis have demonstrated lower incidence of MTPM with HA–coated

implants when compared other non-cemented stems, except one trial [73]. As for the comparison of HA-coated cementless and cemented group, the overall rates of MTPM were very low in the cemented group and displayed lower incidence than HA-coated cementless prosthesis. It is contradictory with a recent meta-analysis of Voight and his coworkers, which demonstrated that use of HA provides the best long-term stability of implants; However, they failed to eliminate potential selection bias because of enrolled studies with hybrid fixation [154]. Another confounding factor was that HA-coated cementless fixation was compared to an inhomogenic group of cemented and uncoated or other-coated cementless fixations. Some other meta-analyses have demonstrated equal stability by using cemented and cementless implants [75,155,156]. Registry data support that risk of revision rate is significantly higher in uncemented TKAs in comparison with cemented prosthesis, and the main reason is aseptic loosening [157,158]. The contradictory conclusions derived from these data can be explained by the selection bias of database analysis.

Clinical outcomes, the KSS and KFS in our meta-analysis demonstrated equal functionality of HA-coated cementless and cemented implants. These scoring systems are validated and responsive methods for assessing objective and subjective outcomes after TKA. KSS is a weighted score which regards to pain intensity, range of motion, stability and flexion deformities, contractures, and poor alignment. The KFS considers mobility parameters of the patient such as the walking distance and stair climbing with deduction for walking aids. In spite of the predictive value of radiological stability, a recent meta-analysis has revealed the differences between postoperative radiological and clinical performance of TKAs at the same time [75]. Our result is consistent with this previous finding.

The final outcome of TKAs can also be linked to factors such as the prosthesis type and the risk of developing certain complications of the patient. Early generation of cementless prosthesis demonstrated poor results due to the suboptimal design of the implants [159]. In order to exclude bias derived from the different design of prosthesis types, we enrolled studies comparing HA-coated prostheses with other prostheses from the same uncemented or cemented series of the manufacturer.

This study has some limitations. Low survival probability and revision rate of the stems are often cited in the literature as predictor of poor outcome and these factors were not considered in the selected trials. Different trials presented some alterations concerning the operative procedure, whose impact on the outcomes were not evaluated. Besides, comparison of KFS in HA-coated and uncemented groups would have limited value due to the low number of studies in the uncemented group. The included RCTs were homogenous with regard to patient

parameters, which, on the one hand provided possibility to exclude selection bias, but on the other hand, the effects of medication, physiotherapy, activity level or systemic diseases (e.g. osteoporosis or osteopenia) could not be evaluated. It would be also important to compare the individual types of cementless knee prosthesis and the outcome of their implantation [160].

6. SUMMARY OF NEW FINDINGS

Our findings confirmed mitochondrial involvement in the pathomechanisms of OA and RA by providing quantitative clinical data on the derangements of mitochondrial functions in human synovium samples. We have demonstrated, for the first time, the substantial differences in the characteristics of mitochondrial dysfunctions in OA and RA. We also highlighted the decisive role of Complex I and disruption of the ETC integrity in the impairment of the inner mitochondrial membrane.

We have demonstrated improved drug delivery with EP in the conservative treatment of arthritis. We have confirmed the direct action of EP-enhanced transdermal diclofenac sodium delivery on the synovial microcirculation as proven by the decreased rolling and the reduced sticking of leukocytes. The biochemical measurements also demonstrated that diclofenac achieved an efficient tissue concentration in the synovium since inflammatory enzyme activities decreased. In summary, EP-enhanced transdermal diclofenac sodium delivery attenuated the microcirculatory deterioration and the consecutive stages of tissue inflammation; therefore, this type of mechanism might be an interesting focus for therapeutic strategies in arthritis.

Our review on implant outcomes provided evidence that HA-coated cementless prosthesis outperforms other cementless prostheses types in stability and functionality. Cemented fixation of prostheses provides the best stability in a 2-year follow up; however, functional results are not superior to HA-coated cementless fixation. Based on these results, HA-coated cementless TKA is a recommended option for treating end-stage arthritis of the knee, and clinicians consider together with patients the factors associated with the risk of revision when choosing the most appropriate procedure.

7. ACKNOWLEDGMENTS

I am grateful to Professor Endre Varga for encouraging my scientific career parallel to my clinical work at the Department of Traumatology of the University of Szeged. I am thankful to Dr. Petra Hartmann, who guided my scientific activity in the Institute of Surgical Research, helped me to acquire the basic experimental skills and granted me unlimited daily assistance in performing studies and writing publications. I am also grateful to Dr. Dávid Kurszán Jász, who guided my research work requiring high-resolution respirometry analysis. Furthermore, I would like to thank Dr. Endre Csonka and Dr. Péter Jávor the valuable advice they provided me in clinical research.

8. REFERENCES

1. Vincent, T.L., *Mechanoflammation in osteoarthritis pathogenesis.* Seminars in Arthritis and Rheumatism, **2019**. 49: p. S36-S38.
2. Silman, A.J. and J.E. Pearson, *Epidemiology and genetics of rheumatoid arthritis.* Arthritis Research & Therapy, **2002**. 4: p. S265-S272.
3. Scott, D.L., F. Wolfe, and T.W.J. Huizinga, *Rheumatoid arthritis.* Lancet, **2010**. 376(9746): p. 1094-1108.
4. Reginster JY. *The prevalence and burden of arthritis*. Rheumatology (Oxford), **2002**. 41(Suppl 1):3–6.
5. Helmick, C.G.; Felson, D.T.; Lawrence, R.C. et al. *Estimatesoftheprevalence of arthritis and other rheumatic conditions in the United States. Part I*. Arthritis Rheum, **2008**. 58(1):15–25.
6. Peterson, K.; McDonagh, M.; Thakurta, S. et al. *Drug class review: non- steroidal anti inflammatory drugs (NSAIDs). Final update 4 report*. Portland (OR): Oregon Health & Science University, **2010**.
7. Pavelka, K. *A comparison of the therapeutic efficacy of diclofenac in osteoarthritis: a systematic review of randomised controlled trials.* Curr Med Res Opin, **2012**. 28(1):163–178.
8. Hussain, S.M.; Neilly, D.W.; Baliga, S. et al. *Knee osteoarthritis: a review of management options.* Scott Med J, **2016** Feb;61(1):7-16. doi: 10.1177/0036933015619588.
9. Adam, J.M.; Jeffrey, D.S.; Langan, S.S. et al, *Results of Cemented vs Cementless Primary Total Knee Arthroplasty Using the Same Implant Design* Arthroplasty, **2018** Apr;33(4):1089-1093. doi: 10.1016/j.arth.2017.11.048.
10. Pap, K.; Vasarhelyi, G.; Gal, T. et al. *Evaluation of clinical outcomes of cemented vs uncemented knee prostheses covered with titanium plasma spray and hydroxyapatite: A minimum two years follow-up*. Eklem Hastalik Cerrahisi, **2018**. Aug;29(2):65-70. doi: 10.5606/ehc.2018.61076.
11. Ebell, M.H. *Osteoarthritis: Rapid Evidence Review*. Am Fam Physician, **2018**. Apr 15;97(8):523-526.
12. Martel-Pelletier, J.; Barr, A.J.; Cicuttini, F.M. et al. *Osteoarthritis*. Nat Rev Dis Primers**, 2016**. Oct 13;2:16072. doi: 10.1038/nrdp.2016.72.
13. Osteoarthritis. Pereira D, Ramos E, Branco J.Acta Med Port. 2015 Jan-Feb;28(1):99-106. doi: 10.20344/amp.5477.
14. Rafaelani, L.; Taruc-Uy, M.D.; , Lynch, S.A. *Diagnosis and Treatment of Osteoarthritis _RSS*. Primary Care: Clinics in Office Practice, **2013.** Volume 40, Issue 4, Pages 821-836.
15. Ten Berg, P.W.L.; Heeg, E. et al. *Narrowing in Patients With Pisotriquetral Osteoarthritis*. Joint Space Hand, **2017**. PMID: 28832198.
16. Marcucci, E.; Bartoloni, E.; Alunno, A. et al. *Extra-articular rheumatoid arthritis.* Reumatismo, **2018.** Dec 20;70(4):212-224. doi: 10.4081/reumatismo.2018.1106.
17. SZENDRŐI M. Ortopédia Semmelweis Kiadó, **2006.**
18. Porter, B.J.; Brittain, A. *Splinting and hand exercise for three common hand deformities in rheumatoid arthritis: a clinical perspective*. Curr Opin Rheumatol, **2012.** Mar;24(2):215-21. doi: 10.1097/BOR.0b013e3283503361.
19. Sharif, K.; Sharif, A.; Jumah, F. *Rheumatoid arthritis in review: Clinical, anatomical, cellular and molecular points of view.* Clin Anat, **2018.** Mar;31(2):216-223. doi: 10.1002/ca.22980.
20. Jacob, D.J.; Sartoris, S.; Kursunoglu, D. P. et al. *Distal interphalangeal joint*

involvement in rheumatoid arthritis. Arthritis Rheum, **1986**. Jan;29(1):10-5. doi: 10.1002/art.1780290102.
21. Chang, M.H.; Nigrovic, P.A. *Antibody-dependent and -independent mechanisms of inflammatory arthritis.* JCI Insight, **2019**. Mar 7;4(5):e125278. doi: 10.1172/jci.insight.125278.
22. Klareskog, L.; Rönnelid, J.; Gudmundsson, S. *Rheumatoid arthritis*. Curr Opin Immunol, **1991**. Dec;3(6):912-6. doi: 10.1016/s0952-7915(05)80013-5.
23. Sang-Tae Choi, Kwang-Hoon. *Clinical management of seronegative and seropositive rheumatoid arthritis: A comparative study*. Plus One, **2018**. doi.org/10.1371/journal.pone.0195550.
24. Emily, A.; Littlejohn, D.O.; Seetha, U.M. *Early Diagnosis and Treatment of Rheumatoid Arthritis RSS*. Primary Care: Clinics in Office Practice, **2018**. Volume 45, Issue 2, Pages 237-255.
25. Piet, L.C.M van Riel, Lisanne, R. *The Disease Activity Score (DAS) and the Disease Activity Score using 28 joint counts (DAS28) in the management of rheumatoid arthritis*. Clin Exp Rheumatol, **2016**. 34(5 Suppl 101):S40-S44.
26. Röhlich P. Szövettan- Medicina könyvkiadó **2006**.
27. Roy, A.; Ganguly, A.; BoseDasgupta, S. et al. *Mitochondria-dependent reactive oxygen species-mediated programmed cell death induced by 3,3'-diindolylmethane through inhibition of F0F1-ATP synthase in unicellular protozoan parasite Leishmania donovani*. Mol Pharmacol, **2008**. 74:1292–307. doi: 10.1124/mol.108.050161.
28. Kim, J.; Xu, M.; Xo, R, et al. *Mitochondrial DNA damage is involved in apoptosis caused by pro-inflammatory cytokines in human OA chondrocytes*. Osteoarthritis Cartilage, **2009**.18:424–432.
29. Itoh, K.; Hase, H.; Kojima, H. et al. *Central role of mitochondria and p53 in Fas-mediated apoptosis of rheumatoid synovial fibroblasts*. Rheumatology (Oxford), **2004**. Mar;43(3):277-85. PMID: 14623946.
30. Terkeltaub, R.; Johnson, K.; Murphy, A. et al. *Invited review: the mitochondrion in osteoarthritis*. Mitochondrion, **2002**. 1:301–319.
31. Samavati, L.; Lee, I.; Mathes, I. et al. *Tumor necrosis factor alpha inhibits oxidative phosphorylation through tyrosine phosphorylation at subunit I of cytochrome c oxidase*. J Biol Chem, **2008**. Jul 25;283(30):21134-44. doi: 10.1074/jbc.M801954200.
32. Halliwell, B. *Oxidative stress and neurodegeneration: where are we now*? J Neurochem, **2006**. 97(6):1634–1658.
33. Martin, J.A.; Martini, A.; Molinari, A. et al. *Mitochondrial electron transport and glycolysis are coupled in articular cartilage*. Osteoarthritis Cartilage, **2012**. Apr;20(4):323-9. doi: 10.1016/j.joca.2012.01.003.
34. Rego, I.; Fernández-Moreno, M.; Fernández-López, C. et al. *Role of European mitochondrial DNA haplogroups in the prevalence of hip osteoarthritis in Galicia Northern Spain*. Ann Rheum Dis, **2010.** 69:210–3. doi: 10.1136/ard.2008.105254.
35. Maneiro, E.; Martín, M.A.; de Andres, M.C. et al. *Mitochondrial respiratory activity is altered in osteoarthritic human articular chondrocytes*. Arthritis Rheum, **2003**. 48:700–8. doi: 10.1002/art.10837.
36. Gergalova, G.; Lykhmus, O.; Kalashnyk, O. et al. *Mitochondria express α7 nicotinic acetylcholine receptors to regulate Ca^{2+} accumulation and cytochrome c release: study on isolated mitochondria.* PLoS One, **2012**. 7:e31361. doi: 10.1371/journal.pone.0031361.
37. Kalashnyk, O.M.; Gergalova, G.L.; Komisarenko, S.V. et al. *Intracellular localization of nicotinic acetylcholine receptors in human cell lines.* Life Sci, **2012**. Nov 27;91(21-22):1033-7. doi: 10.1016/j.lfs.2012.02.005.
38. Gnaiger, E.; Méndez, G.; Hand, S.C. *High phosphorylation efficiency and depression*

of uncoupled respiration in mitochondria under hypoxia. Proc Natl Acad Sci U S A, **2000**. Sep 26;97(20):11080-5. doi: 10.1073/pnas.97.20.11080.
39. Schöttl, T.; Kappler, L. Fromme, T. et al. *Limited OXPHOS capacity in white adipocytes is a hallmark of obesity in laboratory mice irrespective of the glucose tolerance status.* M.Mol Metab, **2015**. Jul 15;4(9):631-42. doi: 10.1016/j.molmet.2015.07.001.
40. Gnaiger, E. *Bioenergetics at low oxygen: dependence of respiration and phosphorylation on oxygen and adenosine diphosphate supply*. Respir Physiol, **2001**. Nov 15;128(3):277-97. doi: 10.1016/s0034-5687(01)00307-3.
41. Phielix, E.; Szendroedi, J.; Roden, M. *Mitochondrial function and insulin resistance during aging: a mini-review.* Gerontology, **2011**.57(5):387-96. doi: 10.1159/000317691.
42. Domenis, R.; Comelli, M.; Bisetto, E. et al. *Mitochondrial bioenergetic profile and responses to metabolic inhibition in human hepatocarcinoma cell lines with distinct differentiation characteristics*. Bioenerg Biomembr, **2011**. Oct;43(5):493-505. doi: 10.1007/s10863-011-9380-5.
43. Jelenik, T.; Roden, M. *Mitochondrial plasticity in obesity and diabetes mellitus.* Antioxid Redox Signal, **2013.** Jul 20;19(3):258-68. doi: 10.1089/ars.2012.4910.
44. Furst, D.E. *Are there differences among nonsteroidal antiinflammatory drugs? Comparing acetylated salicylates, nonacetylated salicylates, and nonacetylated nonsteroidal antiinflammatory drugs.* Arthritis Rheum, **1994**. Jan;37(1):1-9. doi: 10.1002/art.1780370102.
45. Singh, G.; Ramey, D.R.; Morfeld, D.et al. *Gastrointestinal tract complications of nonsteroidal anti-inflammatory drug treatment in rheumatoid arthritis. A prospective observational cohort study.* Arch Intern Med, **1996**. Jul 22;156(14):1530-6.
46. Kavuncu, V.; Evcik, D. *Physiotherapy in Rheumatoid Arthritis.* MedGenMed, **2004**. 6(2): 3.
47. Cordery, J.C. *Joint protection; a responsibility of the occupational therapist.* Am J Occup Ther, **1965**. Sep-Oct;19(5):285-94.
48. Beasley, J.J. *Osteoarthritis and rheumatoid arthritis:conservative therapeutic management*. Hand Ther, **2012**. Apr-Jun;25(2):163-71; quiz 172. doi: 10.1016/j.jht.2011.11.001.
49. Brunner,M.; Dehghanyar, P.; Seigfried,B. et al. *Favourable dermal penetration of diclofenac after administration to the skin using a novel spray gel formulation*. Br J Clin Pharmacol, **2005**. 60(5):573–577.
50. Heyneman, C.A.; Lawless-Liday, C.; Wall, G.C. *Oral versus topical NSAIDs in rheumatic diseases: a comparison*. Drugs, **2000.** 60(3):555–574.
51. Denet, A.R.; Préat, V. *Transdermal delivery of timolol by electroporation through human skin.* J Control Release, **2003**. 88(2):253–262.
52. Tachibana, K. *Transdermal delivery of insulin to alloxan-diabetc rabbits by ultrasound exposure*. Pharm Res, **1992.** 9(7):952–954.
53. Bommannan, D.; Okuyama, H.; Stauffer, P.et al. *The use of high-frequency ultrasound to enhance transdermal drug delivery*. Pharm Res, **1992**. 9(4):559–564.
54. Prausnitz, M.R.; Bose, V.; Langer, R. et al. *Electroporation of mammalian skin: A mechanism to enhance transdermal drug delivery.* Proc Natl Acad Sci U S A, **1993**. 90(22):10504–10508.
55. Vanbever, R.; Lecouturier, N.; Préat, V.; *Transdermal delivery of metoprolol by electroporation*. Pharm Res, **1994**. 11(11):1657–1662.
56. Riviere, J.E.; Monteiro-Riviere, N.A.; Rogers, R.A. et al. *Pulsatile transder- mal delivery of LHRH using electroporation: drug delivery and skin toxicology*. J Control Release, **1995**. 36(3):229–233.
57. Mir, L.; Orlowski, S. *Mechanisms of electrochemotherapy*. Adv Drug Deliv Rev, **1999**. 35(1):107–118.

58. Heller, R.; Gilbert, R.; Jaroszeski, M.J. *Clinical applications of electro-chemotherapy*. Adv Drug Deliv Rev, **1999**. 35(1):119–129.
59. Lombry, C.; Dujardin, N.; Préat, V. *Transdermal delivery of macromol- ecules using skin electroporation*. Pharm Res, **2000**. 17(1):32–37.
60. Weaver, J.C.; Chizmadzhev, Y.A. *Theory of electroporation: a review*. Bioelectrochem Bioenerg, **1996**. 41(2):135–160.
61. Nugent, M.; Wyatt, M.C.; Frampton, C.M. et al. *Despite Improved Survivorship of Uncemented Fixation in Total Knee Arthroplasty for Osteoarthritis, Cemented Fixation Remains the Gold Standard: An Analysis of a National Joint Registry.* J Arthroplasty, **2019**. Aug;34(8):1626-1633. doi: 10.1016/j.arth.2019.03.047.
62. Verneuil, A.; *De la creation d'une fausse articulation par section ou resection partielle de l'os maxillaire inferieur, comme moyen de remedier a l'ankylose vraie ou fausse de la machoire inferieure.* Arch Gen Med, **1860**. 15(ser5):174.
63. Ferguson, W. *Excision of the knee joint: Recovery with a false joint and a useful limb.* Med Times Gaz, **1861**. 1:601.
64. Walldius, B. *Arthroplasty of the knee with an endoprosthesis.* Acta Chir Scand, **1957**. (113(6)):445–6.
65. Machintosh, D.L. *Hemiarthroplasty of the knee using a space occupying prosthesis for painful varus and valgus deformities*. J Bone Joint Surg Am, **1958**. 40:1431.
66. Gunston, F.H. *Polycentric knee arthroplasty: Prosthetic simulation of normal knee movement.* J Bone Joint Surg Br, **1971.** 53:272.
67. Kim, Y.H.; Park, J.W.; Kim, J.S. et al. *The relationship between the survival of total knee arthroplasty and postoperative coronal, sagittal and rotational alignment of knee prosthesis.* Int Orthop, **2014**. 38(2):379-85. doi: 10.1007/s00264-013-2097-9.
68. Newman, J.M.; Sodhi, N.; Khlopas, A. et al. *Cementless Total Knee Arthroplasty. A Comprehensive Review of the Literature*. Orthop, **2018**. 1; 41(5): 263–273.
69. Bauer, T.W.; Geesink, R.C.; Zimmerman, R. et al. *Hydroxyapatite-coated femoral stems. Histologi- cal analysis of components retrieved at autopsy*. J Bone Joint Surg Am, **1991**. 73(10): 1439–52.
70. Morscher, E.W. *Hydroxyapatite coating of prostheses.* J Bone Joint Surg Br, **1991.** 73(5):705-6. doi: 10.1302/0301-620X.73B5.1894652.
71. Eliaz, N.; Ritman-Hertz, O.; Aronov, D. et al. *The effect of surface treatments on the adhesion of electrochemically deposited hydroxyapatite coating to titanium and on its interaction with cells and bacteria.* J Mater Sci Mater Med, **2011**. 22(7):1741-52. doi: 10.1007/s10856-011-4355-y.
72. Carlsson, A.; Bjorkman, A.; Besjakov, J. et al. *Cemented tibial component fixation performs better than cementless fixation: a randomized radiostereometric study comparing porous-coated, hydroxyapatite- coated and cemented tibial components over 5 years*. Acta Orthop, **2005**. 76 (3): 362–9.
73. Beaupre, L.A.; al-Yamani, M.; Huckell, J.R. et al. *Hydroxyapatite-Coated Tibial Implants Compared with Cemented Tibial Fixation in Primary Total Knee Arthroplasty*. J Bone Joint Surg, **2007**. 89: 2204–11. doi.org/10.2106/JBJS.F. 01431.
74. Klutzny, M.; Singh, G.; Hameister, R. et al. *Screw Track Osteolysis in the Cementless Total Knee Replacement Design*. J Arthroplasty, **2019**. 34(5):965-973. doi: 10.1016/j.arth.2018.12.040.
75. Röhrl, S.M.; Nivbrant, B.; Ström, H. et al. *Effect of augmented cup fixation on stability, wear, and osteolysis: a 5-year follow-up of total hip arthroplasty with RSA*. J Arthroplasty, **2004**. 19(8):962–71. doi.org/10.1016/j.arth.2004.06.024.
76. Braun, H.J.; Gold, G.E. *Diagnosis of osteoarthritis: imaging*. Bone, **2012**. 51:278–288. doi: 10.1016/j.bone.2011.11.019.

77. Kohn, M.D.; Sassoon, A.A.; Fernando, N.D. *Classifications in Brief: Kellgren-Lawrence Classification of Osteoarthritis*. Clin Orthop Relat Res, **2016**. 474(8):1886-1893. doi:10.1007/s11999-016-4732-4.
78. Smith, E.; McGettrick, H.M.; Stone, M.A. et al. *Duffy antigen receptor for chemokines and CXCL5 are essential for the recruitment of neutrophils in a multicellular model of rheumatoid arthritis synovium.* Arthritis Rheum, **2008**. 58(7):1968–1973.
79. Khajuria, D.K.; Razdan, R.; Mahapatra, D.R. *Description of a new method of ovariectomy in female rats*. Rev Bras Reumatol, **2012**. 52(3):462–470.
80. Day, S.M.; Lockhart, J.C.; Ferrell, W.R. et al. *Divergent roles of nitrergic and prostanoid pathways in chronic joint inflammation.* Ann Rheum Dis, **2004**. 63(12):1564–1570.
81. Nelissen, R.G.H.H.; Valstar, E.R.; Rozing, P.M. *The effect of hydroxyapatite on the micromotion of total knee prostheses: A prospective, randomized, double-blind study*. J Bone Jt Surg, **1998**. (11): 1665–1672.
82. Liberati, A.; Altman, D.G.; Tetzlaff, J. et al. *The PRISMA statement for reporting systematic reviews and meta-analyses of studies that evaluate healthcare interventions: explanation and elaboration.* BMJ, **2009**. 339 b2700. doi.org/10.1136/bmj.b2700.
83. Valstar, E.R.; Gill, R.; Ryd, L. et al. *Guidelines for standardization of radiostereometry (RSA) of implants*. Acta Orthop, **2005**. 76(4):563–72. doi.org/10.1080/17453670510041574.
84. Beckman, J.S.; Parks, D.A.; Pearson, J.D. et al. *A sensitive fluorometric assay for measuring xanthine dehydrogenase and oxidase in tissues.* Free Radic Biol Med, **1989**. 6(6):607–615.
85. Strzepa, A.; Pritchard, K.A.; Dittel, B.N. *Myeloperoxidase: A new player in autoimmunity.*Cell Immunol, **2017** 317:1-8. doi: 10.1016/j.cellimm.2017.05.002.
86. Kuebler, W.M.; Abels, C.; Schuerer, L. et al. *Measurement of neutrophil content in brain and lung tissue by a modified myeloperoxidase assay*. Int J Microcirc Clin Exp, **1996**. 16: 89-97.
87. Strifler, G.; Mészáros, A.; Pécz, D. et al. *Examination of liver mitochondria with respirometry*. Magy Seb, **2016**. 69(4):194-198. doi: 10.1556/1046.69.2016.4.8.
88. Wu, J.P.; Walton, M.; Wang, A. et al. *The development of confocal arthroscopy as optical histology for rotator cuff tendinopathy.* J. Microscopy, **2015.** 259 (3), 1-7.
89. Komary, Z.; Tretter, L.; Adam-Vizi, V. *Membrane potential-related effect of calcium on reactive oxygen species generation in isolated brain mitochondria*. Biochim Biophys Acta, **2010**. 6-7: 922-928.
90. Garrido, C.; Galluzzi, L.; Brunet, M. et al. *Mechanisms of cytochrome c release from mitochondria*. Cell Death Differ, **2006**.13(9):1423-33. doi: 10.1038/sj.cdd.4401950.
91. Martinou, I.; Desagher, S.; Eskes, R. et al. *The release of cytochrome c from mitochondria during apoptosis of NGF-deprived sympathetic neurons is a reversible event*. J Cell Biol, **1999**.144(5):883-9. doi: 10.1083/jcb.144.5.883.
92. Hargreaves, K.; Dubner, R.; Brown, F. et al. *A new and sensitive method for measuring thermal nociception in cutaneous hyperalgesia.* Pain, **1998**. 32(1):77–88.
93. Hartmann, P.; Szabó, A.; Eros, G. et al. *Anti-inflammatory effects of phosphatidylcholine in neutrophil leukocyte-dependent acute arthritis in rats*. Eur J Pharmacol, **2009**. 622(1–3):58–64.
94. June, R. K.; Liu-Bryan, R.; Long, F. et al. *Emerging role of metabolic signaling in synovial joint remodelling and osteoarthritis.* J Orthop Res, **2016**. 34(12): 2048–2058.
95 Laende, E.K.; Astephen, W.J.L.; Mills, F. J. et al. *Equivalent 2-year stabilization of uncemented tibial component migration despite higher early migration compared with cemented fixation: an RSA study on 360 total knee arthroplasties.* Acta Orthop, **2019**. 90(2):

172–178.
96. Van Hamersveld, K.T.; Marang-Van, De, Mheen, P.J.; Nelissen, R.G.H.H. et al. *Peri-apatite coating decreases uncemented tibial component migration: long-term RSA results of a randomized controlled trial and limitations of short-term results.* Acta Orthop, **2018**. 89(4):425–430. doi.org/10. 1080/17453674.2018.
97. Van Hamersveld, K.T.; Marang-Van, De, Mheen, P.J.; Nelissen, R.G.H.H. et al. *Fixation and clinical outcome of uncemented peri-apatite-coated versus cemented total knee arthroplasty: five-year follow-up of a randomised controlled trial using radiostereometric analysis (RSA).* Bone Joint J, **2017**. 99-B (11):1467–1476. doi.org/10.1302/0301-620X.99B11.BJJ-2016-1347.R3.
98. Pijls, B.G.; Valstar, E.R.; Kaptein, B.L. et al. *The beneficial effect of hydroxyapatite lasts: a randomized radiostereometric trial comparing hydroxyapatite-coated, uncoated, and cemented tibial components for up to 16 years.* Acta Orthop, **2012.** 83(2): 135–41.
99. Hansson, U.; Ryd, L.; Toksvig-Larsen, S. *A randomised RSA study of Peri-Apatite™ HA coating of a total knee prosthesis.* The Knee, **2008**. Volume 15, Pages 211–216.
100. Nilsson, K.G.; Henricson, A.; Norgren, B. et al. *Uncemented HA-coated implant is the optimum fixation for TKA in the young patient.* Clin Orthop Relat Res, **2006**. 448: 129.
101. Carlsson, A.; Bjorkman, A.; Besjakov, J. et al. *Cemented tibial component fixation performs better than cementless fixation: a randomized radiostereometric study comparing porous-coated, hydroxyapatite-coated and cemented tibial components over 5 years*. Acta Orthop, **2005**. 76 (3): 362–9.
102. Hildebrand, D.R.; Trappmann, C.; Georg, S. et al. *Welchen Effekt hat die Hydroxylapatitbeschichtung beim zementfreien Kniegelenkersatz?* Der Orthopäde, **2003**. 32(4):323–330.
103. Regnér, L.; Carlsson, L.; Ka¨rrholm, J. et al. *Tibial Component Fixation in Porousand Hydroxyapatite-Coated Total Knee Arthroplasty A Radiostereometric Evaluation of Migration and Inducible Displacement After 5 Years.* The Journal of Arthroplasty, **2000**. Vol. 15 No. 6.
104. Toksvig-Larsen, S.; Jorn, L.P.; Ryd, L. et al. *Hydroxyapatite-enhanced tibial prosthetic fixation.* Clin Orthop Relat Res, **2000**. (370):192–200.
105. Nilsson, K.G.; Kärrholm, J.; Carlsson, L. et al. *Hydroxyapatite coating versus cemented fixation of the tibial component in total knee arthroplasty: prospective randomized comparison of hydroxyapatite-coated and cemented tibial components with 5-year follow-up using radiostereometry*. J Arthroplasty, **1999**. 14(1):9–20.
106. Ryd, L.; Albrektsson, B.E.; Carlsson, L. et al. *Roentgen stereophoto- grammetric analysis as a predictor of mechanical loosening of knee prostheses*. J Bone Joint Surg Br, **1995**. 77(3): 377–83.
107. Sharma, L.K.; Lu, J.; Bai, Y. *Mitochondrial respiratory complex I: structure, function and implication in human diseases.* Curr Med Chem, **2009**. 16(10):1266-77. doi: 10.2174/092986709787846578.
108. Lambert, A.J.; Brand, M.D. *Inhibitors of the quinone-binding site allow rapid superoxide production from mitochondrial NADH:ubiquinone oxidoreductase (complex I)* J Biol Chem, 2004;279:39414–39420.
109. Armstrong, J.S. *Mitochondrial medicine: pharmacological targeting of mitochondria in disease.* Br J Pharmacol, **2007**. 151(8):1154-65. doi: 10.1038/sj.bjp.0707288.
110. Detaille, D.; Pasdois, P.; Sémont, A. et al. *An old medicine as a new drug to prevent mitochondrial complex I from producing oxygen radicals.* PLOS ONE, **2019.** 14(5), e0216385. doi:10.1371/journal.pone.0216385.
111. Ahmed, U.; Anwar, A.; Savage, R.S. et al. *Biomarkers of early stage osteoarthritis, rheumatoid arthritis and musculoskeletal health*. Sci Rep, **2015**. 19;5:9259. doi:

10.1038/srep09259.
112. Blanco, F.J.; Valdes, A.M.; Rego-Pérez, *Mitochondrial DNA variation and the pathogenesis of osteoarthritis phenotypes.* Nat Rev Rheumatol, **2018**. 14,327–340. doi.org/10.1038/s41584-018-0001-0.
113. Todd, P.A.; Sorkin, E.M. *Diclofenac sodium. A reappraisal of its pharma- codynamic and pharmacokinetic properties, and therapeutic efficacy*. Drugs, **1988**. 35(3):244–285.
114. Vetter, G. *A comparison of naproxen and diclofenac sodium in the treatment of osteoarthritis in elderly patients*. Br J Clin Pract, **1985**. 39(7):276–281.
115. Davies, N.M.; Anderson, K.E. *Clinical pharmacokinetics of diclofenac. Therapeutic insights and pitfalls*. Clin Pharmacokinet, **1997**. 33(3): 184–213.
116. Mir, L.; Orlowski, S. *Mechanisms of electrochemotherapy*. Adv Drug Deliv Rev, **1999**. 35(1):107–118.
117. Heller, R.; Gilbert, R.; Jaroszeski, M.J. *Clinical applications of electro-chemotherapy.* Adv Drug Deliv Rev, **1999**. 35(1):119–129.
118. Weaver, J.C.; Chizmadzhev, Y.A. *Theory of electroporation: a review.* Bioelectrochem Bioenerg, **1996**. 41(2):135–160.
119. Day, R.O.; McLachlan, A.J.; Graham, G.G. et al. *Pharmacokinet- ics of nonsteroidal anti-inflammatory drugs in synovial fluid.* Clin Pharmacokinet, **1999**. 36(3):191–210.
120. Nishimura, T.; Akimoto, M.; Miyazaki, M. et al. *Developments of transdermal transport system during skin iontophoresis and electroporation*. PIERS Online, **2010**. 6(8):759–763.
121. Blagus, T.; Markelc, B.; Cemazar, M. et al. *In vivo real time monitoring system of electroporation mediated control of transdermal and topical drug delivery*. J Control Release, **2013**. 172(3):862–871.
122. Vanbever, R.; Lecouturier, N.; Préat, V. *Transdermal delivery of metoprolol by electroporation*. Pharm Res, **1994**. 11(11):1657–1662.
123. Lombry, C.; Dujardin, N.; Préat, V. *Transdermal delivery of macromol- ecules using skin electroporation*. Pharm Res, **2000**. 17(1):32–37.
124. Zhen, S.; Heyong, Y.; Xiaoming, Y. et al. *Inhibition of osteoarthritis in rats by electroporation with interleukin-1 receptor antagonist.* J Biomed Sci Eng, **2016**. 9(7):323–336.
125. Cemazar, M.; Sersa, G. *Electrotransfer of therapeutic molecules into tissues*. Curr Opin Mol Ther, **2007**. 9(6):554–562.
126. Feng, S.; Zhu, L.; Huang, Z. et al. *Controlled release of optimized elec- troporation enhances the transdermal efficiency of sinomenine hydro- chloride for treating arthritis in vitro and in clinic.* Drug Des Devel Ther, **2017**. 11:1737–1752.
127. Hagen, M.; Baker, M. *Skin penetration and tissue permeation after topical administration of diclofenac.* Curr Med Res Opin, **2017**. 33(9): 1623–1634.
128. Day, S.M.; Lockhart, J.C.; Ferrell, W.R. et al. *Divergent roles of nitrergic and prostanoid pathways in chronic joint inflammation.* Ann Rheum Dis, **2004**. 63(12):1564–1570.
129. Hansra, P.; Moran, E.L.; Fornasier, V.L. et al. *Carrageenan-induced arthritis in the rat.* Inflammation, **2000**. 24(2):141–155.
130. Cremasco, V.; Graham, D.B.; Novack, D.V. et al. *Vav/ phospholipase C γ 2-mediated control of a neutrophil-dependent murine model of rheumatoid arthritis.* Arthritis Rheum, **2008**. 58(9):2712–2722.
131. Springer, T.A. *Traffic signals for lymphocyte recirculation and leukocyte emigration: the multistep paradigm*. Cell, **1994**. 76(2):301–314.
132. Hartmann, P.; Erős, G.; Varga, R. et al. *Limb ischemia-reperfusion differentially affects the periosteal and synovial microcirculation*. J Surg Res, **2012**. 178(1):216–222.

133. Springer, T.A.; Singer, K.H.; Haynes, B.F. et al. *Immunohistologic analysis of the distribution of cell adhesion molecules within the inflammatory synovial microenvironment*. Arthritis Rheum, **1989**. 32(1):22-30. doi: 10.1002/anr.1780320105.
134. Gilroy, D.W.; Colville-Nash, P.R.; Willis, D. et al. *Inducible cyclooxygenase may have anti-inflammatory properties*. Nat Med, **1999**. 5(6):621–622.
135. Scheja, A.; Forsgren, A.; Marsal, L. et al. *Inhibition of in vivo leucocyte migration by NSAIDs.* Clin Exp Rheumatol, **1985**. 3(1): 53–58.
136. Martinez, L.L.; Oliveira, M.A.; Miguel, A.S. et al. *Enalapril interferes with the effect of diclofenac on leucocyte-endothelium interaction in hypertensive rats.* J Cardiovasc Pharmacol, **2004**. 43(2):258–265.
137. Radhakrishnan, R.; Moore, S.A.; Sluka, K.A. *Unilateral carrageenan injec- tion into muscle or joint induces chronic bilateral hyperalgesia in rats.* Pain, **2003**. 104(3):567–577.
138. Sluka, K.A.; Bailey, K.; Bogush, J. et al. *Treatment with either high or low frequency TENS reduces the secondary hyperalgesia observed after injection of kaolin and carrageenan into the knee joint*. Pain, **1998**. 77(1):97–102.
139. Skyba, D.A.; Radhakrishnan, R.; Sluka, K.A. *Characterization of a method for measuring primary hyperalgesia of deep somatic tissue.* J Pain, **2005**. 6(1):41–47.
140. Hardy, J.D.; Wolff, H.G.; Goodell, H. *Experimental evidence on the nature of cutaneous hyperalgesia.* J Clin Invest, **1950**. 29(1): 115–140.
141. Lee, T.H.; Wang, C.J.; Wu, P.C. et al. *The thermal and mechanical anti-hyperalgesic effects of pre- versus post-intrathecal treatment with lamotrigine in a rat model of inflammatory pain*. Life Sci, **2002.** 70(25):3039–3047.
142. Szabo, P.M.; Kekesi, G.; Nagy, E. et al. *Quantitative characterization of a repeated acute joint inflamma- tion model in rats*. Clin Exp Pharmacol Physiol, **2007**. 34(5–6): 520–526.
143. Beckman, J.S.; Parks, D.A.; Pearson, J.D. et al. *A sensitive fluorometric assay for measuring xanthine dehydrogenase and oxidase in tissues*. Free Radic Biol Med, **1989**. 6(6):607–615.
144. Kennett, E.C.; Davies, M.J. *Glycosaminoglycans are fragmented by hydroxyl, carbonate, and nitrogen dioxide radicals in a site-selective manner: implications for peroxynitrite-mediated damage at sites of inflammation.* Free Radic Biol Med, **2009**. 47(4):389–400.
145. Blake, D.R.; Winyard, P.G.; Marok, R. *The contribution of hypoxia- reperfusion injury to inflammatory synovitis: the influence of reactive oxygen intermediates on the transcriptional control of inflammation.* Ann N Y Acad Sci, **1994**. 723:308–317.
146. Mapp, P.I.; Grootveld, M.C.; Blake, D.R. *Hypoxia, oxidative stress and rheumatoid arthritis*. Br Med Bull, **1995**. 51(2):419–436.
147. Tak, P.P.; Bresnihan, B. *The pathogenesis and prevention of joint dam- age in rheumatoid arthritis: advances from synovial biopsy and tissue analysis.* Arthritis Rheum, **2000.** 43(12):2619–2633.
148. Saricaoglu, F.; Dal, D.; Salman, A.E. et al. *Ketamine sedation during spinal anesthesia for arthroscopic knee sur- gery reduced the ischemia-reperfusion injury markers.* Anesth Analg, **2005**. 101(3):904–909.
149. Hanachi, N.; Charef, N.; Baghiani, A. et al. *Comparison of xanthine oxidase levels in synovial fluid from patients with rheumatoid arthritis and other joint inflammations.* Saudi Med J, **2009**. 30(11):1422–1425.
150. Bedard, K.; Krause, K.H. *The NOX family of ROS-generating NADPH oxidases: physiology and pathophysiology.* Physiol Rev, **2007**. 87(1): 245–313.
151. Higgins, J.P.; Altman, D.G.; Gøtzsche, P.C. et al. *Cochrane Bias Methods Group; Cochrane Statistical Methods Group. The Cochrane Collaboration's tool for assessing risk*

of bias in randomised trials. BMJ, **2011**. 343:d5928. doi.org/10.1136/bmj.d5928.
152. Liberati, A.; Altman, D.G.; Tetzlaff, J. et al. *The PRISMA statement for reporting systematic reviews and meta-analyses of studies that evaluate healthcare interventions: explanation and elaboration.* BMJ, **2009**. 339 b2700. doi.org/10.1136/bmj.b2700.
153. NICE Technology appraisal guidance [TA304]: Total hip replacement and resurfacing arthroplasty for end-stage arthritis of the hip. **2014**.
154. Wang, H.; Lou, H.; Zhang, H. et al. *Similar survival between uncemented and cemented fixation prostheses in total knee arthroplasty: a meta-analysis and systematic comparative analysis using registers.* Knee Surg Sports Traumatol Arthrosc, **2014**. 22(12): 3191–7. doi.org/10.1007/s00167- 013-2806-3.
155. Zhou, K.; Yu, H.; Li, J. et al. *No difference in implant survivorship and clinical outcomes between full-cementless and full-cemented fixation in primary total knee arthroplasty: A systematic review and meta-analysis*. Int J Surg, **2018**. 53: 312–319. doi.org/10.1016/j.ijsu.2018.04.015.
156. Voigt, J.D.; Mosier, M. *Hydroxyapatite (HA) coating appears to be of benefit for implant durability of tibial components in primary total knee arthroplasty*. Acta Orthop, **2011**. 82(4): 448–459. doi.org/10. 3109/17453674.2011.590762.
157. Gandhi, R.; Tsvetkov, D.; Davey, J. R. et al. *Survival and clinical function of cemented and unce- mented prostheses in total knee replacement: a meta-analysis*. J Bone Joint Surg Br, **2009**. 91(7): 889–95. doi.org/10.1302/0301-620X.91B7.21702.
158. Australian Orthopaedic Association National Joint Replacement Registry (AOANJRR) Annual report **2018**. *Available: https://aoanjrr.sahmri.com*.
159. Ryd, L. *Micromotion in knee arthroplasty*. Acta Orthop,**1986**. 57 (S220): 3–80.
160. Selvik, G. *Roentgen stereophotogrammetry. A method for the study of the kinematics of the skeletal system*. Acta Orthop Scand Suppl, **1989**. 232: 1–51.

9. ANNEX

Drug Design, Development and Therapy

Dovepress
open access to scientific and medical research

Open Access Full Text Article

ORIGINAL RESEARCH

Electroporation-enhanced transdermal diclofenac sodium delivery into the knee joint in a rat model of acute arthritis

This article was published in the following Dove Press journal:
Drug Design, Development and Therapy

Petra Hartmann[1]
Edina Butt[2]
Ágnes Fehér[1]
Ágnes Lilla Szilágyi[1]
Kurszán Dávid Jász[1]
Boglárka Balázs[3]
Mónika Bakonyi[3]
Szilvia Berkó[3]
Gábor Erős[4]
Mihály Boros[1]
Gyöngyi Horváth[5]
Endre Varga[2]
Erzsébet Csányi[3]

[1]Institute of Surgical Research, University of Szeged, Szeged, Hungary; [2]Department of Traumatology, University of Szeged, Szeged, Hungary; [3]Department of Pharmaceutical Technology, University of Szeged, Szeged, Hungary; [4]Department of Pathology, University of Szeged, Szeged, Hungary; [5]Department of Physiology, University of Szeged, Szeged, Hungary

Purpose: Since electroporation (EP) can increase the permeability of biological membranes, we hypothesized that it offers an opportunity to enhance the transdermal delivery of drugs for intra-articular indications. Our aim was to compare the anti-inflammatory and analgesic efficacy of EP-combined topical administration of diclofenac sodium hydrogel (50 mg mL^{-1} in 230 µL volume) with that of an equivalent dose of oral (75 mg kg^{-1}) and simple topical administration.
Methods: Arthritis was induced with the injection of 2% λ-carrageenan and 4% kaolin into the right knee joints of male Sprague Dawley rats. EP was applied for 8 min with 900 V high-voltage pulses for 5 ms followed by a 20 ms break. Drug penetration into the synovial fluid and plasma was detected by high-performance liquid chromatography. Leukocyte–endothelial interactions were visualized by intravital videomicroscopy on the internal surface of the synovium. Inflammation-induced thermal and mechanical hyperalgesia reactions, knee joint edema, and inflammatory enzyme activities were assessed at 24 and 48 h after arthritis induction.
Results: EP significantly increased the plasma level of diclofenac as compared with the topical controls 10 min after the 2% λ-carrageenan and 4% kaolin injection. Increased leukocyte–endothelial interactions were accompanied by joint inflammation, which was significantly reduced by oral and EP diclofenac (by 45% and by 30%, respectively) and only slightly ameliorated by simple topical diclofenac treatment (by 18%). The arthritis-related secondary hyperalgesic reactions were significantly ameliorated by oral and EP-enhanced topical diclofenac treatments. The knee cross-section area (which increased by 35%) was also reduced with both approaches. However, simple topical application did not influence the development of joint edema and secondary hyperalgesia.
Conclusion: The study provides evidence for the first time of the potent anti-inflammatory and analgesic effects of EP-enhanced topical diclofenac during arthritis. The therapeutic benefit provided by EP is comparable with that of oral diclofenac; EP is a useful alternative to conventional routes of administration.

Keywords: diclofenac, transdermal delivery, HPLC, intravital videomicroscopy

Introduction

Arthritis is a collective term encompassing many diseases with distinct etiologies but common symptoms, such as joint pain and inflammation. Owing to its high incidence, it is of significant public health and economic importance, yet therapeutic options are limited to pain relief and reduction of inflammation.[1,2] Today, the "gold standard" therapy for alleviating arthritis-related pain is diclofenac, a nonsteroidal anti-inflammatory drug (NSAID) of the phenylacetic acid class.[3,4]

Unfortunately, the side effects of such an effective compound are also significant. Diclofenac usages are associated with the NSAID category risk of dose-related

Correspondence: Petra Hartmann
Institute of Surgical Research, University of Szeged, Szőkefalvi-Nagy B. u. 6, H-6720 Szeged, Hungary
Tel +36 62 545 103
Fax +36 62 545 743
Email hartmann.petra@med.u-szeged.hu

submit your manuscript | www.dovepress.com
Dovepress
http://dx.doi.org/10.2147/DDDT.S161703

gastrointestinal, cardiovascular, and renal adverse effects; topical preparations were thus developed to limit the potentially serious complications of systemic treatments. Diclofenac is a lipophilic organic acid, but formulations with salts are water-soluble, and this property renders the compound capable of penetrating the skin and the synovial lining of diarthrodial joints. The systemic absorption of topically administered diclofenac is 3%–5% of that of oral products, and the dosage reaches the site of action ten times later as compared with that of an equivalent oral dose.[5,6] On the whole, since passive transdermal passage after topical administrations is rather slow and therapeutic drug levels cannot always be reached, new delivery methods are needed to achieve locally effective drug concentrations directly at the application site.[7]

Various skin penetration techniques have been developed to improve transdermal drug delivery and bioavailability, including ultrasound and electroporation (EP).[8–14] With EP, applications of short, high-voltage pulses cause transitory structural perturbations in the lipid bilayer of the membranes. Lipophilic or hydrophilic molecules, neutral or highly charged compounds, can thus be transported through or into membranes of bacteria or mammalian cells, if they are up to 40 kDa in molecular weight.[15] Common fields of indication for EP are biological and artificial membranes, but complex structures such as the stratum corneum or the synovium can also be targeted.[16,17]

Based on this background, we hypothesized that EP can amplify the transport of topical diclofenac into the joints, and thus the effectiveness of local administration increases. The aims were to compare the penetration properties of diclofenac hydrogel into the synovial fluid after different administration routes and to estimate the analgesic and anti-inflammatory reactions after oral and topical drug deliveries in a standardized rat model of carrageenan/kaolin (C/K)-induced knee joint monoarthritis.

Materials and methods

The experiments were performed on male Sprague Dawley rats (average weight 300±50 g). The animals were housed in plastic cages in a thermoneutral environment and provided standard laboratory chow and water ad libitum. The experimental protocol complied with EU Directive 2010/63 for the Protection of Animals Used for Scientific Purposes and was approved by Hungary's National Scientific Ethical Committee on Animal Experimentation (National Competent Authority) under license number V./148/2013. This study also satisfied the criteria in the US National Institutes of Health Guidelines for the Care and Use of Laboratory Animals.

Arthritis induction

For arthritis induction, the animals were anesthetized with intraperitoneal (IP) ketamine (50 mg kg^{-1}) and xylazine (12 mg kg^{-1}), and the skin over the knees was disinfected with povidone iodide. Then a single intra-articular injection of a 75 µL mixture of 2% λ-carrageenan (Sigma-Aldrich, St Louis, MO, USA) and 4% kaolin in saline was administered to the right knee joint.[18,19] The contralateral knee was injected with saline.

Experimental protocols

The goal of the first experimental series was to assess the serum and the synovial concentrations of diclofenac by high-performance liquid chromatography (HPLC). The animals were anesthetized with IP sodium pentobarbital (45 mg kg^{-1}) and placed in a supine position on a heating pad to maintain body temperature between 36°C and 37°C. In the first group (n=16), diclofenac sodium gel (50 mg mL^{-1} in 230 µL volume) was applied topically above the knee joint. In the second group (n=16), after dispersion of the diclofenac gel over the knee joint, EP was applied for 8 min. Samples of blood from the inferior vena cava and of synovial washing fluid from the knee joint were collected at 10, 30, 60, and 120 min of the experiment. The samples were frozen at –80°C until the HPLC measurement. At the end of the last sampling point, the animals were sacrificed with a single overdose of anesthetic (Figure 1).

In the second series of experiments, inflammation-related changes to the synovial microcirculation were evaluated directly by intravital videomicroscopy (IVM). The animals were anesthetized with IP sodium pentobarbital (45 mg kg^{-1}) and divided into four groups according to the administration route of diclofenac: The animals were treated with per os diclofenac (75 mg kg^{-1} diclofenac sodium, Novartis Hungaria Kft., Budapest, Hungary) in Group 1 (n=6), with topical diclofenac gel (50 mg mL^{-1} in 230 µL volume; n=6) in Group 2, and with EP-combined topical diclofenac gel (50 mg mL^{-1} in 230 µL volume; n=6) in Group 3. Group 4 served as a per os saline-treated control (n=6). The treatments were always applied 2 h before (t= –2 h) and 2 h after (t=2 h) the arthritis induction (Figure 1).

In the third experimental series, the effectiveness of different routes of diclofenac treatment on nociception and inflammatory edema formation was compared in C/K-induced arthritis. The animals were divided into four groups (n=6) according to the administration route of diclofenac: 1) per os diclofenac sodium, 2) topical diclofenac gel, 3) EP-enhanced topical diclofenac gel, and 4) sham

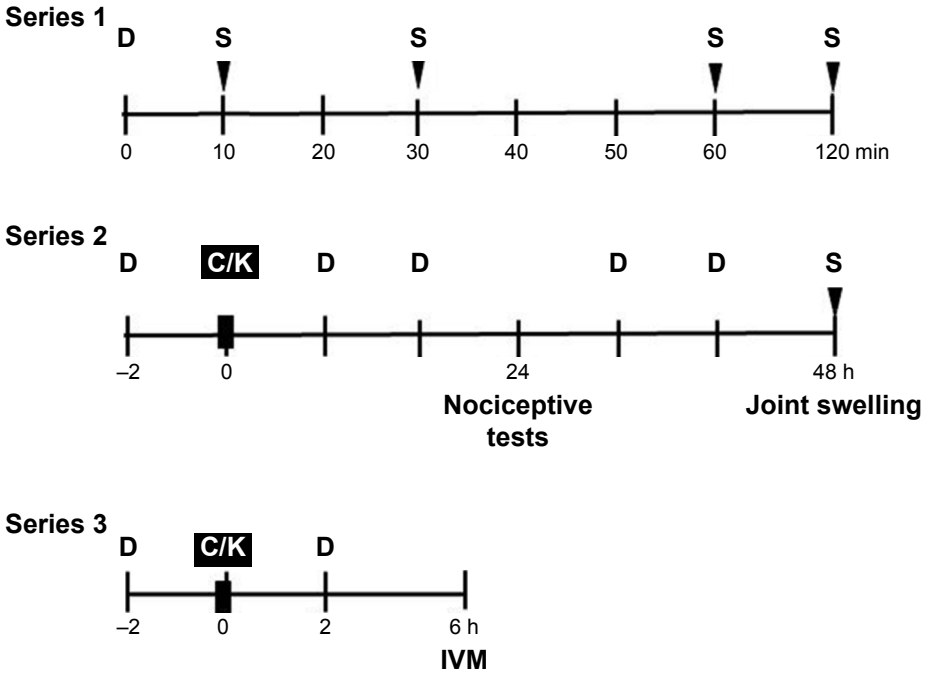

Figure 1 Time sequence of interventions.
Notes: In the first series, the diclofenac concentration in the serum and the synovial washing fluid was measured by HPLC. In the second experimental series, tests for secondary mechanical touch sensitivity and heat-provoked paw withdrawal were performed 24 h after arthritis induction with C/K and for knee joint swelling measurements 48 h after the challenge. In the third series, IVM examinations of the synovial membrane were performed 6 h after the challenge.
Abbreviations: C/K, carrageenan/kaolin; D, diclofenac treatment; HPLC, high-performance liquid chromatography; IVM, intravital videomicroscopy; S, sample taken.

(per os saline-treated). Treatments were applied twice daily (every 12 h). The nociceptive tests were performed 24 h after the C/K injection, while knee joint swelling was evaluated at the peak of edema formation 48 h after arthritis induction. At the end of the experiments, the animals were anesthetized with IP sodium pentobarbital (45 mg kg^{-1}) for sample taking and thereafter sacrificed with a single overdose of anesthetic. Synovial washing fluid samples and synovium tissue specimens were collected for biochemical measurements and histology. Tissue biopsies were stored at –20°C until the examinations (Figure 1).

Diclofenac-containing hydrogel formulation

The hydrogel was prepared using the following procedure. Five w/w% diclofenac sodium (Sigma-Aldrich) was dissolved in a mixture of purified water and 30 w/w% ethanol (Sigma-Aldrich). Two w/w% hydroxypropyl methylcellulose (METHOCEL E4M Premium, Dow Chemical, Midland, MI, USA) was added to this solution. The pH value was adjusted to 8.0±0.1 to ensure the dissolution of the active substance by adding triethanolamine (2 w/w% solution, Hungaropharma Ltd., Budapest, Hungary) if necessary (Supplementary materials).

Electroporation protocols

The noninvasive skin EP treatment was performed with a Mezoforte Duo Mez 120905-D instrument (Dr Derm Equipment Ltd., Budapest, Hungary). A polypropylene-covered treating handpiece with a 25 mm diameter plate electrode was used (modulation with 900 V pulses, a 5 ms voltage pulse was followed by a 20 ms break). Two hundred thirty µL diclofenac hydrogel was used, and the EP treatment time was 8 min.

HPLC measurements

The synovial washing fluid and plasma samples were analyzed using an Agilent HPLC system (Agilent Technologies, Palo Alto, CA, USA) equipped with an automated solvent delivery system, which has an integrated degasser (1260 Infinity Quaternary Pump, Agilent Technologies), an Agilent 1260 Infinity autosampler (Agilent Technologies) and a 1024-element diode array detector (1260 Infinity Diode Array Detector, Agilent Technologies). The system control and data acquisition were performed with Agilent ChemStation B.04.03 software (Agilent Technologies). The chromatographic parameters and the sample extraction procedure have been provided in the Supplementary materials.

Nociceptive tests

Mechanical hyperalgesia was quantified using a plantar aesthesiometer (Dynamic Plantar Aesthesiometer mod-37450; UgoBasile, Comerio, Italy) and was expressed as paw withdrawal thresholds. Thermal hyperalgesia was detected with the paw withdrawal test using a Hargreaves apparatus.[20] Baseline measurements were performed before the induction of arthritis, while the development of inflammation was investigated at the peak of nociceptive sensitivity 24 h after C/K injection.

Knee joint swelling (morphological assessment)

Joint inflammation was characterized by the changes in the diameter of the joints 48 h after C/K injection. The anteroposterior and mediolateral diameters were measured with a caliper square, and the cross-sectional area was calculated.

Analysis of gastric effects

Gastric lesions potentially associated with diclofenac toxicity were assessed at 48 h. After retrieving and washing with saline, photographs were taken of the freshly prepared stomachs. The location (near the pylorus, lesser curvature of the fundus, or diffuse) was recorded, and the extent of the lesions was evaluated by planimetric analysis using the ImageJ software (National Institutes of Health, Bethesda, MD, USA).

Synovial sampling

The skin over the knee was disinfected with povidone iodide, and 75 µL PBS was injected into the knee to collect synovial fluid. The fluid was centrifuged at 4°C for 5 min at 4,000 *g* in Eppendorf tubes. Then the samples were frozen at −80°C until they could be tested.

TNF-α levels

The cytokine content of the synovial washing fluid was measured with commercially available enzyme-linked immunosorbent assay kits (Quantikine Ultrasensitive ELISA kit; Biomedica Hungaria Ltd., Budapest, Hungary).

MPO activity

Tissue MPO activity was measured in synovium and periosteum biopsies using the method developed by Kuebler et al.[21] Briefly, the tissue was homogenized with Tris-HCl buffer (0.1 M, pH 7.4) containing 0.1 M polymethylsulfonyl fluoride to block tissue proteases and then centrifuged at 4°C for 20 min at 24,000 *g*. The MPO activities of the samples were measured at 450 nm (UV-1601 spectrophotometer; Shimadzu, Kyoto, Japan), and the data were corrected for the protein content.

XOR activity

Tissue biopsies were homogenized in a phosphate buffer (pH 7.4) containing 50 mM Tris-HCl, 0.1 mM EDTA, 0.5 mM dithiotreitol, 1 mM phenylmethylsulfonyl fluoride, 10 µg mL^{-1} soybean trypsin inhibitor, and 10 µg mL^{-1} leupeptin. The homogenate was centrifuged at 4°C for 20 min at 24,000 *g*, and the supernatant was loaded into centrifugal concentrator tubes. The activity of XOR was determined in the ultrafiltered supernatant by fluorometric kinetic assay based on the conversion of pterine to isoxanthopterine in the presence (total XOR) or absence (XOR activity) of the electron acceptor methylene blue.[22]

Surgical procedure for the IVM examinations

A detailed description of the surgical procedure can be found elsewhere. In brief, the animals were anesthetized with IP sodium pentobarbital (45 mg kg^{-1}) 6 h after the intra-articular C/K injection.[23] The jugular vein was cannulated for further supplementary doses of anesthetic. Cannulation of the trachea maintained the patent airway, and the arterial pressure was monitored through a carotid artery cannule (Statham P23Db transducer; Experimetria Ltd., Budapest, Hungary). The animals were placed on a specially designed heating pad in a supine position for the IVM examination, during which the slightly flexed knee joint of the hind limb was opened with a microsurgical technique. Surgical preparation included a longitudinal skin incision and a transverse cut of the quadriceps femoris tendon. After a circumferential cut on the joint capsule, the patella was turned aside, and the synovial membrane on the medial condyle of the tibia was visible.

IVM examinations

Synovial microcirculation was investigated by means of fluorescent IVM (Zeiss Axiotech Vario 100 HD microscope, 100 W HBO mercury lamp, Acroplan 20× water immersion objective), while the synovial membrane was superfused with 37°C saline. Erythrocytes were labeled with fluorescent isothiocyanate (0.2 mL intravenously, Sigma-Aldrich Chemicals) and leukocytes were stained with rhodamine-6G (0.1 mL intravenously, Sigma-Aldrich).

Video analysis

IVM records were analyzed offline and frame-to-frame using image analysis software (IVM, Pictron Ltd., Budapest,

Hungary). Polymorphonuclear leukocytes (PMNs) were defined as cells adherent (stickers) to the endothelial lining within an observation period of 30 s. The number of adherent cells per mm^2 of endothelial surface was counted in 5 postcapillary venules (diameter ranges from 11 to 15 μm) per animal.

Statistical analysis

Data analysis was performed with the SPSS 17.0 software (SPSS Inc., Chicago, IL, USA). Changes in variables within and between groups were analyzed by two-way analysis of variance, followed by the Holm–Sidak test. All data are expressed as means ± standard deviation of the mean. *P*-values <0.05 were considered statistically significant.

Results

Plasma and synovial diclofenac concentrations

The plasma and the serum concentrations of diclofenac were the highest 10 min after the EP treatment; they then decreased at 30 min and remained constant at 60 and 120 min. EP-enhanced diclofenac delivery exhibited a significantly higher plasma level of diclofenac as compared with the simple topical application 10 min after the application (Figure 2). There were no significant differences in the diclofenac content of the synovial fluid and the plasma after the EP-combined application. However, simple topical application did not result in detectable diclofenac content in the synovial fluid at the same point in time (Figure 2).

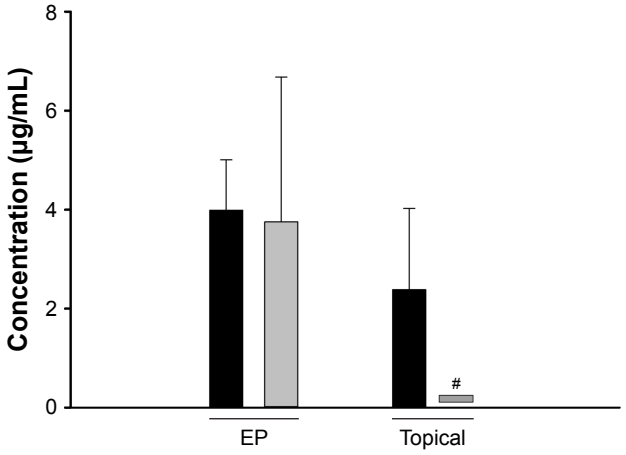

Figure 2 Diclofenac concentrations in the serum (black columns) and the synovial washing fluid (gray columns) measured by HPLC (Series 1).
Notes: Diclofenac sodium gel was applied topically above the knee joint (topical), or EP was applied for 8 min over the knee joint (EP) after the diclofenac gel dispersed. Samples of blood and synovial washing fluid were collected 10 min after application. Data are presented as means ± SD. #$p<0.05$ vs serum level (two-way ANOVA and Holm–Sidak test).
Abbreviations: ANOVA, analysis of variance; EP, electroporation; HPLC, high-performance liquid chromatography; SD, standard deviation of the mean.

Leukocyte–endothelial interactions

In the second experimental series, the microcirculatory consequences of the joint inflammation were quantified via IVM, and the PMN–endothelial interactions (rolling and sticking) in the postcapillary venules of the synovial membrane were determined. The rolling fraction of the PMNs in the postcapillary synovial venules exhibited a large degree of dispersion, and no baseline differences were observed between the C/K- and saline-injected knees or between the groups which participated in the treatment protocols (data not shown). However, the injection of C/K was accompanied by a statistically significant increase in PMN adherence (sticking) to the endothelial layer as compared to the control side (Figure 3). This reaction was considerably reduced with the administration of oral diclofenac. However, it was only moderately ameliorated by the EP-enhanced diclofenac hydrogel, and there were no changes in response to the simple topical application of the hydrogel.

Inflammatory enzyme activities and cytokine production

XOR activity was significantly increased in response to arthritis induction, in comparison with the saline-injected knee joint. These values were significantly decreased when diclofenac was applied orally or topically (Figure 4A).

In the C/K-injected limbs, the MPO activity of the synovial tissue was significantly increased as compared with that of the saline-injected controls. In the oral diclofenac and EP-enhanced topical diclofenac-treated groups, MPO activity was significantly lower than in the nontreated animals. However, conventional topical treatment did not influence the increased MPO activity (Figure 4B).

The C/K injection resulted in a significant increase in TNF-α concentration in the synovial lavage fluid, which was diminished by both the oral intake and EP-enhanced topical treatment (Figure 4C).

Nociception and inflammatory edema

In the third series, the extent of inflammation was estimated with functional tests 24 h after arthritis induction. The mechanical touch sensitivity was considerably increased in response to arthritis as the C/K-injected limbs responded to a lower level of trigger than the saline-injected control limbs in animals receiving the saline vehicle (Figure 5A). This parameter was significantly diminished in response to oral and EP-enhanced topical diclofenac treatments, albeit that complete restoration was not achieved. The thermal nociceptive latency (Figure 5B) was also significantly decreased

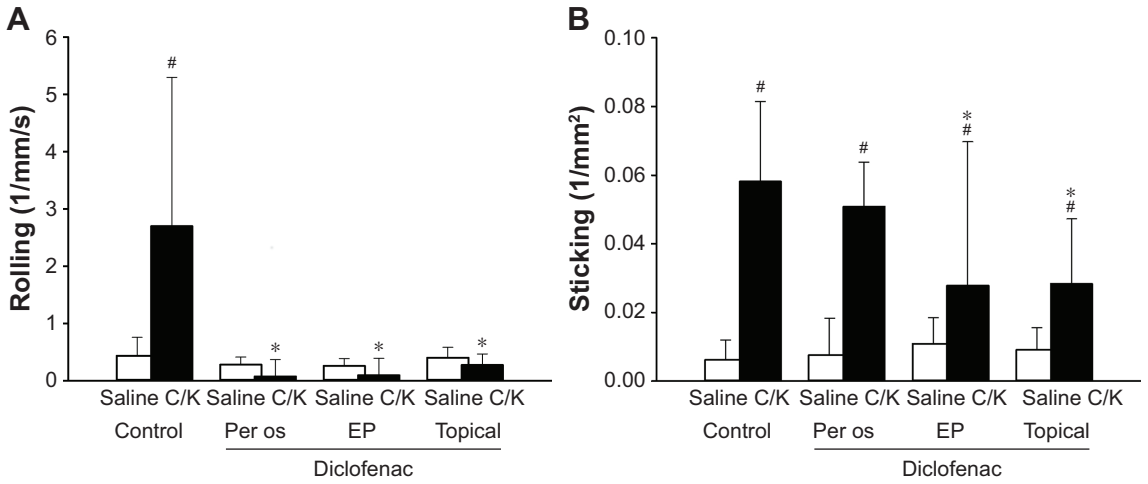

Figure 3 The effects of diclofenac treatments on the number of rolling (**A**) and sticking (**B**) leukocytes in the postcapillary venules of the synovial membrane (Series 3).
Notes: Knees were injected with C/K (black columns), or contralateral knees were treated with a saline vehicle (white columns). Data are presented as means ± SD. #$p<0.05$ vs control limb; *$p<0.05$ vs C/K + oral saline (two-way ANOVA and Holm–Sidak test).
Abbreviations: ANOVA, analysis of variance; C/K, carrageenan/kaolin; SD, standard deviation of the mean.

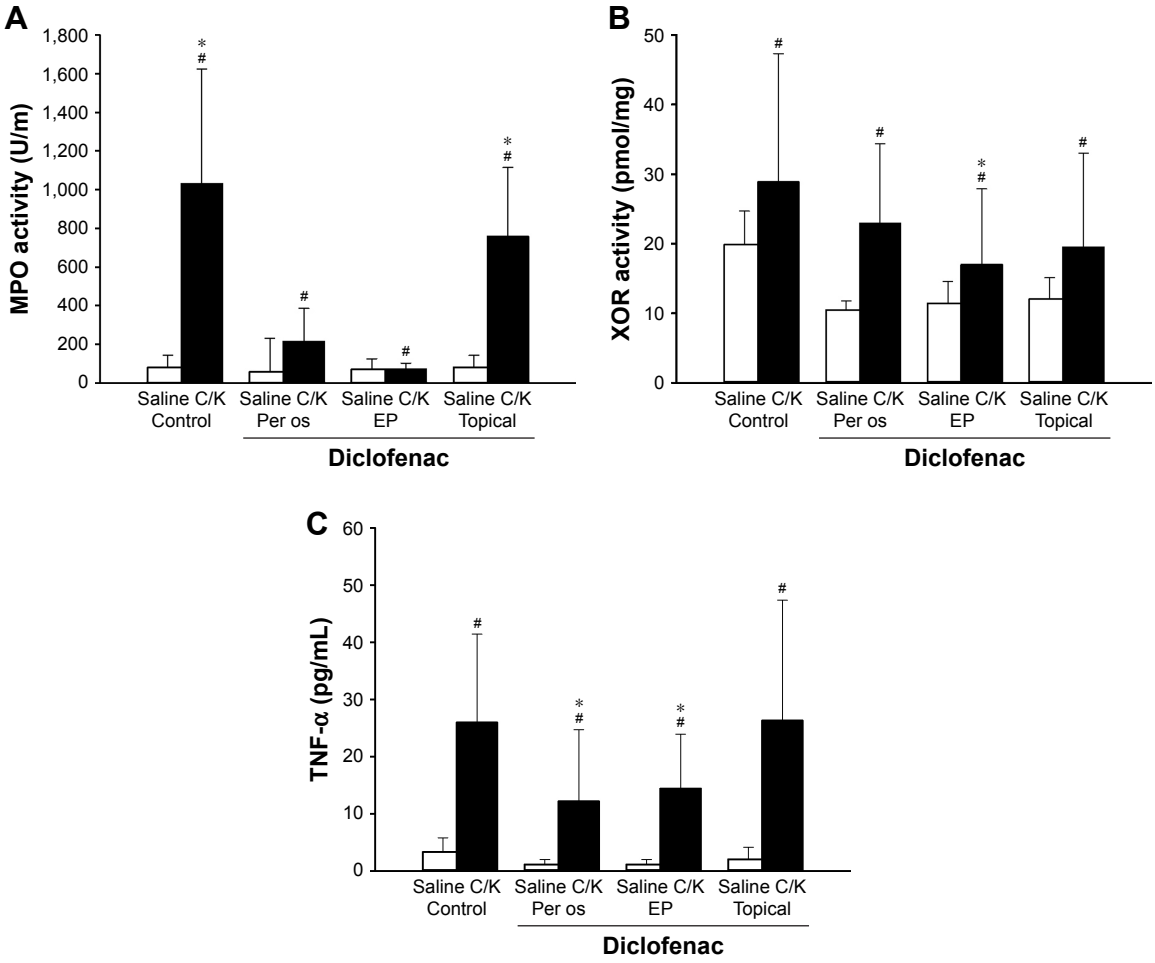

Figure 4 The effects of diclofenac treatments on the C/K-induced changes in MPO activity (**A**), XOR activity (**B**), and TNF-α levels (**C**) (Series 2).
Notes: Knees were injected with C/K (black columns), or contralateral knees were treated with a saline vehicle (white columns). Data are presented as means ± SD. #$p<0.05$ vs control limb; *$p<0.05$ vs C/K + oral saline (two-way ANOVA and Holm–Sidak test).
Abbreviations: ANOVA, analysis of variance; C/K, carrageenan/kaolin; SD, standard deviation of the mean.

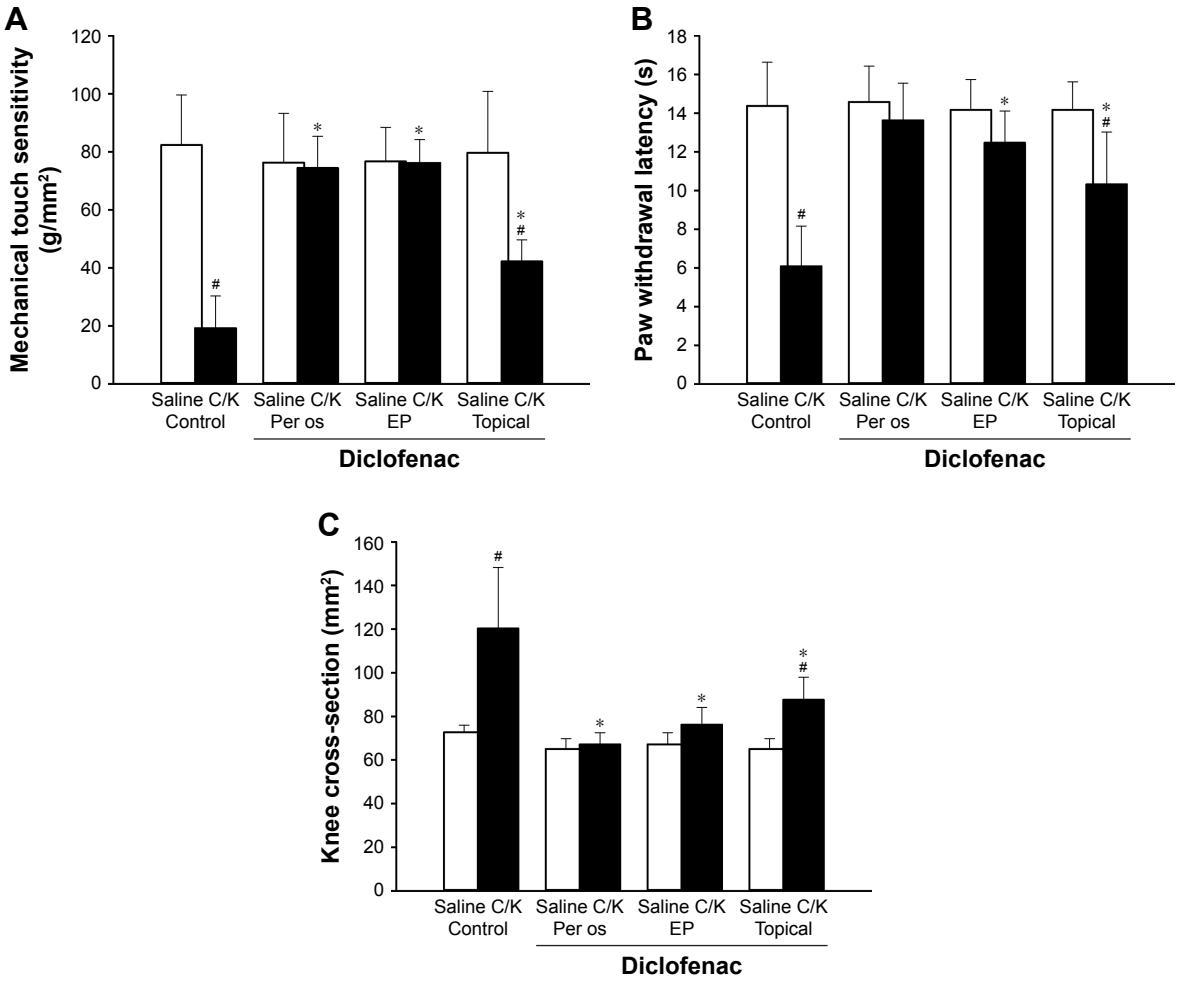

Figure 5 The effects of diclofenac treatments on the C/K-induced changes in mechanical touch sensitivity (**A**), heat-provoked paw withdrawal latency (**B**), and changes in knee joint swelling (**C**) (expressed as a knee cross-section) (Series 2).

Notes: Knees were injected with C/K (black columns), or contralateral knees were treated with a saline vehicle (white columns). Data are presented as means ± SD. $^{\#}p<0.05$ vs control limb; $^{*}p<0.05$ vs C/K + oral saline (two-way ANOVA and Holm–Sidak test).

Abbreviations: ANOVA, analysis of variance; C/K, carrageenan/kaolin; SD, standard deviation of the mean.

in the injured leg in the saline-treated group, and oral and EP-enhanced topical diclofenac treatments exerted similar protective effects to those seen with the von Frey test.

The changes in knee cross-section (Figure 5C) furnish a direct and objective measure of joint inflammation. The cross-sectional area in the C/K-injected knees was significantly enlarged 48 h after the challenge but was significantly reduced by both the conventional topical and the EP-enhanced topical diclofenac treatments. In the case of oral diclofenac administration, complete restoration to the level for the saline-injected knees was achieved.

Adverse effects of diclofenac intake

The gastric adverse effects of diclofenac intake were assessed by planimetric analysis of ulcers in the gastric mucosa. The topically applied diclofenac sodium with or without EP had no deleterious effect on gastric mucosa; however, an equivalent dose of oral diclofenac sodium resulted in ulcer formation in 70% of the animals. The location of gastric ulcerations in the rat stomach was variable and included only mild lesions with edema, irritation, and petechia formation (Supplementary materials; Figure S1).

Discussion

This study has demonstrated the added value of EP to the transdermal delivery of diclofenac into the knee joint in experimental arthritis. The analgesic effect of EP-enhanced delivery was comparable to that of the oral administration and manifested in decreased nociceptive sensitivity, reduced joint swelling, and lower cytokine concentration in the synovial fluid and lower inflammatory enzyme activities in the synovial tissue. The EP treatment also influenced the number

of PMN–endothelial interactions at the level of the synovial microcirculation.

Following oral administration, diclofenac absorbs rapidly through the gastrointestinal tract. However, due to first-pass metabolism, only 60% of the dose reaches the systemic circulation, where it bonds extensively to plasma proteins, mainly albumin.[24] Substantial concentration of the drug is attained in synovial fluid, which may be one of the sites of action of diclofenac. It has been shown that the antinociceptive and anti-inflammatory action of diclofenac is directly proportional to its concentration in the synovial fluid.[25] Diclofenac has a short biological half-life (approx 2 h) and is eliminated following biotransformation to glucuroconjugated and sulfate metabolites, which are excreted in urine.[26] The pharmacological action of oral drugs depends on the absorption into the circulation and subsequent distribution to the peripheral tissues; in contrast, efficacy of topical drugs relies on penetration through the skin.

EP is promising among skin penetration enhancement techniques; apart from transdermal delivery, application of EP has been widely investigated in cell biology, biotechnology, and electrochemotherapy.[13,14,16] EP applies high-voltage pulses to the biological membranes and results in conformation changes in their stereo structures. Transdermal drug penetration into the joint cavity is mostly limited by the low permeability of the stratum corneum of the skin, the thickness of the surrounding tissue layer, and the special physicochemical barrier function of the synovial membrane, which is commonly referred to as the "blood–joint barrier."[27] However, EP is capable of opening transitory pores on complex structures, such as the multilamellar lipid bilayer of the stratum corneum and the synovial membrane.[28,29] Macromolecules of up to 40 kDa can thus be transported through and/or into the skin.[11,15]

Electroporation is now widely used as an alternative to small interfering RNA or naked DNA delivery for targeted suppression of therapeutic genes into the knee joint in arthritis.[30,31] However, electrotransfer of painkiller drugs into the knee joint is less widespread.[32] According to a recent review, plasma levels of diclofenac after topical administration decrease from 0.2% to 8% of those after oral administration.[33] Unfortunately, the resultant synovial concentration is also decreased, as compared to an equivalent oral dose. Effective concentrations in target tissues can be augmented with EP.[32] In accordance with literature data, our results revealed that EP causes higher concentration values in the serum as compared with the topical administration. The diclofenac concentration in the synovia was equal to the serum concentrations; however, conventional topical treatment did not result in a detectable amount of diclofenac sodium in the synovial fluid.

Intra-articular injection of C/K is a well-established model of an acute onset monoarthritis resembling osteoarthritis. In this model, arthritis is probably initiated by mechanical damage to the inner surface of the synovium resulting in an inflammatory response indirectly to the activation of the endothelial side of the synovial barrier. It is characterized by an initial nonphagocytic edema and rapid uptake of the late phagocytic inflammatory phase, where PMNs accumulate in the affected area.[19,34] It has been demonstrated that PMNs are primed within 1 h and are in the majority up to 12 h after the arthritis induction; subsequently, they are replaced by predominating macrophages until the resolution of the inflammation at 48 h.[27] It has also been found that the rate of PMN infiltration is directly related to severity of inflammation in the synovial membrane.[35,36] Based on the pivotal role of PMNs in the initiation and maintenance of joint disorders, we employed the PMN-derived experimental model of inflammatory arthritis in these studies.

Adhesive cell-to-cell interactions are regulated by β2 integrins (CD11/CD18) expressed on PMNs and their associated endothelial ligands (ICAMs and VCAMs).[37] The presence of adhesion molecules on postcapillary endothelial cells in the inflammatory synovial microenvironment has previously been shown and proven to be an appropriate marker for estimating inflammation.[23,38,39] These reactions can be quantitatively assessed by IVM, and the efficacy of various therapeutic interventions can also be judged objectively. PMN accumulation peaks very early, usually at 6–8 h in this model, and (at approx 24 h) macrophages predominate in the exudates thereafter.[40] Like other nonselective cyclooxygenase inhibitors, diclofenac diminishes the number of PMN–endothelial interactions.[41,42] Sticking in the synovial vessels was considerably reduced with the oral administration of diclofenac. However, it was only moderately ameliorated by the EP-enhanced diclofenac hydrogel, and there were no changes in response to the simple topical application of the hydrogel.

Administration of C/K injection into the knee joint results in primary and secondary hyperalgesia in the inflammatory monoarthritis.[43] Secondary hyperalgesia develops at the paw to heat and mechanical stimuli, and primary hyperalgesia is present over the inflamed knee joint.[44,45] Secondary hyperalgesia develops as a result of the sensitization of the dorsal horn neurons neighboring the spinal representation of the injured tissue.[46] Secondary hyperalgesia reactions

were investigated at the peak of the joint inflammation and demonstrated a significant amelioration as a consequence of diclofenac treatment.[47] Like the oral diclofenac treatment, EP completely restored thermal nociceptive sensitivity and increased mechanical touch sensitivity, but to a lesser extent. Knee swelling, which is an objective parameter of joint inflammation, was significantly reduced with both the oral and the EP-enhanced diclofenac treatment.[48] Again, this increased volume was significantly reduced by both oral and EP-enhanced diclofenac treatments 48 h after arthritis induction.

The C/K-induced arthritis is also an appropriate model for the evaluation of the analgesic and anti-inflammatory properties of diclofenac. The TNF-α response is an early marker in carrageenan-induced inflammation, and thus the changes were measured in the synovial fluid 48 h after intra-articular C/K or saline injections. Free radical formation has been demonstrated in the synovial fluid and synovial membrane under clinical conditions and proposed as a causative factor in joint disorders.[22,49] Specifically, oxidoreductive stress has been shown to play a fundamental role in the pathogenesis of arthrosis as a result of increased pressure in the synovial cavity, reduced capillary density and vascular changes, and due to the increased metabolic rate of synovial tissue in joint inflammation.[50–52] Being a source of the oxygen free radical formation located in synovial cells, XOR activity has been shown to increase in joint inflammation.[36,53] Moreover, joint inflammation was also associated with enhanced XOR activity in the synovial fluid.[54] Our present findings demonstrated increases in XOR activity in response to arthritis attenuated by diclofenac treatment, applied either by oral or simple topical routes of administration, the latter being more accentuated in the case of EP. PMNs are also important sources of free radicals through their NADPH oxidase 2 activities.[55] As for microcirculatory inflammatory reactions induced by inflammation, the increase in both the primary and secondary forms of PMN–endothelial interactions (rolling and firm adherence) were confined to the periosteal postcapillary venules. In this model, C/K-induced monoarthritis was the positive control. This aggressive arthritis model, which is associated with severe tissue destruction, is also known to be mediated by infiltrating PMNs.[19,23] Data regarding the final step of PMN–endothelial interactions (ie, sticking) were well correlated with the tissue accumulation of PMNs, as determined by MPO activity. Diclofenac treatment attenuated the MPO activity in the inflamed synovial tissue, applied either via oral or EP-enhanced topical routes of administration.

The present study has provided evidence for the direct action of EP-enhanced transdermal diclofenac sodium delivery on the synovial microcirculation as proven by the decreased rolling and the reduced sticking of leukocytes. The biochemical measurements also demonstrated that diclofenac achieved an efficient tissue concentration in the synovium since inflammatory enzyme activities decreased. In summary, EP-enhanced transdermal diclofenac sodium delivery attenuated the microcirculatory deterioration and the consecutive stages of tissue inflammation; therefore, this type of mechanism might be an interesting focus for therapeutic strategies in arthritis.

Conclusion

EP-enhanced diclofenac delivery is well tolerated and possesses superior efficacy compared to simple topical application in experimental arthritis. The plasma and the joint concentrations of EP diclofenac are similar to those in oral administration. Further investigations are needed to determine the optimal parameters of EP and to diminish the plasma level of diclofenac.

Acknowledgments

The authors would like to thank Dr Derm Clinic of Anti-aging Dermatology, Aesthetic Laser and Plastic Surgery (1026 Budapest, Hungary) for providing the Mezoforte Duo Mez120905-D instrument. The study was supported by grants from the National Research Development and Innovation Office (NKFI K120232) and Economic Development and Innovation Operational Program (GINOP-2 .3.2-15-2016-00015). PH and EB contributed equally to this study.

Disclosure

The authors report no conflicts of interest in this work.

References

1. Reginster JY. The prevalence and burden of arthritis. *Rheumatology (Oxford)*. 2002;41(Suppl 1):3–6.
2. Helmick CG, Felson DT, Lawrence RC, et al. Estimates of the prevalence of arthritis and other rheumatic conditions in the United States. Part I. *Arthritis Rheum*. 2008;58(1):15–25.
3. Peterson K, McDonagh M, Thakurta S, et al. Drug class review: nonsteroidal anti inflammatory drugs (NSAIDs). Final update 4 report. Portland (OR): Oregon Health & Science University; 2010.
4. Pavelka K. A comparison of the therapeutic efficacy of diclofenac in osteoarthritis: a systematic review of randomised controlled trials. *Curr Med Res Opin*. 2012;28(1):163–178.
5. Brunner M, Dehghanyar P, Seigfried B, Martin W, Menke G, Muller M. Favourable dermal penetration of diclofenac after administration to the skin using a novel spray gel formulation. *Br J Clin Pharmacol*. 2005; 60(5):573–577.

6. Heyneman CA, Lawless-Liday C, Wall GC. Oral versus topical NSAIDs in rheumatic diseases: a comparison. *Drugs*. 2000;60(3):555–574.
7. Denet AR, Préat V. Transdermal delivery of timolol by electroporation through human skin. *J Control Release*. 2003;88(2):253–262.
8. Tachibana K. Transdermal delivery of insulin to alloxan-diabetc rabbits by ultrasound exposure. *Pharm Res*. 1992;9(7):952–954.
9. Bommannan D, Okuyama H, Stauffer P, Guy RH. Sonophoresis. I. The use of high-frequency ultrasound to enhance transdermal drug delivery. *Pharm Res*. 1992;9(4):559–564.
10. Prausnitz MR, Bose V, Langer R, Weaver JC. Electroporation of mammalian skin: A mechanism to enhance transdermal drug delivery. *Proc Natl Acad Sci U S A*. 1993;90(22):10504–10508.
11. Vanbever R, Lecouturier N, Préat V. Transdermal delivery of metoprolol by electroporation. *Pharm Res*. 1994;11(11):1657–1662.
12. Riviere JE, Monteiro-Riviere NA, Rogers RA, et al. Pulsatile transdermal delivery of LHRH using electroporation: drug delivery and skin toxicology. *J Control Release*. 1995;36(3):229–233.
13. Mir L, Orlowski S. Mechanisms of electrochemotherapy. *Adv Drug Deliv Rev*. 1999;35(1):107–118.
14. Heller R, Gilbert R, Jaroszeski MJ. Clinical applications of electrochemotherapy. *Adv Drug Deliv Rev*. 1999;35(1):119–129.
15. Lombry C, Dujardin N, Préat V. Transdermal delivery of macromolecules using skin electroporation. *Pharm Res*. 2000;17(1):32–37.
16. Weaver JC, Chizmadzhev YA. Theory of electroporation: a review. *Bioelectrochem Bioenerg*. 1996;41(2):135–160.
17. Denet A, Vanbever R, Préat V. Skin electroporation for transdermal and topical delivery. *Adv Drug Deliv Rev*. 2004;56(5):659–674.
18. Khajuria DK, Razdan R, Mahapatra DR. Description of a new method of ovariectomy in female rats. *Rev Bras Reumatol*. 2012;52(3):462–470.
19. Day SM, Lockhart JC, Ferrell WR, McLean JS. Divergent roles of nitrergic and prostanoid pathways in chronic joint inflammation. *Ann Rheum Dis*. 2004;63(12):1564–1570.
20. Hargreaves K, Dubner R, Brown F, Flores C, Joris J. A new and sensitive method for measuring thermal nociception in cutaneous hyperalgesia. *Pain*. 1998;32(1):77–88.
21. Kuebler WM, Abels C, Schuerer L, Goetz AE. Measurement of neutrophil content in brain and lung tissue by a modified myeloperoxidase assay. *Int J Microcirc Clin Exp*. 1996;16(2):89–97.
22. Beckman JS, Parks DA, Pearson JD, Marshall PA, Freeman BA. A sensitive fluorometric assay for measuring xanthine dehydrogenase and oxidase in tissues. *Free Radic Biol Med*. 1989;6(6):607–615.
23. Hartmann P, Szabó A, Eros G, et al. Anti-inflammatory effects of phosphatidylcholine in neutrophil leukocyte-dependent acute arthritis in rats. *Eur J Pharmacol*. 2009;622(1–3):58–64.
24. Todd PA, Sorkin EM. Diclofenac sodium. A reappraisal of its pharmacodynamic and pharmacokinetic properties, and therapeutic efficacy. *Drugs*. 1988;35(3):244–285.
25. Vetter G. A comparison of naproxen and diclofenac sodium in the treatment of osteoarthritis in elderly patients. *Br J Clin Pract*. 1985;39(7):276–281.
26. Davies NM, Anderson KE. Clinical pharmacokinetics of diclofenac. Therapeutic insights and pitfalls. *Clin Pharmacokinet*. 1997;33(3):184–213.
27. Day RO, McLachlan AJ, Graham GG, Williams KM. Pharmacokinetics of nonsteroidal anti-inflammatory drugs in synovial fluid. *Clin Pharmacokinet*. 1999;36(3):191–210.
28. Nishimura T, Akimoto M, Miyazaki M, Nomoto M, Miyakawa M. Developments of transdermal transport system during skin iontophoresis and electroporation. *PIERS Online*. 2010;6(8):759–763.
29. Blagus T, Markelc B, Cemazar M, et al. In vivo real time monitoring system of electroporation mediated control of transdermal and topical drug delivery. *J Control Release*. 2013;172(3):862–871.
30. Zhen S, Heyong Y, Xiaoming Y, et al. Inhibition of osteoarthritis in rats by electroporation with interleukin-1 receptor antagonist. *J Biomed Sci Eng*. 2016;9(7):323–336.
31. Cemazar M, Sersa G. Electrotransfer of therapeutic molecules into tissues. *Curr Opin Mol Ther*. 2007;9(6):554–562.
32. Feng S, Zhu L, Huang Z, et al. Controlled release of optimized electroporation enhances the transdermal efficiency of sinomenine hydrochloride for treating arthritis in vitro and in clinic. *Drug Des Devel Ther*. 2017;11:1737–1752.
33. Hagen M, Baker M. Skin penetration and tissue permeation after topical administration of diclofenac. *Curr Med Res Opin*. 2017;33(9):1623–1634.
34. Hansra P, Moran EL, Fornasier VL, Bogoch ER. Carrageenan-induced arthritis in the rat. *Inflammation*. 2000;24(2):141–155.
35. Cremasco V, Graham DB, Novack DV, Swat W, Faccio R. Vav/phospholipase Cγ2-mediated control of a neutrophil-dependent murine model of rheumatoid arthritis. *Arthritis Rheum*. 2008;58(9):2712–2722.
36. Smith E, McGettrick HM, Stone MA, et al. Duffy antigen receptor for chemokines and CXCL5 are essential for the recruitment of neutrophils in a multicellular model of rheumatoid arthritis synovium. *Arthritis Rheum*. 2008;58(7):1968–1973.
37. Springer TA. Traffic signals for lymphocyte recirculation and leukocyte emigration: the multistep paradigm. *Cell*. 1994;76(2):301–314.
38. Hartmann P, Erős G, Varga R, et al. Limb ischemia-reperfusion differentially affects the periosteal and synovial microcirculation. *J Surg Res*. 2012;178(1):216–222.
39. Hale LP, Martin ME, McCollum DE, et al. Immunohistologic analysis of the distribution of cell adhesion molecules within the inflammatory synovial microenvironment. *Arthritis Rheum*. 1989;32(1):22–30.
40. Gilroy DW, Colville-Nash PR, Willis D, Chivers J, Paul-Clark MJ, Willoughby DA. Inducible cyclooxygenase may have anti-inflammatory properties. *Nat Med*. 1999;5(6):621–622.
41. Scheja A, Forsgren A, Marsal L, Wollheim F. Inhibition of in vivo leucocyte migration by NSAIDs. *Clin Exp Rheumatol*. 1985;3(1):53–58.
42. Martinez LL, Oliveira MA, Miguel AS, et al. Enalapril interferes with the effect of diclofenac on leucocyte-endothelium interaction in hypertensive rats. *J Cardiovasc Pharmacol*. 2004;43(2):258–265.
43. Radhakrishnan R, Moore SA, Sluka KA. Unilateral carrageenan injection into muscle or joint induces chronic bilateral hyperalgesia in rats. *Pain*. 2003;104(3):567–577.
44. Sluka KA, Bailey K, Bogush J, Olson R, Ricketts A. Treatment with either high or low frequency TENS reduces the secondary hyperalgesia observed after injection of kaolin and carrageenan into the knee joint. *Pain*. 1998;77(1):97–102.
45. Skyba DA, Radhakrishnan R, Sluka KA. Characterization of a method for measuring primary hyperalgesia of deep somatic tissue. *J Pain*. 2005;6(1):41–47.
46. Hardy JD, Harold G, Goodell W, Goodell H. Experimental evidence on the nature of cutaneous hyperalgesia. *J Clin Invest*. 1950;29(1):115–140.
47. Lee TH, Wang CJ, Wu PC, Buerkle H, Lin SH, Yang LC. The thermal and mechanical anti-hyperalgesic effects of pre- versus post-intrathecal treatment with lamotrigine in a rat model of inflammatory pain. *Life Sci*. 2002;70(25):3039–3047.
48. Peter-Szabo M, Kekesi G, Nagy E, Sziver E, Benedek G, Horvath G. Quantitative characterization of a repeated acute joint inflammation model in rats. *Clin Exp Pharmacol Physiol*. 2007;34(5–6):520–526.
49. Kennett EC, Davies MJ. Glycosaminoglycans are fragmented by hydroxyl, carbonate, and nitrogen dioxide radicals in a site-selective manner: implications for peroxynitrite-mediated damage at sites of inflammation. *Free Radic Biol Med*. 2009;47(4):389–400.
50. Blake DR, Winyard PG, Marok R. The contribution of hypoxia-reperfusion injury to inflammatory synovitis: the influence of reactive oxygen intermediates on the transcriptional control of inflammation. *Ann N Y Acad Sci*. 1994;723:308–317.
51. Mapp PI, Grootveld MC, Blake DR. Hypoxia, oxidative stress and rheumatoid arthritis. *Br Med Bull*. 1995;51(2):419–436.

52. Tak PP, Bresnihan B. The pathogenesis and prevention of joint damage in rheumatoid arthritis: advances from synovial biopsy and tissue analysis. *Arthritis Rheum*. 2000;43(12):2619–2633.
53. Saricaoglu F, Dal D, Salman AE, Doral MN, Kilinç K, Aypar U. Ketamine sedation during spinal anesthesia for arthroscopic knee surgery reduced the ischemia-reperfusion injury markers. *Anesth Analg*. 2005;101(3):904–909.
54. Hanachi N, Charef N, Baghiani A, et al. Comparison of xanthine oxidase levels in synovial fluid from patients with rheumatoid arthritis and other joint inflammations. *Saudi Med J*. 2009;30(11):1422–1425.
55. Bedard K, Krause KH. The NOX family of ROS-generating NADPH oxidases: physiology and pathophysiology. *Physiol Rev*. 2007;87(1):245–313.

Supplementary materials

Characterization of the diclofenac sodium-containing hydrogel

Rheological investigations and pH measurements were designed to characterize the hydrogel.

The pH of the semisolid formulations was measured with a Testo 206 pH meter (Testo SE & Co. KGaA, Lenzkirch, Germany). The probe of the device was immersed into three different parts of the sample. The pH was adjusted to 8.0±0.1.

The rheological properties were studied with a Physica MCR101 rheometer (Anton Paar, Graz, Austria). The measuring device was of the parallel plate type (with a 25 mm diameter and a gap height of 0.10 mm). The flow and viscosity curve were recorded over the shear rate range from 0.1 to 100 and from 100 to 0.1 s^{-1} at 32°C.

The flow curve of the gel can provide information on the viscosity changes under flow conditions and on the time dependency of the structure breakdown and recovery.

The flow curve of the gel presented shear thinning behavior, which means that the shear stress continuously increases with the shear rate, but the rate of the increase decreases. The curves showed slight thixotropy, which means the structure regeneration is time-dependent.

High-performance liquid chromatography (HPLC) measurements of the synovial washing fluid and plasma samples

The quantitative measurement of diclofenac sodium was carried out with the HPLC method.

Chemicals and reagents for HPLC

Methanol, orthophosphoric acid (85% v/v), potassium dihydrogen phosphate, isopropanol, and n-hexane were bought from VWR International GmbH (Darmstadt, Germany). All reagents and solutions used were analytical grade, except the methanol, which was HPLC grade. The purified water for the HPLC was acquired from TKA Smart2Pure device (TKA, Burladingen, Germany).

HPLC system and conditions

The HPLC analysis of diclofenac sodium was conducted using an Agilent HPLC system (Agilent Technologies, Palo Alto, CA, USA) equipped with an automated solvent delivery system, which has an integrated degasser (1260 Infinity Quaternary Pump, Agilent Technologies), an Agilent 1260 Infinity autosampler, and a 1024-element diode array detector (1260 Infinity Diode Array Detector, Agilent Technologies). The system control and data acquisition were performed with Agilent ChemStation B.04.03 software (Agilent Technologies). The chromatographic parameters are provided in Table S1.

The chromatographic separations were performed on Kromasil® 100 5C188 (250×4, 6 mm ID, 5 µm) (Phenomenex Inc., Torrance, CA, USA) analytical column. The column temperature was maintained at a constant 35°C. Separations were performed in gradient mode. The mobile phase was eluted at a flow rate of 1.5 mL min^{-1}, and effluent was monitored at 254 nm.

The mobile phase consisted of two components. Component A was a mixture of methanol and PBS buffer at a ratio of 80:20 volume/volume percentage (potassium hydrogen phosphate, 5 mM and diluted orthophosphoric acid buffer, 5 mM, pH 2.5, adjusted by adding 85% orthophosphoric acid). Component B was a 20:80 (v/v) mixture of methanol and PBS buffer.

The preliminary ratio was 30:70 (v/v) A:B for 1 min; then the volume for B was increased from 70% to 100% after 4.1 min and sustained for 1 min before being returned to the initial conditions after 5 min. After a measurement, 2 min at 154 bar pressure for equilibration of the column was performed before the next injection. The retention time for diclofenac sodium was 4.5±0.054 min (relative standard deviation =0.29%) (Table S1).

Preparation of standard solutions and calibration samples

A stock solution of diclofenac sodium (1,000 µg/mL) was prepared in a 50:50 (v/v) mixture of methanol and HPLC water. External standard calibration solutions were prepared by dilution of the stock solution with the 50:50 (v/v) mixture of methanol and HPLC water to produce solutions with

Table S1 Parameters of the chromatographic measurement

Mobile phase	Mixture of methanol and PBS buffer
pH	2.5
Flow rate	1 mL/min
Injection volume	20 µL
Elution type	Gradient elution
Detection wavelength	254 nm
Column	Kromasil 100 5C18, 5 µm 250×4.6 mm
Temperature	35°C
Evaluation	External standard calibration, 6 conc (n=3)
Time	20 min

Abbreviation: conc, concentrations.

concentrations of 0 (as blank), 10, 20, 50, 100, and 150 µg/mL (six standard solutions).

Sample extraction procedure

An aliquot of plasma (1 mL) was combined with 100 µL of the internal standard solution (added amount 1.25 µg). The sample was acidified by adding 2 mL of 0.83 M phosphoric acid and 4 mL of hexane isopropyl alcohol (90:10). The mixtures were shaken for 10 min on a rotating shaker at 250 rpm and then centrifuged at 1,500 *g* for 10 min. The aqueous phase was frozen, and the organic phase was transferred to another tube and evaporated to dryness with nitrogen gas at room temperature. The dried residue was reconstituted with 300 µL of mobile phase and shaken for 15 s on a vortex mixer, and then a 20 µL aliquot was injected into the HPLC system.

An aliquot of 1.2 mL of synovial fluid was added to 2 mL of orthophosphoric acid (0.83 M) and 0.6 mL of isopropyl alcohol and vortexed for a few seconds. After that, 5.4 mL of *n*-hexane was added, and the mixture was centrifuged at 9,000 *g* for 5 min. The organic phase was transferred to a clean tube, and the solvent was evaporated to dryness with nitrogen gas at 30°C. The residue was dissolved in 1.2 mL of the mobile phase by vortexing. An aliquot of 20 µL was injected into the chromatograph.

Linearity

Linearity was studied by preparing standard solutions in the range of 0–150 µg mL^{-1} (n=6), plotting a graph of concentration against area under the curve and determining the linearity. Two methods (the short and long methods) were compared to choose the optimal one for the HPLC analysis (Table S2).

Based on the linearity test and the low relative standard deviation % values, the short method is recommended. The advantage is a runtime shortened by 42% (35–20 min; Figure S2).

Table S2 Comparison of the parameters of the long and short methods

Parameters of the HPLC method	Long method	Short method
Linear regression equation	$y = 20.491x - 7.4762$	$Y = 20.338x - 1.9623$
Coefficient of determination	$R^2 = 0.9999$	$R^2 = 0.9999$
Number of samples	n=15	n=15
Runtime (min)	35	20
RTDs (min), mean ± standard deviation	18.721±0.054	14.610±0.002
RSD – RTDs (%)	0.29	0.02
RSD – AUC (%)	1.70	1.52
RSD – maximum limit (%)	2.00	2.00

Abbreviations: AUC, area under the curve; HPLC, high-performance liquid chromatography; RSD, relative standard deviation; RTDs, residence time distributions.

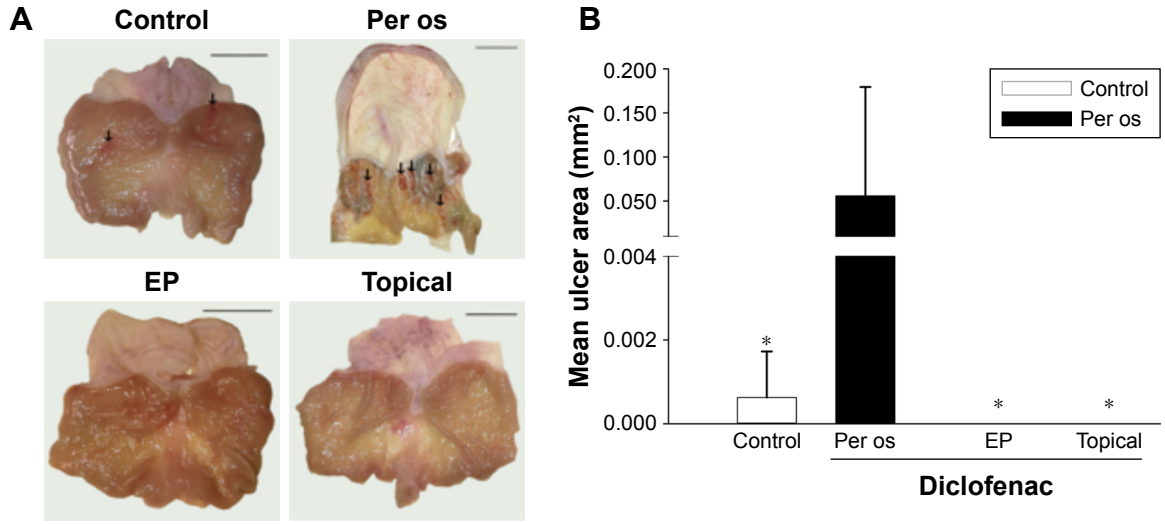

Figure S1 Gastric adverse effects of diclofenac intake.
Notes: The effects of diclofenac treatment on the gastric mucosa. (**A**) Diclofenac treatment-induced gastric adverse effects. Scale bars represent 10 mm. Black arrows show edema, irritation, and petechia formation. (**B**) Mean area of gastric lesions. The white column represents the control group (per os saline-treated), and the black column represents the per os diclofenac-treated group. The pale and dark columns (not visible, as values are 0.000) represent the topical and EP-combined topical diclofenac-treated groups, respectively. Data are presented as means ± SD. *$p<0.05$ vs per os diclofenac-treated group (Kruskal–Wallis one-way analysis and Dunnet test).
Abbreviations: EP, electroporation; SD, standard deviation of the mean.

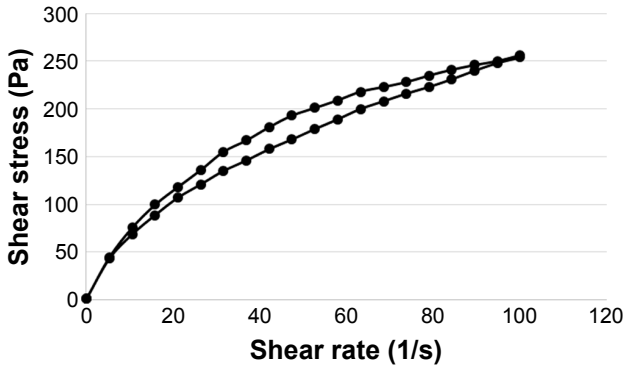

Figure S2 The flow curve of the diclofenac sodium-containing hydrogel.

PLOS ONE

RESEARCH ARTICLE

Hydroxyapatite-coated implants provide better fixation in total knee arthroplasty. A meta-analysis of randomized controlled trials

Tamara Horváth[1], Lilla Hanák[2], Péter Hegyi[2], Edina Butt[3], Margit Solymár[2], Ákos Szűcs[4], Orsolya Varga[5], Bui Quoc Thien[5], Zsolt Szakács[2,6], Endre Csonka[3], Petra Hartmann[1]*

1 Institute of Surgical Research, University of Szeged, Szeged, Hungary, **2** Institute for Translational Medicine, Medical School, University of Pécs, Pécs, Hungary, **3** Department of Traumatology, University of Szeged, Szeged, Hungary, **4** Department of Surgery, University of Semmelweis, Budapest, Hungary, **5** Department of Preventive Medicine, Faculty of Public Health, University of Debrecen, Debrecen, Hungary, **6** Szentágothai Research Centre, Medical School, University of Pécs, Pécs, Hungary

* hartmann.petra@med.u-szeged.hu

Citation: Horváth T, Hanák L, Hegyi P, Butt E, Solymár M, Szűcs Á, et al. (2020) Hydroxyapatite-coated implants provide better fixation in total knee arthroplasty. A meta-analysis of randomized controlled trials. PLoS ONE 15(5): e0232378. https://doi.org/10.1371/journal.pone.0232378

Editor: Thomas Webster, Northeastern University, UNITED STATES

Received: November 28, 2019

Accepted: April 14, 2020

Published: May 12, 2020

Data Availability Statement: All relevant data are within the paper and its Supporting Information files.

Funding: PH and TH have recieved the National Research Development and Innovation Office grant: NKFI K120232 https://nkfih.gov.hu/palyazoknak, the Economic Development and Innovation Operative Program Grant (GINOP-2.3.2-15-2016-00015) https://www.palyazat.gov.hu/ and Human Resource Development Operational Program (EFOP-3.6.2-16-2017-0006). https://

Abstract

Background

The potential advantages of hydroxyapatite (HA)-coated cementless total knee arthroplasty (TKA) implants are bone stock preservation and biological fixation. Studies comparing the outcomes of HA-coated cementless, non HA-coated cementless (uncemented) and cemented TKA implants reported contradictory data. Our aim was to provide a comparison of the effects of HA coating of tibial stem on the stability and functionality of TKA implants.

Methods

A systematic literature search was performed using MEDLINE, Scopus, EMBASE and the CENTRAL databases up to May 31st, 2019. The primary outcome was Maximum Total Point Motion (MTPM) of the tibial stem. This parameter is determined by radiosterometric analysis and refers to the migration pattern of the prosthesis stems. The clinical outcomes of the implanted joints were evaluated by the Knee Society Knee Score (KSS) and the Knee Society Function Score (KFS). Weighted mean difference (WMD) with 95% confidence interval (CI) were calculated with the random-effects model.

Results

Altogether, 11 randomized controlled trials (RCTs) with 902 patients for primary TKA implants were included. There was a statistically significant difference in the MTPM values with the use of HA-coated and uncoated uncemented implants (WMD = +0.28, CI: +0.01 to +0.56, $P<0.001$). However, HA-coated stems showed significantly higher migration when compared with the cemented prostheses (WMD = -0.29, CI: -0.41 to -0.16, $P<0.001$). The KSS values of HA-coated implants were significantly higher than those for the uncemented

www.palyazat.gov.hu/doc/4379 ZS, LH, PH, and MS have recieved the Economic Development and Innovation Operative Program Grant GINOP 2.3.2-15-2016-00048. https://www.palyazat.gov.hu/ The funders had no role in study design, data collection and analysis, decision to publish, or preparation of the manuscript.

Competing interests: The authors have declared that no competing interests exist.

Abbreviations: BMI, body mass index; CI, confidence interval; HA, hydroxyapatite; KFS, knee society function score; KSS, knee society knee score; MTPM, maximum total point motion; RCT, randomized controlled trials; RSA, radiosterometrical analysis; TKA, total knee arthroplasty; TSA, trial sequential analysis; WMD, weighted mean difference.

implants; moreover, KSS and KFS outcome scores were statistically not different between the HA-coated and cemented prosthesis cases.

Conclusion

HA-coating yields better stability than other, uncemented prostheses. More importantly, the HA-coating is not outperformed by cemented prosthesis in providing good functional outcome.

Introduction

Since the introduction of cementless prostheses, manufacturers came up with new materials with better biocompatibility and porous, rough surface to increase stability [1]. Among them, hydroxyapatite (HA) is a promising coating material with the potential to achieve biological fixation of implants [2]. In terms of its chemical structure, HA is an osteoconductive calcium phosphate molecule similar to human bone, which accelerates and induces insertion of implants, called osteointegration [2, 3]. Numerous studies investigated the outcomes of HA-coated stems with conflicting results. Some of them reported improved initial and late stability of stems, directly correlating with prosthetic life [3]. However, further investigations did not confirm these benefits and signs of osteolysis or early stem migration were observed [4].

Five previous systematic reviews and national registries have summarized the available evidences, but each of these has limitations [5–11]. Registries were based on observational data with potential sources of bias including the lack of worldwide consensus on implants taxonomy. Moreover, learning curve effects and differences between a high volume center and the wide community practice were also not explicitly addressed in these tables [12]. One systematic review [7] failed to eliminate potential selection bias because a few of the studies enrolled hybrid fixation (such as cemented femoral and uncemented tibial stem). Others included quasi-randomized and observational studies as well [9]. Two reviews allocated only a limited number of studies into *de facto* statistical analysis (3 and 2, respectively) [7–8] despite of a relatively large number of selected publications. As confusing results, HA-coated cementless prostheses were compared with cemented and not with other porous-coated or non-coated cementless (uncemented) prostheses in 4 meta-analyses [3,13,14,15].

Therefore, the aim of our study was to update current knowledge and compare up-to-date data on the quality of fixation in TKA implants under two conditions: with HA-coated cementless prosthesis and with uncemented or cemented fixation. The primary outcome was MTPM of the tibial stem determined by radiostereometrical analysis (RSA). The secondary endpoints were clinical outcomes including the KSS and the KFS.

Materials and methods

This study is reported in accordance with the PRISMA 2009 (Preferred Reporting Items in Systematic Reviews and Meta-Analysis) statement (**S1 Table**) [16]. The review protocol was registered with the National Institute for Health Research PROSPERO system under registration number CRD42019129619.

Search

A systematic literature search was performed using EMBASE, MEDLINE, Scopus and CENTRAL. The query was designed based on Medical Subject Headings (MeSH) terms combined with various free-text terms for hydroxyapatite and uncemented or cemented prosthesis and total knee arthroplasty. No language limitation was applied (**S1 Fig**). The date of final literature search was May 31th, 2019.

Selection and eligibility criteria

Inclusion criteria specified any RCTs comparing the radiological and clinical outcomes of HA-coated tibial stem with those uncemented or cemented stems for primary TKA implants. Reoperations (revision prostheses), hybrid fixation, unicompartmental knee arthroplasty, non-clinical and uncontrolled studies were excluded. RCTs missing outcomes of our study were also excluded. Two authors (T.H. and E.B.) reviewed all studies upon the search strategy and controversies were resolved by discussion with a third author (P.H.). Full-text versions of potentially relevant studies were evaluated for inclusion using an eligibility pro forma screening document that was based on pre-specified criteria. At the end of literature search, 11 RCTs involving 902 patients were enrolled to analysis (**Fig 1**).

Outcomes

The primary outcome was the MTPM of the tibial stem. MTPM is determined by RSA using the UMRSA software (RSA Biomedical, Umeå, Sweden) according to guideline [17] and is defined clearly in the articles as the total three-dimensional vector displacement of the marker to the greatest motion.

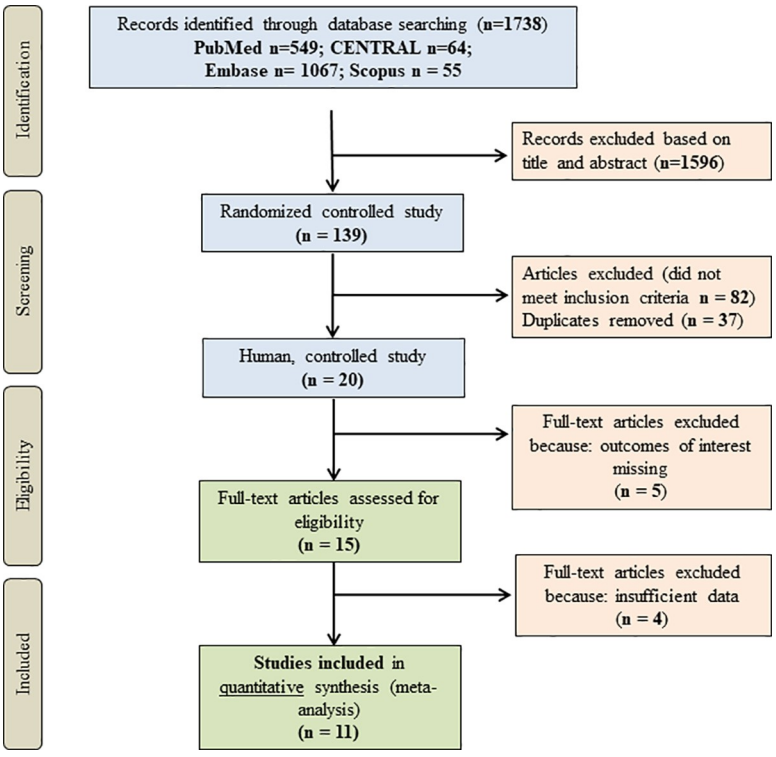

Fig 1. Flowchart of the meta-analysis.

https://doi.org/10.1371/journal.pone.0232378.g001

When useful data were presented in graphic plots, we quantified them by using open source PlotDigitizer for Windows software (Version 2.6.8, Joseph A. Huwaldt). Where mean with standard deviation was not reported, they were estimated from median, interquartiles and range by using the method of Xiang Wan [18]. The median (range) was transformed to mean ±standard deviation (SD). Disagreements were resolved by discussion with a senior author or by contacting the corresponding author.

The secondary outcomes were validated using scoring systems including KSS and KFS referring to the function of the implant in everyday life. The KSS evaluates the clinical profile with regards to pain intensity, range of motion and stability, flexion deformities, contractures and poor alignment. In contrast, KFS considers only walking distance and stair climbing with deduction for walking aids.

Data extraction and risk of bias assessment

We used the Cochrane risk-of-bias tool to assess the risk of bias for each study (**Fig 2**) [19]. Demographic, quality, and outcome data were extracted independently into Microsoft Excel by two authors (T.H. and E.B.). Data were taken from all articles describing the studies. Any questions in data extraction were settled by discussion with a third author.

Quality of evidence

In order to estimate the quality of evidence on the outcomes in our meta-analysis, we have used the Grading of Recommendations Assessment, Development, and Evaluation (GRADE) approach (**S4 Table**).

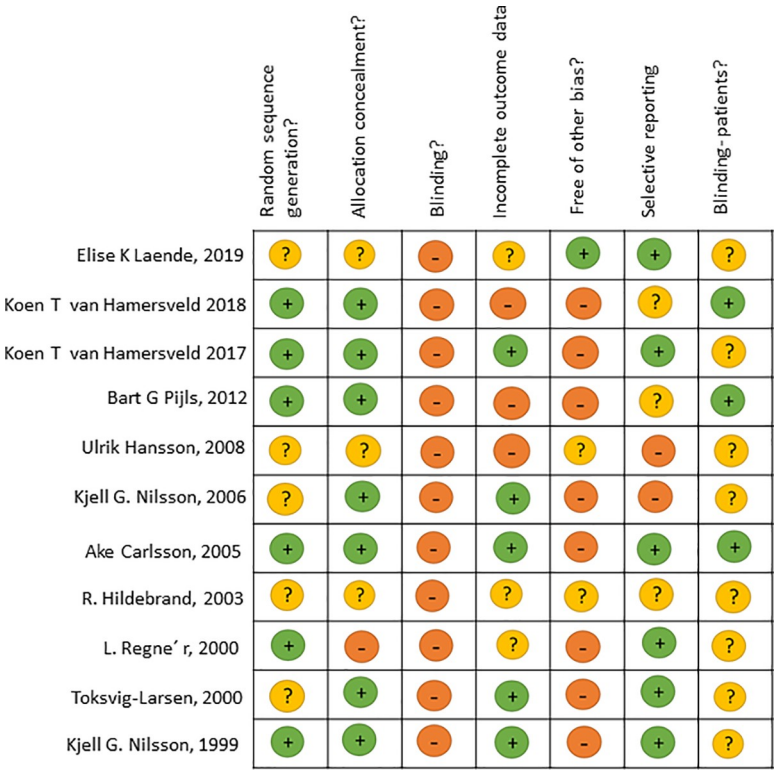

Fig 2. Risk of bias—Review of authors' judgments about each risk of bias item for each study included.

https://doi.org/10.1371/journal.pone.0232378.g002

Statistical analysis

The statistical analysis of this study was performed by a dedicated statistician (L.H.) using Stata 15 SE (Stata Corp) pooled weighted mean difference (WMD) with 95% CI was calculated for continuous outcomes. Random effect model was was applied to all analyses with DerSimonian-Laird estimation. Statistical heterogeneity was analysed using the I^2 and the chi-square statistic to gain probability-values; I^2 represents the magnitude of the heterogeneity (moderate: 30–60%, substantial: 50–90%, considerable: 75–100%).

Publication bias was evaluated by visual inspection of the funnel plot, and the presence of this bias was considered in the case of an asymmetrical rather than a symmetrical graph. These funnel plots were automatically generated by the Stata software using the effect size and the standard error of the effect size for each study. Due to the low number of included studies per analysis (less than 10), the conditions of the Egger's test were not met. We performed trial sequential analysis (TSA) for primary outcomes. We used TSA program version 0.9 beta (available from www.ctu.dk/tsa) to determine whether further randomized trials are needed in this investigation (**S2 Fig**).

Results

Eleven RCTs were included in quantitative synthesis, in which TKA implants with a HA-coated tibial stem was compared to other tibial fixations (cemented and uncemented prosthesis). All trials were homogenous with respect to demographic characteristics. (**Table 1**).

Radiological outcome

The MTPM of the tibial stem at 2 years is the primary outcome in this analysis. If the MTPM exceeds 0.2 mm, the prosthesis is classified as unstable, which greatly increases the likelihood of other complications such as aseptic loosening. If the MTPM is less than 0.2 mm, the

Table 1. Characteristics of the studies included.

Author, Year	Design	Country	Recruitment period	Patients' characteristics					
				Patients	N^0 of knees	Age (y)		Gender (male%)	BMI
						Mean	SD		Mean
Carlsson 2005 [4]	prospective randomized	Sweden	1992–1995	30	72	72,6	6	21,3	ND
Laende 2019 [14]	prospective randomized	Australia	2002–2015	ND	360	65	7,8	61	31,6
Pijls 2012 [15]	prospective randomized	Sweden	ND	ND	68	62	ND	18,3	26,5
Hildebrand 2003 [20]	prospective randomized	Germany	1992–1993	48	27	70,7	ND	ND	ND
Regne´ r 2000 [21]	prospective randomized	Sweden	ND	68	51	66,5	ND	16	ND
Nilsson 1999 [22]	prospective randomized	Sweden	1991–1992	53	27	67	ND	17	ND
Nilsson 2006 [23]	prospective randomized	Sweden	1997–2003	85	69	55,7	ND	62	ND
Toksvig 2000 [24]	prospective randomized	Sweden	ND	60	62	71	ND	ND	ND
Hansson 2008 [25]	prospective randomized	Sweden	1997–1999	60	49	ND	ND	ND	ND
Hamersveld 2018 [26]	prospective randomized	Sweden	2007–2008	58	25	66	7,4	17,3	ND
Hamersveld 2017 [27]	prospective randomized	Sweden	2009–2010	60	60	66,2	7,2	16	28,3

https://doi.org/10.1371/journal.pone.0232378.t001

prosthesis can be considering as stable in a long run [28]. Thirteen studies were enrolled to the MTPM analysis. The analysis showed that the MTPM values of the HA-coated cementless stems are significantly lower than that of the uncemented stems (WMD = 0.28, 95% CI: 0.01–0.56, $P = 0.045$) (Fig 3A).

When HA-coated implants were compared to cemented prostheses, the latter displayed lower MTPM (WMD = -0.29, 95% CI: -0.41 to 0.16, $P < 0.001$) (Fig 3B).

(Fig 3C and 3D). In these two plots show the funnel plot, but we couldn't run Egger's test on it.

Clinical outcomes

The secondary outcomes were KSS and KFS. Four RCTs were enrolled to the analysis. The analysis showed that KSS of HA-coated cementless prostheses is not significantly different from that of the uncemented group (WMD = -0.64, 95% CI: -3.02–1.73, $P = 0.596$) (Fig 4A);

Of interest, there was no statistically significant difference between the KSS of HA-coated cementless and cemented prosthesis (WMD = -0.29, 95% CI: -2.27 to 1.69, $P = 0.775$) (Fig 4B). Similar results could be obtained from the analysis of KFS, however, have limited value due to the lack of the comparison between HA-coated and uncemented groups. As such, no significant difference could be observed between HA-coated cementless and cemented implants (WMD = -4.95, 95% CI: -13.59 to 3.69 $P = 0.069$). However, comparison between HA-coated and uncemented groups was not performed due to the low number of studies in the uncemented group. (Fig 5A). (**Figs 4C, 4D and 5B)** KSS data are shown on the funnel plot, but unfortunately we couldn't run Egger's test on it.

Discussion

This study reviews the current evidence on and updates knowledge of the use of HA-coated tibial stem for primary TKA implants. The treatment groups were homogenous in terms of characteristics of patients, thus the prediction of primary and secondary outcomes (i.e. MTPM and KSS and KFS) was likely independent from individual risk variables, patient selection or the overall severity of osteoporosis at prosthesis implantation. Direct meta-analysis comparison was made and the sample size of included trials was large enough to provide good evidence that HA-coating yields better stability than other, uncemented prostheses. However, cement fixation of prostheses stems still performs greater anchorage against migration. More importantly, the HA-coating is not outperformed by cemented prosthesis in providing good functional outcome with regards to pain intensity, range of motion and walking distance.

The survival probability of the stems is often cited in the literature as predictor of prosthesis outcome. However, the TKA implants outcomes are generally good with a mean survivorship rate (or projected rates) of 95% or more at 10 years. Hence, this parameter is less sensitive to evaluate the quality of stem fixation, than radiological results [29]. The migration analysis with RSA is a standardized and objective method with low susceptibility to different interpretations [17]. This technique allows movements between the implant and host bone measured with an accuracy of 0.2 mm [28,30]. As a primary outcome of our study, the migration pattern of the prosthesis stems was determined as the maximum total point motion (MTPM) of the tibial stem measured by RSA. The MTPM value is the unit of measurement for the largest 3D migration of any point on the prosthesis surface. The migration pattern was defined as at least 2 postoperative follow-up moments within the first 2 years of follow-up [28]. MTPM mainly depends on mechanical factors such as the bone-implant interface or different biological reactions at the implant-bone interface therefore is a reliable parameter to assess the added value of HA-coating in implant surface.

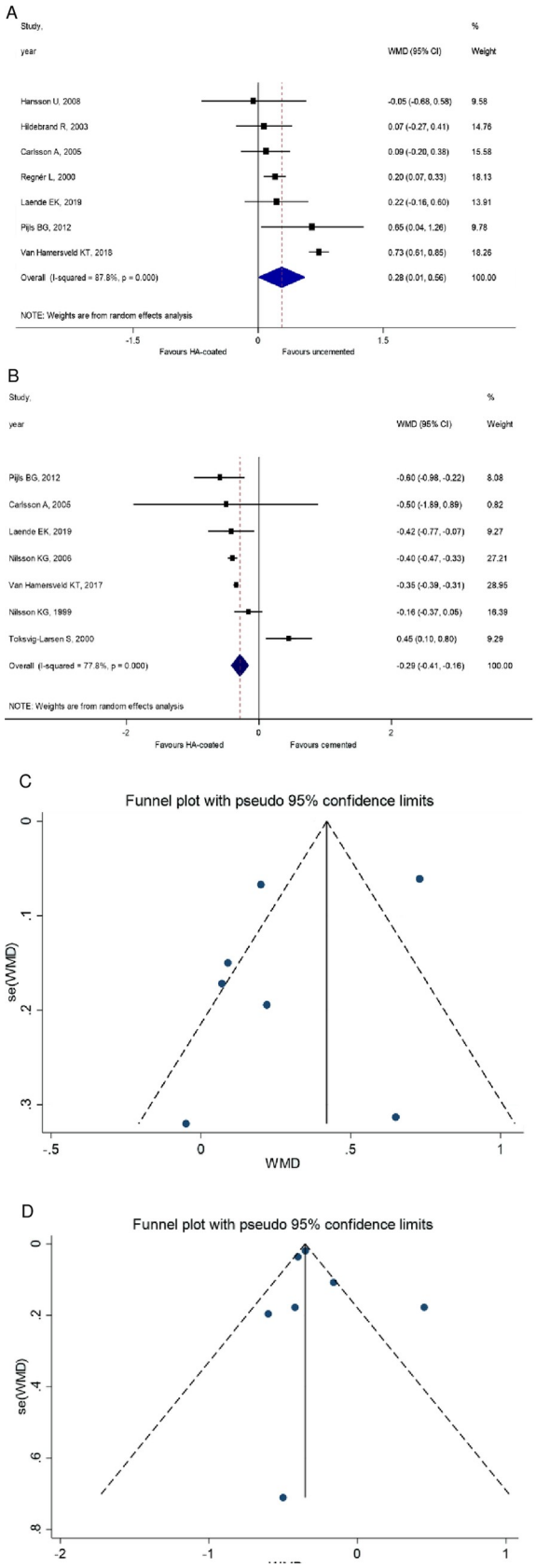
A
Study, year
WMD (95% CI)
%
Weight
Hansson U, 2008
-0.05 (-0.68, 0.58)
9.58
Hilebrand R, 2003
0.07 (-0.27, 0.41)
14.76
Carlsson A, 2005
0.09 (-0.20, 0.38)
15.58
Regnér L, 2000
0.20 (0.07, 0.33)
18.13
Laende EK, 2019
0.22 (-0.16, 0.60)
13.91
Pijls BG, 2012
0.65 (0.04, 1.26)
9.78
Van Hamersveld KT, 2018
0.73 (0.61, 0.85)
18.26
Overall (I-squared = 87.8%, p = 0.000)
0.28 (0.01, 0.56)
100.00
NOTE: Weights are from random effects analysis
-1.5
0
1.5
Favours HA-coated
Favours uncemented
B
Study, year
WMD (95% CI)
%
Weight
Pijls BG, 2012
-0.60 (-0.98, -0.22)
8.08
Carlsson A, 2005
-0.50 (-1.89, 0.89)
0.82
Laende EK, 2019
-0.42 (-0.77, -0.07)
9.27
Nilsson KG, 2006
-0.40 (-0.47, -0.33)
27.21
Van Hamersveld KT, 2017
-0.35 (-0.39, -0.31)
28.95
Nilsson KG, 1999
-0.16 (-0.37, 0.05)
16.39
Toksvig-Larsen S, 2000
0.45 (0.10, 0.80)
9.29
Overall (I-squared = 77.8%, p = 0.000)
-0.29 (-0.41, -0.16)
100.00
NOTE: Weights are from random effects analysis
-2
0
2
Favours HA-coated
Favours cemented
C
Funnel plot with pseudo 95% confidence limits
se(WMD)
0
.1
.2
.3
-.5
0
.5
1
WMD
D
Funnel plot with pseudo 95% confidence limits
se(WMD)
0
.2
.4
.6
.8
-2
-1
0
1

Fig 3. **A** MTPM analysis of the cemented and HA-coated cementless group. The value of cemented MTPM lesser than HA-coated cementless group. **B** MTPM analysis of uncemented vs. HA-coated cementless group. The MTPM values of uncemented prostheses are significantly higher than HA-coated. **C** Funnel plot 2 years follow-up; HA-coated cementless vs. uncemented group. **D** Funnel plot 2 years follow-up; HA-coated cementless vs. cemented group.

https://doi.org/10.1371/journal.pone.0232378.g003

RCTs in our meta-analysis have demonstrated lower incidence of MTPM with HA–coated implants when compared to other non-cemented stems, except one trial [31]. As for the comparison of HA-coated cementless and cemented group, the overall rates of MTPM were very low in the cemented group and displayed lower incidence than HA-coated cementless prosthesis. It is contradictory with a recent meta-analysis of Voight and his coworkers, which demonstrated that use of HA provide the best long-term stability of implants. However, they failed to eliminate potential selection bias because of enrolled studies with hybrid fixation [7]. Another confounding factor was that HA-coated cementless fixation was compared to an inhomogenic group of cemented and uncoated or other-coated cementless fixations. Some other meta-analyses have demonstrated equal stability by using cemented and cementless implants [5,6,8]. Registry data support that risk of revision rate is significantly higher in uncemented TKA implants in comparison with cemented prosthesis, and the main reason is aseptic loosening [10–11]. The contradictory conclusions derived from these data can be explained by the selection bias of database analysis.

Clinical outcomes, the KSS and KFS in our meta-analysis demonstrated equal functionality of HA-coated cementless and cemented implants. These scoring systems are validated and responsive methods for assessing objective and subjective outcomes after TKA implants. KSS is a weighted score which regards to pain intensity, range of motion, stability and flexion deformities, contractures and poor alignment. The KFS considers mobility parameters of the patient such as the walking distance and stair climbing with deduction for walking aids. In spite of the predictive value of radiological stability, a recent meta-analysis has revealed the differences between postoperative radiological and clinical performance of TKA implants at the same time [5]. Our result is consistent with this previous finding.

The final outcome of TKA implants can also be linked to factors such as the prosthesis type and the risk of developing certain complications of the patient. Early generation of cementless prosthesis demonstrated poor results due to the suboptimal design of the implants [32]. In order to exclude bias derived from the different design of prosthesis types, we enrolled studies comparing HA-coated prostheses with other prostheses from the same uncemented or cemented series of the manufacturer (**S2 Table**).

This study has some limitations. Low survival probability and revision rate of the stems are often cited in the literature as predictor of poor outcome and these factors were not considered in the selected trials. Different trials presented some alterations concerning the operative procedure, whose impact on the outcomes were not evaluated. Besides, comparison of KFS in HA-coated and uncemented groups would have limited value due to the low number of studies in the uncemented group. The included RCTs were homogenous with regard to patient parameters, which, on the one hand provided possibility to exclude selection bias, but on the other hand, the effects of medication, physiotherapy, activity level or systemic diseases (e.g. osteoporosis or osteopenia) could not be evaluated. It would be also important to compare the individual types of cementless knee prosthesis and the outcome of their implantation [33].

Conclusion

In conclusion, this review provides the best available evidence that HA-coated cementless prosthesis outperforms other cementless prostheses both in respect to stability and

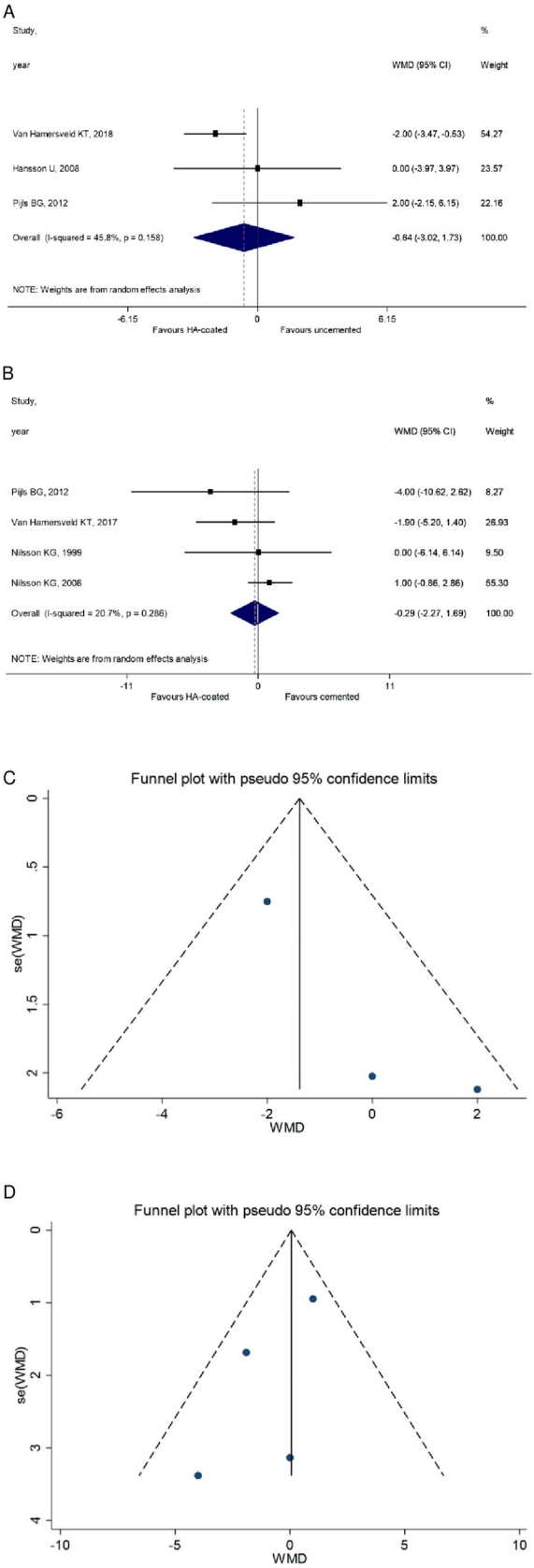
A
Study,
year
WMD (95% CI)
%
Weight
Van Hamersveld KT, 2018
-2.00 (-3.47, -0.53)
54.27
Hansson U, 2008
0.00 (-3.97, 3.97)
23.57
Pijls BG, 2012
2.00 (-2.15, 6.15)
22.16
Overall (I-squared = 45.8%, p = 0.158)
-0.84 (-3.02, 1.73)
100.00
NOTE: Weights are from random effects analysis
-6.15
0
6.15
Favours HA-coated
Favours uncemented
B
Study,
year
WMD (95% CI)
%
Weight
Pijls BG, 2012
-4.00 (-10.62, 2.62)
8.27
Van Hamersveld KT, 2017
-1.90 (-5.20, 1.40)
26.93
Nilsson KG, 1999
0.00 (-6.14, 6.14)
9.50
Nilsson KG, 2006
1.00 (-0.86, 2.86)
55.30
Overall (I-squared = 20.7%, p = 0.286)
-0.29 (-2.27, 1.69)
100.00
NOTE: Weights are from random effects analysis
-11
0
11
Favours HA-coated
Favours cemented
C
Funnel plot with pseudo 95% confidence limits
se(WMD)
0
.5
1
1.5
2
-6
-4
-2
0
2
WMD
D
Funnel plot with pseudo 95% confidence limits
se(WMD)
0
1
2
3
4
-10
-5
0
5
10
WMD

Fig 4. **A** KSS analysis 2 years follow-up; HA-coated. cementless vs uncemented. The value of the uncemented is lesser than of HA-coated cementless group. **B** KSS of the HA-coated cementless vs. cemented group. The value of cemented KSS did not differ significantly from that of HA-coated. **C** Funnel plot 2 years follow-up; HA-coated cementless vs. uncemented group. **D** Funnel plot 2 years follow-up; HA-coated cementless vs. cemented group.

https://doi.org/10.1371/journal.pone.0232378.g004

functionality. Cemented fixation of prostheses provide the best stability in a 2-year follow-up, however, functional results are not superior to HA-coated cementless fixation. Based on these results, HA-coated cementless TKA implants is a recommended option for treating end-stage

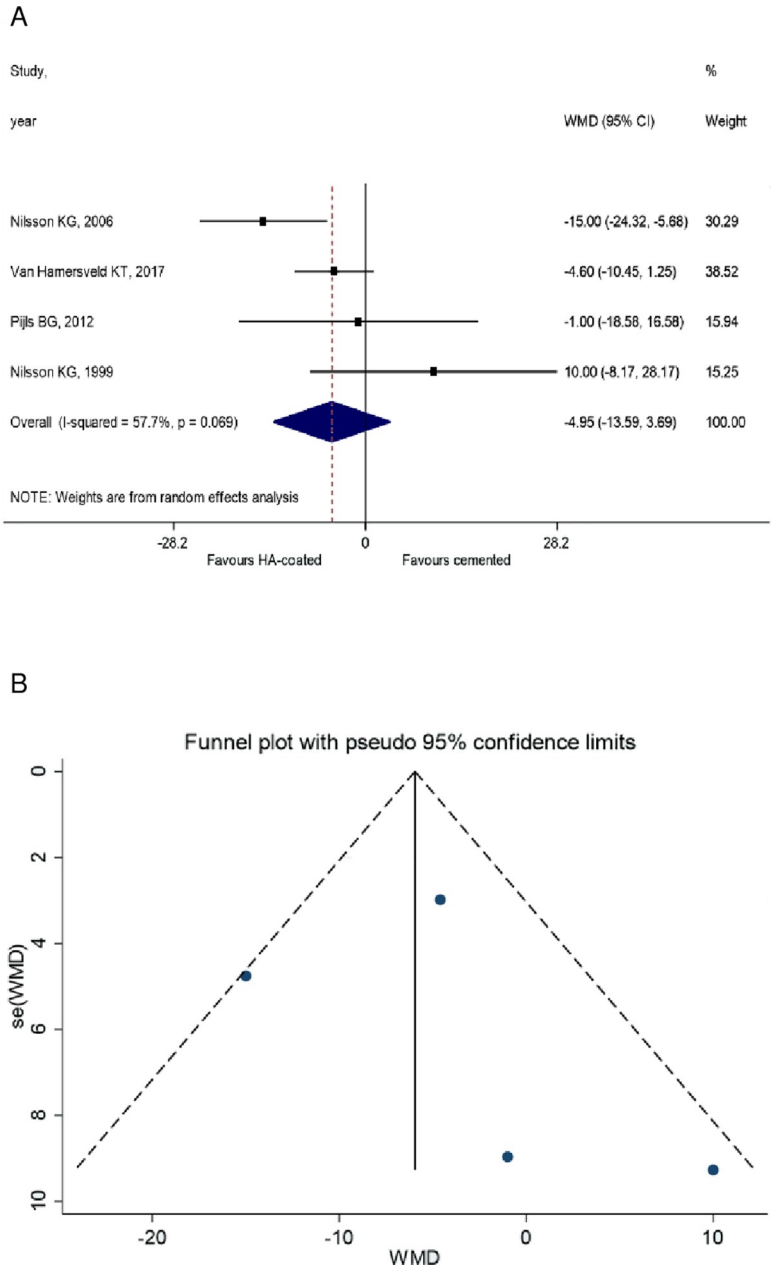

Fig 5. **A** KFS value of the cemented and the HA-coated cementless group. The value of cemented is not significantly different from the HA-coated cementless group. **B** Funnel plot 2 years follow-up; HA-coated cementless vs. uncemented group.

https://doi.org/10.1371/journal.pone.0232378.g005

arthritis of the knee, and clinicians consider together with patients the factors associated with the risk of revision when choosing the most appropriate procedure.

Supporting information

S1 Table. PRISMA checklist for preferred reporting items for systematic reviews and meta-analyses.
(PDF)

S2 Table. Type of prosthesis.
(PDF)

S3 Table. KSS and KFS data together with the MTPM values.
(PDF)

S4 Table. Quality of evidence.
(PDF)

S1 Fig. Search strategy.
(PDF)

S2 Fig. Trial sequential analysis of the primary outcomes. A: The cumulative z-curve surpassed the conventional boundary for statistical significance. However, none of the trial sequential monitoring boundaries have been surpassed in the TSA. Therefore, the result is inconclusive, the required information size (1723) has not yet been achieved. B: The cumulative z-curve crossed both the conventional boundary and the trial sequential monitoring boundary, and the required information size has been achieved. There is no need to include further studies to confirm the significant result.
(PDF)

Author Contributions

Conceptualization: Tamara Horváth, Petra Hartmann.

Formal analysis: Tamara Horváth, Edina Butt, Endre Csonka.

Funding acquisition: Petra Hartmann.

Investigation: Tamara Horváth, Edina Butt.

Methodology: Lilla Hanák, Endre Csonka.

Project administration: Zsolt Szakács.

Software: Lilla Hanák.

Supervision: Péter Hegyi, Margit Solymár.

Writing – original draft: Tamara Horváth, Petra Hartmann.

Writing – review & editing: Péter Hegyi, Margit Solymár, Ákos Szűcs, Orsolya Varga, Bui Quoc Thien, Zsolt Szakács.

References

1. Newman JM, Sodhi N, Khlopas A, Sultan AA, Chughtai M, Abraham R, et al. Cementless Total Knee Arthroplasty. A Comprehensive Review of the Literature, Orthop. 2018; 1; 41(5): 263–273.

2. Bauer TW, Geesink RC, Zimmerman R, McMahon JT. Hydroxyapatite-coated femoral stems. Histological analysis of components retrieved at autopsy. J Bone Joint Surg Am. 1991; 73(10): 1439–52. PMID: 1748693

3. Hamadouche M, Sedel L. Ceramics in orthopaedics. J Bone Joint Surg Br. 2000; 82(8):1095–9. https://doi.org/10.1302/0301-620x.82b8.11744 PMID: 11132264

4. Carlsson A, Bjorkman A, Besjakov J, Onsten I. Cemented tibial component fixation performs better than cementless fixation: a randomized radiostereometric study comparing porous-coated, hydroxyapatite-coated and cemented tibial components over 5 years. Acta Orthop. 2005; 76 (3): 362–9. PMID: 16156464

5. Röhrl SM, Nivbrant B, Ström H, Nilsson KG. Effect of augmented cup fixation on stability, wear, and osteolysis: a 5-year follow-up of total hip arthroplasty with RSA. J Arthroplasty. 2004; 19(8):962–71. https://doi.org/10.1016/j.arth.2004.06.024 PMID: 15586331

6. Zhou K, Yu H, Li J, Wang H Zhou Z, Pei F. No difference in implant survivorship and clinical outcomes between full-cementless and full-cemented fixation in primary total knee arthroplasty: A systematic review and meta-analysis. Int J Surg. 2018; 53: 312–319. https://doi.org/10.1016/j.ijsu.2018.04.015 PMID: 29656129

7. Wang H, Lou H, Zhang H, Jiang J, Liu K. Similar survival between uncemented and cemented fixation prostheses in total knee arthroplasty: a meta-analysis and systematic comparative analysis using registers. Knee Surg Sports Traumatol Arthrosc. 2014; 22(12): 3191–7. https://doi.org/10.1007/s00167-013-2806-3 PMID: 24337525

8. Voigt JD, Mosier M. Hydroxyapatite (HA) coating appears to be of benefit for implant durability of tibial components in primary total knee arthroplasty. Acta Orthop. 2011; 82(4): 448–459. https://doi.org/10.3109/17453674.2011.590762 PMID: 21657975

9. Nakama GY, Peccin MS, Almeida GJM, Lira Neto ODA, Queiroz AAB, Navarro RD. Cemented, cementless or hybrid fixation options in total knee arthroplasty for osteoarthritis and other non-traumatic diseases (Review). Cochrane Database Syst Rev. 2012; 10: CD006193. https://doi.org/10.1002/14651858.CD006193.pub2 PMID: 23076921

10. Gandhi R, Tsvetkov D, Davey J R, Mahomed NN. Survival and clinical function of cemented and uncemented prostheses in total knee replacement: a meta-analysis. J Bone Joint Surg Br. 2009; 91(7): 889–95. https://doi.org/10.1302/0301-620X.91B7.21702 PMID: 19567852

11. Australian Orthopaedic Association National Joint Replacement Registry (AOANJRR) Annual report 2018. Available: https://aoanjrr.sahmri.com.

12. National Joint Replacement Registry of England, Wales, and Northern Ireland (NJR)) Annual report 2018. Available: http://www.njrcentre.org.uk/njrcentre/default.aspx.

13. Hughes RE, Batra A, Hallstrom BR. Arthroplasty registries around the world: valuable sources of hip implant revision risk data. Curr Rev Musculoskelet Med. 2017; 10(2): 240–252. https://doi.org/10.1007/s12178-017-9408-5 PMID: 28337731

14. Laende EK, Astephen Wilson JL, Mills Flemming J, Valstar ER, Richardson CG, Dunbar MJ. Equivalent 2-year stabilization of uncemented tibial component migration despite higher early migration compared with cemented fixation: an RSA study on 360 total knee arthroplasties. Acta Orthop. 2019; 90(2): 172–178. https://doi.org/10.1080/17453674.2018.1562633 PMID: 30669909

15. Pijls BG, Valstar ER, Kaptein BL, Fiocco M, Nelissen RG. The beneficial effect of hydroxyapatite lasts: a randomized radiostereometric trial comparing hydroxyapatite-coated, uncoated, and cemented tibial components for up to 16 years. Acta Orthop. 2012a; 83(2): 135–41. https://doi.org/10.3109/17453674.2012.665330 PMID: 22329667

16. Nelissen RGHH, Valstar ER, Rozing PM. The effect of hydroxyapatite on the micromotion of total knee prostheses: A prospective, randomized, double-blind study. J Bone Jt Surg. 1998; (11): 1665–1672.

17. Liberati A, Altman DG, Tetzlaff J, Mulrow C, Gøtzsche PC, Ioannidis JP, et al. The PRISMA statement for reporting systematic reviews and meta-analyses of studies that evaluate healthcare interventions: explanation and elaboration. BMJ. 2009; 339 b2700. https://doi.org/10.1136/bmj.b2700 PMID: 19622552

18. Wan X., Wang W., Liu J., Tong T. Estimating the sample mean and standard deviation from the sample size, median, range and/or interquartile range. BMC Med Res Methodol, 2014; 14(1) p. 135.

19. Valstar ER, Gill R, Ryd L, Flivik G, Börlin N, Kärrholm J. Guidelines for standardization of radiostereometry (RSA) of implants. Acta Orthop. 2005; 76(4):563–72. https://doi.org/10.1080/17453670510041574 PMID: 16195075

20. Hildebrand D R., Trappmann C, Georg S, at el. Welchen Effekt hat die Hydroxylapatitbeschichtung beim zementfreien Kniegelenkersatz? Der Orthopäde. 2003; 32(4):323–330. https://doi.org/10.1007/s00132-002-0443-5 PMID: 12707697

21. Regnér L., MD, Carlsson L., MD, Ka¨rrholm J., MD, and Herberts P., MD Tibial Component Fixation in Porousand Hydroxyapatite-Coated Total Knee Arthroplasty A Radiostereometric Evaluation of Migration and Inducible Displacement After 5 Years. The Journal of Arthroplasty. 2000; Vol. 15 No. 6.

22. Nilsson KG, Kärrholm J, Carlsson L, Dalén T. Hydroxyapatite coating versus cemented fixation of the tibial component in total knee arthroplasty: prospective randomized comparison of hydroxyapatite-coated and cemented tibial components with 5-year follow-up using radiostereometry. J Arthroplasty. 1999; 14(1):9–20. https://doi.org/10.1016/s0883-5403(99)90196-1 PMID: 9926947

23. Nilsson KG, Henricson A, Norgren B, Dalen T. Uncemented HA-coated implant is the optimum fixation for TKA in the young patient. Clin Orthop Relat Res. 2006; 448: 129. https://doi.org/10.1097/01.blo.0000224003.33260.74 PMID: 16826107

24. Toksvig-Larsen S, Jorn LP, Ryd L, Lindstrand A. Hydroxyapatite-enhanced tibial prosthetic fixation. Clin Orthop Relat Res. 2000; (370):192–200. https://doi.org/10.1097/00003086-200001000-00018 PMID: 10660713

25. Hansson Ulrik, Ryd Leif, Toksvig-Larsen Sören. A randomised RSA study of Peri-Apatite™ HA coating of a total knee prosthesis. The Knee. 2008; Volume 15, Pages 211–216. https://doi.org/10.1016/j.knee.2008.01.013 PMID: 18329882

26. Van Hamersveld KT, Marang-Van De Mheen PJ, Nelissen RGHH, Toksvig-Larsen S. Peri-apatite coating decreases uncemented tibial component migration: long-term RSA results of a randomized controlled trial and limitations of short-term results. Acta Orthop. 2018; 89(4):425–430. https://doi.org/10.1080/17453674.2018.1469223 PMID: 29741133

27. Van Hamersveld KT, Marang-van de Mheen PJ, Tsonaka R, Valstar ER, Toksvig-Larsen. Fixation and clinical outcome of uncemented peri-apatite-coated versus cemented total knee arthroplasty: five-year follow-up of a randomised controlled trial using radiostereometric analysis (RSA). Bone Joint J. 2017; 99-B (11):1467–1476. https://doi.org/10.1302/0301-620X.99B11.BJJ-2016-1347.R3 PMID: 29092985

28. Ryd L, Albrektsson BE, Carlsson L, Dansgard F, Herberts P, Lindstrand A, et al. Roentgen stereophotogrammetric analysis as a predictor of mechanical loosening of knee prostheses. J Bone Joint Surg Br. 1995; 77(3): 377–83. PMID: 7744919

29. Higgins JP, Altman DG, Gøtzsche PC, Jüni P, Moher D, Oxman AD, et al. Cochrane Bias Methods Group; Cochrane Statistical Methods Group. The Cochrane Collaboration's tool for assessing risk of bias in randomised trials. BMJ. 2011; 343:d5928. https://doi.org/10.1136/bmj.d5928 PMID: 22008217

30. NICE Technology Appraisal Guidance TA304: Total hip replacement and resurfacing arthroplasty for end-stage arthritis of the hip (review of technology appraisal guidance 2 and 44; 2014.

31. Beaupré LA, PhD, PT, al-Yamani M., MD, Huckell JR., BSc, MDCM, FRCS(C), and Johnston DWC., MD, FRCS(C) Hydroxyapatite-Coated Tibial Implants Compared with Cemented Tibial Fixation in Primary Total Knee Arthroplasty. J Bone Joint Surg. 2007; 89: 2204–11. https://doi.org/10.2106/JBJS.F.01431 PMID: 17908897

32. Ryd L. Micromotion in knee arthroplasty. Acta Orthop. 1986; 57 (S220): 3–80.

33. Selvik G. Roentgen stereophotogrammetry. A method for the study of the kinematics of the skeletal system. Acta Orthop Scand Suppl. 1989; 232: 1–51. PMID: 2686344

PLOS ONE

Mitochondrial dysfunction affects the synovium of patients with rheumatoid arthritis and osteoarthrosis differently

--Manuscript Draft--

Manuscript Number:	PONE-D-21-09721
Article Type:	Research Article
Full Title:	Mitochondrial dysfunction affects the synovium of patients with rheumatoid arthritis and osteoarthrosis differently
Short Title:	Mitochondrial dysfunction in rheumatoid arthritis and osteoarthrosis
Corresponding Author:	Petra Hartmann University of Szeged, Hungary Szeged, HUNGARY
Keywords:	rheumatoid arthritis; osteoarthrosis; mitochondrial respiration; complex I; cytochrome C
Abstract:	Background : There is growing evidence for the role of mitochondrial dysfunction in osteoarthritis (OA) and rheumatoid arthritis (RA). However, quantitative comparison of mitochondrial derangements in these main arthritis forms in clinical settings is missing. Therefore, our aim was to characterize altered mitochondrial functions in synovial membranes of OA and RA patients. Methods : Prospective clinical study was conducted on adult patients undergoing knee surgery. Patients were allocated into RA and OA groups based on disease specific clinical scores, while patients without arthritis and under 40 years of age served as controls. Synovial tissue samples were taken intraoperatively and subjected to high-resolution respirometry (Oxygraph-2k, Oroboros Instruments, Austria) to analyze mitochondrial oxygen consumption. The oxidative phosphorylation (OxPhos) capacity and the relative contribution of respiratory complexes I and II were determined, together with the coupling of the mitochondrial respiratory chain (coupling control ratio, CCR). The release of cytochrome C (shuttles electrons between complexes III and IV) was also determined, in parallel with biochemical and histopathological evaluation of the samples. Results : From the total of 528 patients, 71 cases were enrolled to the study (17 RA, 31 OA and 23 control patients) between 01 September 2019 and 30 November 2020. The complex I-related OxPhos, CCR and cytochrome c release were significantly decreased in the synovial samples of RA patients as compared to OA patients (61.9±14.8 pmol/s/ml vs 92.3±17.2 pmol/s/ml), while both displayed reduced complex I OxPhos activity than the control group (115.2±26.2 pmol/s/ml). However, no significant difference was found in complex II-related activity. Biochemical parameters and histopathology confirmed chronic inflammation in both arthritis groups. Conclusions: According to our findings, in contrast to complex I, complex II does not play a central role in mitochondrial dysfunction in RA and OA. Consequently, focusing on complex I specific mitochondrial protective agents in arthritis research may have major benefits.
Order of Authors:	Péter Jávor
	Attila Mácsai
	Edina Butt
	Bálint Baráth
	Dávid Kurszán Jász
	Tamara Horváth
	Bence Baráth
	Ákos Csonka
	László Török
	Endre Varga
	Petra Hartmann

Opposed Reviewers:	
Additional Information:	
Question	Response
Financial Disclosure Enter a financial disclosure statement that describes the sources of funding for the work included in this submission. Review the submission guidelines for detailed requirements. View published research articles from *PLOS ONE* for specific examples. This statement is required for submission and **will appear in the published article** if the submission is accepted. Please make sure it is accurate. **Unfunded studies** Enter: *The author(s) received no specific funding for this work.* **Funded studies** Enter a statement with the following details: • Initials of the authors who received each award • Grant numbers awarded to each author • The full name of each funder • URL of each funder website • Did the sponsors or funders play any role in the study design, data collection and analysis, decision to publish, or preparation of the manuscript? • **NO** - Include this sentence at the end of your statement: *The funders had no role in study design, data collection and analysis, decision to publish, or preparation of the manuscript.* • **YES** - Specify the role(s) played. * typeset	The study was supported by the following National Research Development and Innovation Office grants: NKFI K120232. (P.H.) (https://nkfih.gov.hu/) It was further supported by Human Resource Development Operational Program EFOP 3.6.3-VEKOP-16-2017-00009. (P.J.)(https://ec.europa.eu/regional_policy/en/atlas/programmes/2014-2020/hungary) The funders had no role in study design, data collection and analysis, decision to publish, or preparation of the manuscript.
Competing Interests Use the instructions below to enter a competing interest statement for this submission. On behalf of all authors, disclose any competing interests that could be perceived to bias this work—acknowledging all financial support and any other relevant financial or non-financial competing interests.	The authors have declared that no competing interests exist.

This statement is required for submission and **will appear in the published article** if the submission is accepted. Please make sure it is accurate and that any funding sources listed in your Funding Information later in the submission form are also declared in your Financial Disclosure statement. View published research articles from *PLOS ONE* for specific examples. **NO authors have competing interests** Enter: *The authors have declared that no competing interests exist.* **Authors with competing interests** Enter competing interest details beginning with this statement: *I have read the journal's policy and the authors of this manuscript have the following competing interests: [insert competing interests here]* * typeset	
Ethics Statement Enter an ethics statement for this submission. This statement is required if the study involved: • Human participants • Human specimens or tissue • Vertebrate animals or cephalopods • Vertebrate embryos or tissues • Field research Write "N/A" if the submission does not require an ethics statement. General guidance is provided below. Consult the submission guidelines for detailed instructions. **Make sure that all**	The study was conducted in accordance with the Declaration of Helsinki and has been approved by the local medical ethics committee at the University of Szeged (Humán Orvosbiológiai Intézményi és Regionális Kutatásetikai Bizottsága) under reference number 85/2019-SZTE. Written ethical consent has been obtained.

information entered here is included in the Methods section of the manuscript. **Format for specific study types** **Human Subject Research (involving human participants and/or tissue)** • Give the name of the institutional review board or ethics committee that approved the study • Include the approval number and/or a statement indicating approval of this research • Indicate the form of consent obtained (written/oral) or the reason that consent was not obtained (e.g. the data were analyzed anonymously) **Animal Research (involving vertebrate animals, embryos or tissues)** • Provide the name of the Institutional Animal Care and Use Committee (IACUC) or other relevant ethics board that reviewed the study protocol, and indicate whether they approved this research or granted a formal waiver of ethical approval • Include an approval number if one was obtained • If the study involved *non-human primates*, add *additional details* about animal welfare and steps taken to ameliorate suffering • If anesthesia, euthanasia, or any kind of animal sacrifice is part of the study, include briefly which substances and/or methods were applied **Field Research** Include the following details if this study involves the collection of plant, animal, or other materials from a natural setting: • Field permit number • Name of the institution or relevant body that granted permission	
Data Availability Authors are required to make all data underlying the findings described fully available, without restriction, and from the time of publication. PLOS allows rare exceptions to address legal and ethical	Yes - all data are fully available without restriction

concerns. See the PLOS Data Policy and FAQ for detailed information. A Data Availability Statement describing where the data can be found is required at submission. Your answers to this question constitute the Data Availability Statement and **will be published in the article**, if accepted. **Important:** Stating 'data available on request from the author' is not sufficient. If your data are only available upon request, select 'No' for the first question and explain your exceptional situation in the text box. Do the authors confirm that all data underlying the findings described in their manuscript are fully available without restriction?	
Describe where the data may be found in full sentences. If you are copying our sample text, replace any instances of XXX with the appropriate details. • If the data are **held or will be held in a public repository**, include URLs, accession numbers or DOIs. If this information will only be available after acceptance, indicate this by ticking the box below. For example: *All XXX files are available from the XXX database (accession number(s) XXX, XXX.*). • If the data are all contained **within the manuscript and/or Supporting Information files**, enter the following: *All relevant data are within the manuscript and its Supporting Information files.* • If neither of these applies but you are able to provide **details of access elsewhere**, with or without limitations, please do so. For example: *Data cannot be shared publicly because of [XXX]. Data are available from the XXX Institutional Data Access / Ethics Committee (contact via XXX) for researchers who meet the criteria for access to confidential data.*	All relevant data are within the manuscript and its Supporting Information files.

The data underlying the results presented in the study are available from (include the name of the third party and contact information or URL). • This text is appropriate if the data are owned by a third party and authors do not have permission to share the data. * typeset	
Additional data availability information:	

Szegedi Tudományegyetem
SZENT-GYÖRGYI ALBERT KLINIKAI KÖZPONT
ÁLTALÁNOS ORVOSTUDOMÁNYI KAR

TRAUMATOLÓGIAI KLINIKA
Igazgató:
PROF. DR. VARGA ENDRE
tanszékvezető egyetemi tanár
✉ H-6725 Szeged, Semmelweis u. 6.
☎ *(36-62) 545-531 Fax: (36-62) 545-530*

Emily Chenette
Editor-in-Chief
PLOS ONE

Petra Hartmann
Institute of Surgical Research
University of Szeged

March 22, 2021.

Research Article

"Mitochondrial dysfunction differently affects the synovium of patients with rheumatoid arthritis and osteoarthrosis" by Jávor P. et al.

Dear Prof. Chenette,

we have submitted the attached manuscript for consideration for publication in *PLOS ONE*.

There is growing evidence for the role of mitochondrial dysfunction in osteoarthritis (OA) and rheumatoid arthritis (RA). However, due to the small amount of quantitative clinical data available in the literature, the characteristics of mitochondrial derangements in OA and RA have not been compared yet.
Our present record is a prospective clinical study that makes OA and RA comparable with regards to mitochondrial dysfunctions. High-resolution respirometry, biochemical analyses and histopathological evaluation were performed on human synovial membrane samples to provide quantitative data on oxidative phosphorylation capacity, cytochrome C-release, pathways of reactive oxygen species production, and disease severity.
Besides several similarities, substantial differences could be revealed between the features of mitochondrial impairment in OA and RA. Furthermore, our findings strongly suggest the central role of mitochondrial Complex I in both diseases, highlighting it as a target for future disease-modifying drugs.

We hope that these data will be judged to be of sufficient interest to the readership of the Journal. All authors have read, and approved submission of the manuscript and it has not been published and is not being considered for publication elsewhere in whole or part in any language. No commercial financial support or other financial interests, which could create a potential conflict of interest, are declared.

We are looking forward to hearing from you at your earliest convenience and thank you for your kind assistance.

Sincerely yours,

Dr. Petra Hartmann
corresponding author

Mitochondrial dysfunction affects the synovium of patients with rheumatoid arthritis and osteoarthrosis differently

Péter Jávor[1¶], Attila Mácsai[1¶], Edina Butt[1], Bálint Baráth[2], Dávid Kurszán Jász[2], Tamara Horváth[2], Bence Baráth[3], Ákos Csonka[1], László Török[1,4], Endre Varga[1], Petra Hartmann[2*]

[1]*Department of Traumatology, University of Szeged, Szeged, Hungary*

[2]*Institute of Surgical Research, University of Szeged, Szeged, Hungary*

[3]*Department of Pathology, University of Szeged, Szeged, Hungary*

[4]*Department of Sports Medicine, University of Szeged, Szeged, Hungary*

*Corresponding author

E-mail: hartmann.petra@med.u-szeged.hu

[¶]These authors contributed equally to this work.

List of abbreviations

ACR/EULAR	American College of Rheumatology/European League Against Rheumatism
ATP	adenosine triphosphate
BMI	body mass index
C	complexes
CCR	coupling control ratio
CLSM	confocal laser scanning endomicroscope
CRP	C-reactive protein
DAMPs	damage-associated molecular patterns
ETC	electron transport chain
HClO	hypochlorous acid
ICD	International Statistical Classification of Diseases and Related Health Problems
KL	Kellgren-Lawrence
MPO	myeloperoxidase
NSAIDs	nonsteroidal anti-inflammatory drugs
NT	nitrotyrosine
OA	osteoarthrosis
RA	rheumatoid arthritis

RANKL	nuclear factor kappa-beta ligand
RCR	respiratory control ratio
ROS	reactive oxygen species
SCID	severe combined immunodeficiency
TP	total protein
TNF-α	tumor necrosis factor alpha
WBC	white blood cell count
XOR	xanthine oxidoreductase

Abstract

Background

There is growing evidence for the role of mitochondrial dysfunction in osteoarthritis (OA) and rheumatoid arthritis (RA). However, quantitative comparison of mitochondrial derangements in these main arthritis forms in clinical settings is missing. Therefore, our aim was to characterize altered mitochondrial functions in synovial membranes of OA and RA patients.

Methods

Prospective clinical study was conducted on adult patients undergoing knee surgery. Patients were allocated into RA and OA groups based on disease specific clinical scores, while patients without arthritis and under 40 years of age served as controls. Synovial tissue samples were taken intraoperatively and subjected to high-resolution respirometry (Oxygraph-2k, Oroboros Instruments, Austria) to analyze mitochondrial oxygen consumption. The oxidative phosphorylation (OxPhos) capacity and the relative contribution of respiratory complexes I and II were determined, together with the coupling of the mitochondrial respiratory chain (coupling control ratio, CCR). The release of cytochrome C (shuttles electrons between complexes III and IV) was also determined, in parallel with biochemical and histopathological evaluation of the samples.

Results

From the total of 528 patients, 71 cases were enrolled to the study (17 RA, 31 OA and 23 control patients) between 01 September 2019 and 30 November 2020. The complex I-related OxPhos, CCR and cytochrome c release were significantly decreased in the synovial samples of RA patients as compared to OA patients (61.9±14.8 pmol/s/ml vs

92.3±17.2 pmol/s/ml), while both displayed reduced complex I OxPhos activity than the control group (115.2±26.2 pmol/s/ml). However, no significant difference was found in complex II-related activity. Biochemical parameters and histopathology confirmed chronic inflammation in both arthritis groups.

Conclusions

According to our findings, in contrast to complex I, complex II does not play a central role in mitochondrial dysfunction in RA and OA. Consequently, focusing on complex I specific mitochondrial protective agents in arthritis research may have major benefits.

Keywords: rheumatoid arthritis; osteoarthrosis; mitochondrial respiration; complex I; cytochrome C

Introduction

Arthritis is a collective term for inflammatory diseases affecting the joints with distinct etiologies ranging from the most common form osteoarthrosis (OA) to rheumatoid arthritis (RA), but joint dysfunction and pain are common characteristics [1]. A growing body of evidence implicates the role of mitochondrial damage and dysfunction in OA and RA [2-6]. Mitochondria are both targets and sources of inflammation-associated injury in the synovial membrane of patients, hence injury and necrosis of synoviocytes induce the release of mitochondrial damage-associated molecular patterns (DAMPs) from damaged mitochondria [7]. DAMPs trigger innate and adaptive immune responses, thus promote the release of proinflammatory mediators and the aggregation of inflammatory cells. Mitochondrial dysfunction has also been implicated in the pathogenesis of primary and post-traumatic OA [8]. Some haplogroups of mitochondrial respiratory genes, and as a consequence, mitochondrial respiratory activity are closely associated with higher prevalence of OA and RA resulting in an increased genetic predisposition to the development of arthritis [9].

RA and OA are common forms of arthritis sharing several similarities despite of different pathogenesis. Chronic synovitis, dysregulation of synovial functions, and progressive destruction of articular cartilage occur in both disorders. In contrast to OA, RA displays more prominent inflammatory processes, and it is also characterized by the presence of an invasive synovial membrane (pannus tissue) [10]. With regards to the etiology, OA is induced by mechanical injuries, while RA is considered as a multifactorial, multigenic autoimmune disease [2]. Although the contribution of mitochondrial impairment is well

known in both diseases, quantitative clinical data on its extent is hardly available in the literature.

As mitochondria are also involved in the development of inflammation and inflammatory damage, they can also be considered as future therapeutic targets for OA and RA [11, 12]. However, in spite of intensive research efforts, the etiology of arthritis-related mitochondrial dysfunction is not completely understood [13], and novel disease-modifying regimens are still not available. Furthermore, the characteristics of mitochondrial derangements in OA and RA have not been compared yet. For these reasons, mitochondrial signaling pathways in the pathophysiology of joint diseases need further investigation, mainly human studies [5, 13, 14].

According to previous studies, mitochondrial dysfunction may affect several pathways that have been implicated in joint degradation, including hypoxia-induced signaling pathways of synovial epithelial cells, defective chondrocyte biosynthesis and growth responses [3, 4, 15]. Impaired electron transport through mitochondrial complexes has also been demonstrated with higher reactive oxygen species (ROS) production and lower ATP levels in chondrocytes of OA patients as compared with healthy patients [16]. Studies demonstrate that the synovium may show significant changes prior to subchondral and cartilage degeneration, thus suggesting its initiative role in joint failure [17]. The arthrogenic role of the synovium has been demonstrated upon transfer of isolated human RA synovial fibroblasts into the knee of severe combined immunodeficiency (SCID) mice, where they induced chronic arthritis [18]. The deteriorative pathways are suspected to be promoted by the derangements of the

mitochondrial respiratory chain complexes (C I-IV), altered ATP-synthesis, cytochrome C release and increased oxidative and nitrosative stress in the synovium [4, 19].

Our present clinical study investigates the role of synovial mitochondrial dysfunction in RA and OA. We provide quantitative clinical data making the two arthritis types comparable with respect to mitochondrial dysfunction. Mitochondrial respiratory activities, cytochrome C release, and pathways of ROS production were studied in homogenates of synovial epithelial cells of RA, OA, and healthy control patients, respectively. In order to give a complex analysis of the joint status of our participants, histopathological examinations and measurements of proinflammatory cytokine levels were also performed. We hope that our results can add to the relatively small amount of scientific information available in this new, promising field of arthritis research.

Materials and Methods

Ethical approval

The study was conducted in accordance with the Declaration of Helsinki and has been approved by the local medical ethics committee at the University of Szeged under reference number 85/2019-SZTE.

Study design

Prospective clinical study was conducted at a single, level I trauma center (Department of Traumatology at the University of Szeged) between 01 September 2019 and 30 November 2020.

Data were collected from consecutive, adult patients (age > 18 years) with signed informed consent undergoing open or arthroscopic knee joint surgery. Pediatric patients

and patients with multiple injuries, septic conditions, inadequate compliance, or incomplete dataset were excluded.

Labor parameters (white blood cell count (WBC), C-reactive protein (CRP), total protein (TP)), clinically relevant information (age, gender, height, weight, Body Mass Index (BMI), International Statistical Classification of Diseases and Related Health Problems (ICD) codes, comorbidities, previous joint injuries, medication, etiology, current activity of OA and type of operation were extracted from electronic database (MedSolution). Additional information regarding subjective life quality, the level of everyday joint pain (according to VAS) and the use of orthoses and walking aids were obtained from a detailed questionnaire.

Patient allocation

Participants were allocated into RA, OA and control groups based on their medical documentation, 2010 American College of Rheumatology/European League Against Rheumatism (ACR/EULAR) rheumatoid arthritis classification criteria and Kellgren-Lawrence (KL) classification. Patients were allocated into the RA group if they have already been diagnosed with RA and fulfilled the 2010 ACR/EULAR score ≥6 criterion. For the diagnosis of OA, the KL classification is the most widely used radiographic clinical tool [20, 21]. AP knee radiographs were graded from 0 to 4, according to KL-criteria, by two independent orthopedic trauma experts (Á.C., A.M.). A grade >1 entailed an allocation to the OA group, independently from the etiology of the disease (both primary and posttraumatic cases were included). The control group consisted of patients under the age of 40 with a KL grade ≤1.

Sampling

Synovial fluid and tissue samples from the knee joint synovium were taken with the permission and signed consent of the patients. Synovial fluid was aspirated prior to incision, with an 18 G needle, and placed into Eppendorf tubes. Synovium tissue samples of 1x1 cm in size were obtained from the suprapatellar pouch, sparing the Hoffa's fat pad. The samples were placed into 4% (v/v) neutral buffered formalin and phosphate buffered saline (PBS), and transported on ice directly to undergo biochemical measurements, histopathological evaluation and high-resolution respirometry respectively [22].

Examination of mitochondrial functions

The efficacy of mitochondrial respiration was assessed from synovium homogenates by high-resolution respirometry (Oxygraph-2k, Oroboros Instruments, Innsbruck, Austria). The tissue samples were homogenized in 200 µl of MiR05 respiration medium [23] with a glass Potter-Elvehjem homogenizer. Subsequently, the homogenates were weighed into the detection chambers, 50 µl in each, which were calibrated to 200 nmol/ml oxygen concentration in room air. Our protocol was used to explore the relative contribution of respiratory complexes to the electron transport chain (ETC) and the oxidative phosphorylation capacity (OxPhos) of mitochondria. First, the steady-state basal oxygen consumption of the homogenates (respiratory flux) was measured. Glutamate (10 mM) and malate (2 mM) were used in combination to induce C I-linked respiration. Complex II-linked baseline respiration (10 mM succinate-fuelled, in the presence of C I inhibitor 0.5 µM rotenone) was determined, then oxidative phosphorylation capacity was measured by adding saturating ADP (5 mM final concentration). Cytochrome C release (an indicator of inner mitochondrial membrane damage) was determined as described previously [24]. The intactness of the inner mitochondrial membrane was assessed after adding

cytochrome C (10 μM). Leak respiration (LEAK) was measured in the presence of C V inhibitor oligomycin (Omy) (1 mM). Thereafter, protonophore agent carbonyl cyanide p-trifluoromethoxy-phenyl-hydrazine (FCCP) (0.5 μM) was added to measure ETC coupling. Finally, residual oxygen consumption (ROX) was determined by adding 1 μM rotenone (Rot) and 1 μM antimycin-A (Ama).

Biochemical analyses

Tissue xanthine oxidoreductase (XOR) activity

Synovial membrane samples were homogenized in phosphate buffer (pH 7.4) containing 50 mM Tris-HCl, 0.1 mM EDTA, 0.5 mM dithiotreitol, 1 mM phenylmethylsulfonyl fluoride, 10 μg ml^{-1} soybean trypsin inhibitor, and 10 μg ml^{-1} leupeptin. The homogenate was centrifuged at 4 ^{o}C for 20 min at 24.000 g, and the supernatant was loaded into centrifugal concentrator tubes. The activity of XOR was determined in the ultrafiltered supernatant by a fluorometric kinetic assay based on the conversion of pterine to isoxanthopterine in the presence (total XOR) or absence (XO activity) of the electron acceptor methylene blue [25].

Tissue myeloperoxidase (MPO) activity

The MPO activity was measured in synovial tissue according to the method of Kuebler et al [26]. Briefly, the synovial tissue was homogenized with Tris-HCl buffer (0.1 M, pH 7.4) containing 0.1 M polymethylsulfonyl fluoride to block tissue proteases, and then centrifuged at 4 °C for 20 min. at 24.000 g. The MPO activity of the samples was measured at 450 nm (UV-1601 spectrophotometer; Shimadzu, Japan). The data was referred to the protein content.

Nitrotyrosine (NT) levels

Free nitrotyrosine, as a marker of peroxynitrite generation, was measured by enzyme-linked immunosorbent assay (Cayman Chemical, Ann Arbor, MI). The synovial fluid was centrifuged at 15,000g. The supernatants were collected and incubated overnight with antinitrotyrosine rabbit IgG and nitrotyrosine acetylcholinesterase tracer in precoated (mouse antirabbit IgG) microplates followed by development with Ellman's reagent. Nitrotyrosine content was normalized to the protein content of the homogenate and expressed in ng/mg.

Laboratory testing of synovial fluid

Proinflammatory cytokines tumor necrosis factor alpha (TNF-α) and receptor activator of nuclear factor kappa-beta ligand (RANKL) levels were measured in the synovial fluid samples using commercially available ELISA kit according to the manufacturer's instruction (Sigma-Aldrich, Budapest, Hungary).

Histopathological analysis

Intraoperatively harvested synovium biopsies were assessed with light microscopy and confocal imaging. Confocal imaging with a laser scanning endomicroscope (CLSM, FIVE1 system, Optiscan, Victoria, Australia) was started immediately after retrieving the synovial sample. The rigid confocal probe (excitation wavelength 488 nm; emission detected at 505–585 nm) was mounted on a specially designed metal frame and gently pressed onto the inner surface of the joint capsule (1 scan/image, 1024 x 512 pixels and 475 x 475 µm per image). For the *in vivo* staining, 0.01% acriflavine (Sigma-Aldrich, Budapest, Hungary) was applied topically [24]. The analysis was performed twice separately by the same investigator (PH) using a semiquantitative histology score (S0-S4) based on widening of synovial lining, neoangiogenesis, collagen fibre disorganization

and fragmentation, as described previously [27]. For traditional light microscopy, the samples were fixed in buffered paraformaldehyde solution (4%) and embedded in paraffin. 5-µm thick sections were cut and then stained with haematoxylin and eosin (H&E).

Statistical analysis

The statistical analysis was performed with SigmaStat 13.0 statistical software (Jandel Corporation, San Rafael, CA, USA). Normal distribution was tested with the Shapiro-Wilk test. In the case of a normal distribution, one-way ANOVA with Tukey's test was used and the data are expressed as mean ± SD. $P < 0.05$ was considered as statistically significant.

Results

Patient characteristics

A total of 528 patients underwent knee joint surgery between 01 September 2019 and 30 November 2020 at the Traumatology Department of the University of Szeged. Inclusion criteria were met in 71 cases, in which 17 patients suffered from RA and 31 from OA. The control group consisted of 23 patients under 40 years of age, without a history of OA and with a need for surgery due to trauma. The mean age of all participants was 51 ± 19 years, 66 ± 9 years in the OA, 56 ± 14 and 27 ± 4 in the RA and control group. The gender ratio was balanced. The members of the OA group had a higher mean Body Mass Index (BMI) compared to the control group. Furthermore, more than 70% of the OA patients had a BMI ≥30. As a well-known fact, a BMI ≥30 doubles the risk of knee OA compared to normal weight or underweight individuals [28]. Most patients in the OA group suffered from a moderate to severe (KL grade 3-4) joint degeneration. Despite of the advanced

255 stages of the disease, only 39% of the OA patients reported a habitual, daily intake of
256 NSAIDs. Prior to surgery, inflammatory markers (CRP, WBC) did not indicate an acute
257 flare up of OA; however, a slightly elevated CRP (<25 mg/L) was measured by more than
258 50% of OA patients. The most common comorbidity of the study population was primary
259 hypertension, affecting 37% of all participants. Samples were taken from the knee joint in
260 72% of the cases. The characteristics of the patients are shown in Table 1.

261

Demographics	All patients (n=71)	RA group (n=17)	OA group (n=31)	Control group (n=23)
Age (y) (mean ± SD)	51 ± 19	56 ± 14	66 ± 9	27 ± 4
Female n (%)	39 (55)	16 (94)	15 (48)	8 (35)
Male n (%)	32 (45)	1 (6)	16 (52)	15 (65)
OA risk factors				
Age >50 years n (%)	41 (58)	11 (65)	30 (97)	0 (0)
BMI (mean ± SD)	29 ± 5	28 ± 4	33 ± 6	26 ± 3
BMI ≥30 n (%)	29 (41)	2 (12)	23 (74)	4 (17)
Joint trauma in the anamnesis n (%)	39 (55)	1 (6)	15 (48)	23 (100)
Disease severity				
ACR/EULAR score (mean ± SD)		7 ± 1		
ACR/EULAR score (median [IQR])		7 [6-7]		
Kellgren-Lawrence Score (mean ± SD)			4 ± 1	
Kellgren-Lawrence Score (median [IQR])			4 [3-4]	
VAS (mean ± SD)		8 ± 2	5 ± 3	
Takes NSAIDs daily n (%)		11 (65)	12 (39)	
Needs walking aid n (%)		8 (47)	16 (52)	
Labor results				
WBC (G/L) (mean ± SD)	9.8 ± 3.6	10.8 ± 3.3	10.3 ± 3.8	8.3 ± 3.0
WBC (G/L) (median [IQR])	9.2 [7.5-12.0]	10.1 [8.8-13.2]	10.0 [7.9-12.1]	7.6 [6.1-10.0]
CRP (mg/L) (mean ± SD)	7.0 ± 7.0	11.2 ± 8.9	7.3 ± 6.1	3.5 ± 4.3
CRP (mg/L) (median [IQR])	5.5 [2.9-8.8]	6.9 [5.4-15.6]	5.6 [3.5-10.4]	2.8 [0.0-5.5]
TP (g/L) (mean ± SD)	70.1 ± 2.9	69.2 ± 2.5	70.5 ± 3.0	70.2 ± 2.7
TP (g/L) (median [IQR])	69.4 [68.5-71.0]	72.2 [67.5-69.8]	69.6 [69.2-71.0]	69.5 [68.5-71.6]
RF positive n (%)		11 (65)		
Comorbidities				
Presence of comorbidities n (%)	38 (54)	14 (82)	21 (68)	3 (13)
Primary hypertension	26 (37)	6 (35)	18 (58)	2 (9)
Diabetes	9 (13)	2 (12)	6 (19)	1 (4)
NIDDM	*8 (11)*	*2 (12)*	*5 (16)*	*1 (4)*
IDDM	*1 (1)*	*0 (0)*	*1 (3)*	*0 (0)*
Gout	3 (4)	1 (6)	2 (6)	0 (0)
Other	22 (31)	12 (71)	10 (32)	0 (0)
Operation type				

Arthroscopy n (%)	32 (45)	2 (12)	9 (29)	21 (91)
Open surgery n (%)	39 (55)	15 (88)	22 (71)	2 (9)

Table 1. Patient characteristics**.** The patients were graded according to Kellgren-Lawrence classification by two independent orthopedic-trauma surgeons. VAS refers to the chronic pain in the joint affected by OA. Acute pain due to acute trauma was not considered. Daily use of NSAIDs refers to habitual drug intake. Taking NSAIDs for a short period after trauma was not regarded as daily use. Crutches, rollators and wheelchairs were categorized as walking aids. Labor parameters were measured prior to joint surgery. CRP levels were not measurable under 2 mg/L, thus a CRP<2 mg/L was considered as 0. OA=osteoarthritis; SD=standard deviation; BMI=body mass index; IQR=interquartile range; VAS=visual analog scale; ACR/EULAR=American College of Rheumatology/European League Against Rheumatism; NSAID=non-steroidal anti-inflammatory drug; WBC=white blood cell; CRP=C-reactive protein; TP=total protein; NIDDM=non-insulin dependent diabetes mellitus; IDDM=insulin dependent diabetes mellitus.

Mitochondrial functional measurements

Changes in mitochondrial respiratory functions were evaluated in the presence of glutamate and malate or succinate in order to differentiate between C I- and C II-based activity. Arthritis groups (92.3 ± 17.2 pmol/s/ml in OA, 61.9 ± 14.8 pmol/s/ml in RA) displayed significantly reduced C I OxPhos activity compared to the control group (115.2 ± 26.2 pmol/s/ml) in the presence of saturating amount of ADP. The decrease in C I-related OxPhos was significantly higher in the synovial samples of RA patients than in OA patients.

Respiratory acceptor control ratio (RCR) and coupling control ratio (CCR) were defined to quantify changes in the coupling of the ETC [24]. RCR is expressed as the OxPhos/LEAK ratio and is directly but non-linearly related to the OxPhos-coupling efficiency. CCR is a flux control ratio at a constant mitochondrial pathway-control state and ranges from 0-1. A reference rate is defined by taking maximum respiratory flux and flux in the electron transfer-state induced by complex-specific substrate, such that the lower and upper limits of the CCR.

In comparison with the control group, C I-based RCR (4.4 ± 1.3 in the control group, 3.0 ± 0.8 in RA) and CCR (0.3 ± 0.1 in the control and OA group, 0.6 ± 0.2 in RA) both indicated a significant impairment of the ETC in the RA group. However, no significant difference was found in C II-related OxPhos, RCR and CCR between the study groups **(Fig. 1.).**

Fig 1. Mitochondrial functional measurements. Complex I (CI) and complex II (CII) related oxidative phosphorylation (OxPhos) capacities of synovial epithelial mitochondria are shown together with the respiratory control ratio (RCR) and coupling control ratio (CCR) of the complexes. Arthritis groups displayed significantly reduced C I activity compared to the control group. The C I-related respiratory control ratio (RCR) of the RA group was significantly lower compared to the control group. C I-related CCR–is significantly higher in the RA group. No significant difference was found in C II-related respiratory activity, RCR and CCR between the study groups. RA group is marked with red columns. Black columns represents the OA group. Control group is marked with white. Data are presented as means ± SD. **P*<0.05 *vs* control; $^{\#}$*P*<0.05 *vs* OA (one-way ANOVA, Tukey's test)

Cytochrome C release

Cytochrome C release was assessed by adding exogenous cytochrome C to the sample in the presence of glutamate and malate or succinate. OA (8.8 ± 2.4 pmol/s/ml) group exhibited significantly higher C I-based response in oxygen consumption compared to the control group (3.9 ± 1.4 pmol/s/ml), indicating lower initial levels of cytochrome C. Furthermore, a significant increase could be detected in the RA group compared with both the control and OA groups in both Complex I- (12.4 ± 2.6 pmol/s/ml) and Complex II-related (3.7 ± 1.1 pmol/s/ml in the control group, 4.6 ± 1.1 pmol/s/ml in OA, 10.5 ± 3.5 pmol/s/ml in RA) activity **(Fig. 2).**

Fig 2. Cytochrome C induced respiration. RA and OA groups displayed significantly elevated O_2-consumption in the presence of glutamate and malate (CI Cytochrome C) compared to the control group. In the presence of succinate (CII Cytochrome C), significantly increased O_2-consumption occurred only in the RA group. RA group is marked with red color. Black color represents the OA group. Control group is marked with

white. Data are presented as means ± SD. *P<0.05 *vs* control; #P<0.05 *vs* OA (one-way ANOVA, Tukey's test). CI=Complex I, CII=Complex II

Proinflammatory cytokines in the synovial fluid

TNF-α and RANKL levels in the synovial fluid samples of the participants were measured using chemiluminescence assays. Concentration of RANKL was significantly increased in the RA group compared to the control group, while TNF-α levels in the RA group were significantly higher compared to not only the control group, but the OA group as well. **(Fig 3.)**

Fig 3. **Inflammatory cytokines.** Significantly elevated TNF-α and RANKL levels were measured in the RA groups compared to OA and control groups. This result confirms the presence of chronic synovitis in RA. RA group is marked with red color. Black color represents the OA group. Control group is marked with white. Data are presented as means ± SD. *P<0.05 vs control; #P<0.05 vs OA (one-way ANOVA, Tukey's test). TNF-α=Tumor Necrosis Factor-α, RANKL=Receptor Activator of Nuclear factor-κB Ligand.

Biochemical analyses

XOR and MPO activity were measured from synovial tissue, while NT levels were determined from synovial fluid as indicators of tissue damage. Significantly higher XOR activities were measured in the synovial membrane homogenates of RA and OA patients compared to the control group. Significant difference in XOR activity occurred also between the RA and OA groups. The synovial tissues of RA patients displayed a significantly higher MPO activity compared to the synovial tissues of OA patients and healthy individuals. In the RA group, significant elevation of NT was present relative to both the OA and control groups, as well as between the OA and control groups **(Fig. 4.).**

Fig 4. Biochemical analyses. Significantly higher MPO activity was detected in the RA group compared to OA and control groups. This result corresponds to the existing literature regarding the role of MPO in autoimmune inflammation. Elevated XOR activity was measured in tissue homogenates of RA and OA patients compared to the control group. Both RA and OA groups displayed significantly elevated NT levels in comparison

with the control group. RA group is marked with red color. Black color represents the OA group. Control group is marked with white. Data are presented as means ± SD. *P<0.05 vs control; #P<0.05 vs OA (one-way ANOVA, Tukey's test). MPO=Myeloperoxidase, XOR=Xanthine Oxidoreductase, NT=Nitrotyrosine.

Histopathological evaluation

CLSEM and H&E staining were used to validate the proper assignment of participants to study groups. Histological assessment was performed independently and blindly on coded slides by two investigators (P.J. and P.H.) using a previously described 0–4-grade histological scoring system, representing a composite of the extent of angiogenesis and fibrosis. Additionally, on H&E stained sections, a thickened synovial membrane, increased cellularity and mild lymphocytic infiltration occurred in samples from patients suffering from OA. **(Fig. 5.F)** More prominent lymphocytic infiltration, fibrosis, and in some cases even extensive fibrosis could be observed in RA samples **(Fig. 5.G).**

Fig 5. Histological changes in the synovium. A, B, C: Tissue sections show the results of in vivo confocal laser scanning endomicroscopy with acriflavine labeling. The bar represents 100 µm. **D**: Histological grade of patients. RA group is marked with red color. Black color represents the OA group. Control group is marked with white. **E, F, G**: Histological sections stained with hematoxylin and eosin. **A**: Healthy synovium with rounded synoviocytes. No signs of inflammation related angiogenesis and fibrosis can be seen. **B**: Osteoarthritic synovium with moderate angiogenesis due to low-grade chronic inflammation. **C**: Synovium of a patient suffering from RA. The large number of vascular cross-sections refers to inflammation-related angiogenesis. Scarring occurs as a result of chronic synovitis. **E:** Joint capsule section with synovial membrane from a healthy joint. Flattened mast cells constitute one, single cell layer. The lamina propria is poor in cells and rich in connective tissue fibers. Adipocytes and cross sections of capillaries can be observed in the deeper layers. **F**: Joint capsule sample from osteoarthritic joint. The synovial membrane is thickened, consists of 3-4 cell layers. Increased cellularity occurs partly due to the mild lymphocytic infiltration that can also be observed in the lamina propria. **G:** Joint capsule sample of a patient suffering from RA. As a result of the extensive scarring, the synovial membrane is unrecognizable. Fibrosis affects more than 50% of the stroma.

Discussion

Our present study provides quantitative clinical data on mitochondrial derangements in RA and OA. Systemic disease activity was evaluated by CRP serum concentrations, proinflammatory cytokines in the synovial fluid samples and clinical scores (KL, ACR/EULAR) of our patients. Additionally, histopathological evaluation and *in vivo* histology with CLSEM were also performed on tissue samples to detect the histological characteristics of RA and OA. Our results complied with the literature as RA patients had significantly higher levels of proinflammatory cytokines and hyperactive pathways of ROS production. Additionally, histopathology revealed signs of chronic inflammation such as neoangiogenesis, increased mean lining thickness and fibrosis in both OA and RA patients; however, with a much higher extent in the latter [29].

The capacities of the ETC complexes in the study groups were tested with high resolution respirometry. Interestingly, C I activity was strongly diminished in the RA group, while there was no significant difference in C II activity between the groups. This result highlights the central role of C I in mitochondrial dysfunction in RA, setting it as the main target of future RA therapies. C I is the first, largest, and most complicated component of the respiratory chain. Furthermore, as the major entry point for electrons to the respiratory chain, C I is considered as the rate-limiting factor in overall respiration [30]. Additionally, it generates significant levels of ROS, especially during reverse electron transport [31, 32]. As a consequence, C I has already stood in the focus of researchers investigating potential mitochondrial protective drugs. According to this, a recent study demonstrated the C I specific ROS-production inhibiting effect of OP2113 (5-(4-Methoxyphenyl)-3H-1,2-dithiole-3-thione, CAS 532-11-6) and raised its role in the therapies for Parkinson’s and

Alzheimer's diseases [33]. Additional to aging-related diseases, based on our findings, we emphasize the importance of C I related ROS blockers in autoimmune diseases including RA.

Compared to patients suffering from RA, members of the OA group displayed a milder, but still notable decrease in C I activity compared to healthy individuals in the control group. Again, a significant deficit in C II activity did not occur. This result complies with literature data accentuating the importance of C I in aging related diseases. Based on our findings, we suggest putting the focus on C I specific pharmaceutical agents in the research for novel therapeutic options for OA. Beyond highly effective conservative treatment options, prognostic biomarkers for disease progression and early-stage osteoarthritis are also lacking [34]. A recent study suggested that certain mitochondrial DNA (mtDNA) haplogroups may be suitable to aid the recognition of early-stage OA and also have a prognostic potential for disease progression [11]. Cytochrome C serves as an electron shuttle in the respiratory chain, in the mitochondrial intermembrane space. It is well-known that inflammatory stimuli promote the release of cytochrome C from the intermembrane space to the cytosol, where it facilitates apoptosis through initiating the proteolytic maturation of caspases [35, 36]. Based on our findings, further studies investigating other mitochondrial parameters such as C I activity or cytochrome C release as prognostic markers for disease progression are warranted.

Bone destruction is a common feature of inflammatory arthritis and is mediated by osteoclasts. Both synovium secreted soluble-factors, namely RANKL and TNF-α, which have the ability to directly induce osteoclastogenesis, were significantly elevated in RA patients in our study [37]. Mitochondria are considered an early target in TNFα-induced

cytotoxicity, since TNF-α induces mitochondrial damage through suppression of respiratory complexes I-IV [38]. Aberrant expression of RANKL, an inducer of osteoclast differentiation has been linked to synovial fibroblasts and bone pathology in RA. Moreover, increased ROS production results in oxidation of mitochondrial lipids, sulfhydryl groups and iron sulfur complexes of mitochondrial respiratory enzymes ~~that~~ leading to the impairment of OxPhos [39].

Our present study demonstrated increased synovial tissue levels of XOR and NT in both arthritis study groups as compared to healthy controls, while MPO was elevated only in RA patients. XOR is an important enzyme in purine catabolism. Besides converting xanthine to uric acid, XOR also catalyzes the reduction of nitrates and nitrites into nitric oxide. This process is accompanied by the production of ROS, which can result in cellular disruption. Nitric oxide reacts in a diffusion-limited manner with superoxide anion to form peroxynitrite, a powerful oxidant that has been linked to tissue injury. Being a stable end product of peroxynitrite formation, NT reflects disease-associated tissue damage in the joint, thereby serves as a potential biomarker for disease activity [40, 41]. MPO plays a central role in the pathogenesis of autoimmune inflammation through initiating the production of hypochlorous acid (HClO) and other reactive agents causing tissue damage. According to the literature, elevated MPO levels are observed in a number of autoimmune diseases including multiple sclerosis and RA [42].

Conclusions

Our present study provides quantitative clinical data making RA and OA comparable with respect to mitochondrial dysfunction. The characteristics of mitochondrial derangements in OA and RA share several similarities including increased ROS production and C I

related diminution of respiratory activity. Differences are reflected mainly in the extent of respiratory deficit (RA>OA), ROS formation (RA>OA), and cytochrome C release (RA>OA). According to our findings, in contrast to C I, C II does not play a central role in altered mitochondrial functions in the two arthritis types. Consequently, focusing on C I specific mitochondrial protective agents in OA and RA research may have major benefits.

Author contributions

Conceptualization: P.H., P.J.; Methodology: E.B., Á.C., A.M., B.Be., B.Bá.; Formal Analysis: T.H.; Investigation: D.K.J., T.H., B.Bá., A.M.; Statistician: B.Bá.; Writing – Original Draft Preparation: P.J., P.H.; Writing Review & Editing: P.H., E.V.; Supervision: P.H., L.T., E.V.; Funding Acquisition: P.H.

References

1. Reginster JY. The prevalence and burden of arthritis. Rheumatology (Oxford). 2002;41 Supp 1:3-6. PubMed PMID: 12173279.

2. Da Sylva TR, Connor A, Mburu Y, Keystone E, Wu GE. Somatic mutations in the mitochondria of rheumatoid arthritis synoviocytes. Arthritis Res Ther. 2005;7(4):R844-51. doi: 10.1186/ar1752. PubMed PMID: 15987486; PubMed Central PMCID: PMCPMC1175034.

3. Fearon U, Canavan M, Biniecka M, Veale DJ. Hypoxia, mitochondrial dysfunction and synovial invasiveness in rheumatoid arthritis. Nat Rev Rheumatol. 2016;12(7):385-97. doi: 10.1038/nrrheum.2016.69. PubMed PMID: 27225300.

4. Blanco FJ, Rego I, Ruiz-Romero C. The role of mitochondria in osteoarthritis. Nat Rev Rheumatol. 2011;7(3):161-9. doi: 10.1038/nrrheum.2010.213. PubMed PMID: 21200395.

5. Lepetsos P, Papavassiliou AG. ROS/oxidative stress signaling in osteoarthritis. Biochim Biophys Acta. 2016;1862(4):576-91. doi: 10.1016/j.bbadis.2016.01.003. PubMed PMID: 26769361.

6. Rego-Perez I, Duran-Sotuela A, Ramos-Louro P, Blanco FJ. Mitochondrial Genetics and Epigenetics in Osteoarthritis. Front Genet. 2019;10:1335. doi:

10.3389/fgene.2019.01335. PubMed PMID: 32010192; PubMed Central PMCID: PMCPMC6978735.

7. Roh JS, Sohn DH. Damage-Associated Molecular Patterns in Inflammatory Diseases. Immune Netw. 2018;18(4):e27. doi: 10.4110/in.2018.18.e27. PubMed PMID: 30181915; PubMed Central PMCID: PMCPMC6117512.

8. Martin JA, Martini A, Molinari A, Morgan W, Ramalingam W, Buckwalter JA, et al. Mitochondrial electron transport and glycolysis are coupled in articular cartilage. Osteoarthritis Cartilage. 2012;20(4):323-9. doi: 10.1016/j.joca.2012.01.003. PubMed PMID: 22305999; PubMed Central PMCID: PMCPMC3634328.

9. Rego I, Fernandez-Moreno M, Fernandez-Lopez C, Gomez-Reino JJ, Gonzalez A, Arenas J, et al. Role of European mitochondrial DNA haplogroups in the prevalence of hip osteoarthritis in Galicia, Northern Spain. Ann Rheum Dis. 2010;69(1):210-3. doi: 10.1136/ard.2008.105254. PubMed PMID: 19224903.

10. Woetzel D, Huber R, Kupfer P, Pohlers D, Pfaff M, Driesch D, et al. Identification of rheumatoid arthritis and osteoarthritis patients by transcriptome-based rule set generation. Arthritis Res Ther. 2014;16(2):R84. doi: 10.1186/ar4526. PubMed PMID: 24690414; PubMed Central PMCID: PMCPMC4060460.

11. Blanco FJ, Valdes AM, Rego-Perez I. Mitochondrial DNA variation and the pathogenesis of osteoarthritis phenotypes. Nat Rev Rheumatol. 2018;14(6):327-40. doi: 10.1038/s41584-018-0001-0. PubMed PMID: 29670212.

12. Mao X, Fu P, Wang L, Xiang C. Mitochondria: Potential Targets for Osteoarthritis. Front Med (Lausanne). 2020;7:581402. doi: 10.3389/fmed.2020.581402. PubMed PMID: 33324661; PubMed Central PMCID: PMCPMC7726420.

13. Wang Y, Zhao X, Lotz M, Terkeltaub R, Liu-Bryan R. Mitochondrial biogenesis is impaired in osteoarthritis chondrocytes but reversible via peroxisome proliferator-activated receptor gamma coactivator 1alpha. Arthritis Rheumatol. 2015;67(8):2141-53. doi: 10.1002/art.39182. PubMed PMID: 25940958; PubMed Central PMCID: PMCPMC4519411.

14. Panga V, Kallor AA, Nair A, Harshan S, Raghunathan S. Mitochondrial dysfunction in rheumatoid arthritis: A comprehensive analysis by integrating gene expression, protein-protein interactions and gene ontology data. PLoS One. 2019;14(11):e0224632. doi: 10.1371/journal.pone.0224632. PubMed PMID: 31703070; PubMed Central PMCID: PMCPMC6839853.

15. Liu H, Li Z, Cao Y, Cui Y, Yang X, Meng Z, et al. Effect of chondrocyte mitochondrial dysfunction on cartilage degeneration: A possible pathway for osteoarthritis pathology at the subcellular level. Molecular Medicine Reports. 2019. doi: 10.3892/mmr.2019.10559.

16. Maneiro E, Martin MA, de Andres MC, Lopez-Armada MJ, Fernandez-Sueiro JL, del Hoyo P, et al. Mitochondrial respiratory activity is altered in osteoarthritic human articular chondrocytes. Arthritis Rheum. 2003;48(3):700-8. doi: 10.1002/art.10837. PubMed PMID: 12632423.

17. Mathiessen A, Conaghan PG. Synovitis in osteoarthritis: current understanding with therapeutic implications. Arthritis Res Ther. 2017;19(1):18. doi: 10.1186/s13075-017-1229-9. PubMed PMID: 28148295; PubMed Central PMCID: PMCPMC5289060.

18. Lehmann J, Jungel A, Lehmann I, Busse F, Biskop M, Saalbach A, et al. Grafting of fibroblasts isolated from the synovial membrane of rheumatoid arthritis (RA) patients induces chronic arthritis in SCID mice-A novel model for studying the arthritogenic role of RA fibroblasts in vivo. J Autoimmun. 2000;15(3):301-13. doi: 10.1006/jaut.2000.0435. PubMed PMID: 11040071.

19. Gavriilidis C, Miwa S, von Zglinicki T, Taylor RW, Young DA. Mitochondrial dysfunction in osteoarthritis is associated with down-regulation of superoxide dismutase 2. Arthritis Rheum. 2013;65(2):378-87. doi: 10.1002/art.37782. PubMed PMID: 23138846.

20. Kohn MD, Sassoon AA, Fernando ND. Classifications in Brief: Kellgren-Lawrence Classification of Osteoarthritis. Clin Orthop Relat Res. 2016;474(8):1886-93. doi: 10.1007/s11999-016-4732-4. PubMed PMID: 26872913; PubMed Central PMCID: PMCPMC4925407.

21. Braun HJ, Gold GE. Diagnosis of osteoarthritis: imaging. Bone. 2012;51(2):278-88. doi: 10.1016/j.bone.2011.11.019. PubMed PMID: 22155587; PubMed Central PMCID: PMCPMC3306456.

22. Smith MM, Cake MA, Ghosh P, Schiavinato A, Read RA, Little CB. Significant synovial pathology in a meniscectomy model of osteoarthritis: modification by intra-articular hyaluronan therapy. Rheumatology (Oxford). 2008;47(8):1172-8. doi: 10.1093/rheumatology/ken219. PubMed PMID: 18565987; PubMed Central PMCID: PMCPMC2468886.

23. Komary Z, Tretter L, Adam-Vizi V. Membrane potential-related effect of calcium on reactive oxygen species generation in isolated brain mitochondria. Biochim Biophys Acta. 2010;1797(6-7):922-8. doi: 10.1016/j.bbabio.2010.03.010. PubMed PMID: 20230776.

24. Strifler G, Tuboly E, Szel E, Kaszonyi E, Cao C, Kaszaki J, et al. Inhaled Methane Limits the Mitochondrial Electron Transport Chain Dysfunction during Experimental Liver Ischemia-Reperfusion Injury. PLoS One. 2016;11(1):e0146363. doi: 10.1371/journal.pone.0146363. PubMed PMID: 26741361; PubMed Central PMCID: PMCPMC4720186.

25. Beckman JS, Parks DA, Pearson JD, Marshall PA, Freeman BA. A sensitive fluorometric assay for measuring xanthine dehydrogenase and oxidase in tissues. Free Radic Biol Med. 1989;6(6):607-15. doi: 10.1016/0891-5849(89)90068-3. PubMed PMID: 2753392.

26. Kuebler WM, Abels C, Schuerer L, Goetz AE. Measurement of neutrophil content in brain and lung tissue by a modified myeloperoxidase assay. Int J Microcirc Clin Exp. 1996;16(2):89-97. doi: 10.1159/000179155. PubMed PMID: 8737712.

27. Wu JP, Walton M, Wang A, Anderson P, Wang T, Kirk TB, et al. The development of confocal arthroscopy as optical histology for rotator cuff tendinopathy. J Microsc. 2015;259(3):269-75. doi: 10.1111/jmi.12260. PubMed PMID: 25919432.

28. June RK, Liu-Bryan R, Long F, Griffin TM. Emerging role of metabolic signaling in synovial joint remodeling and osteoarthritis. J Orthop Res. 2016;34(12):2048-58. doi: 10.1002/jor.23420. PubMed PMID: 27605370; PubMed Central PMCID: PMCPMC5365077.

29. Baeten D, Demetter P, Cuvelier C, Van Den Bosch F, Kruithof E, Van Damme N, et al. Comparative study of the synovial histology in rheumatoid arthritis, spondyloarthropathy, and osteoarthritis: influence of disease duration and activity. Ann Rheum Dis. 2000;59(12):945-53. doi: 10.1136/ard.59.12.945. PubMed PMID: 11087697; PubMed Central PMCID: PMCPMC1753054.

30. Sharma LK, Lu J, Bai Y. Mitochondrial respiratory complex I: structure, function and implication in human diseases. Curr Med Chem. 2009;16(10):1266-77. doi: 10.2174/092986709787846578. PubMed PMID: 19355884; PubMed Central PMCID: PMCPMC4706149.

31. Lambert AJ, Brand MD. Inhibitors of the quinone-binding site allow rapid superoxide production from mitochondrial NADH:ubiquinone oxidoreductase (complex I). J Biol Chem. 2004;279(38):39414-20. doi: 10.1074/jbc.M406576200. PubMed PMID: 15262965.

32. Armstrong JS. Mitochondrial medicine: pharmacological targeting of mitochondria in disease. Br J Pharmacol. 2007;151(8):1154-65. doi: 10.1038/sj.bjp.0707288. PubMed PMID: 17519949; PubMed Central PMCID: PMCPMC2189819.

33. Detaille D, Pasdois P, Semont A, Dos Santos P, Diolez P. An old medicine as a new drug to prevent mitochondrial complex I from producing oxygen radicals. PLoS One. 2019;14(5):e0216385. doi: 10.1371/journal.pone.0216385. PubMed PMID: 31048932; PubMed Central PMCID: PMCPMC6497312 patent applications related to the molecule OP2113 described in this work (USA US62/215,215; France 15 184 217.6; France EP 17 159 691.9). P.D. is one of the founders of the OP2 drugs company. The funding sources had no role in the study design or the analysis and interpretation of data or in the decision to submit the article for publication. This does not alter our adherence to PLOS ONE policies on sharing data and materials.

34. Ahmed U, Anwar A, Savage RS, Costa ML, Mackay N, Filer A, et al. Biomarkers of early stage osteoarthritis, rheumatoid arthritis and musculoskeletal health. Sci Rep. 2015;5:9259. doi: 10.1038/srep09259. PubMed PMID: 25788417; PubMed Central PMCID: PMCPMC4365413.

35. Garrido C, Galluzzi L, Brunet M, Puig PE, Didelot C, Kroemer G. Mechanisms of cytochrome c release from mitochondria. Cell Death Differ. 2006;13(9):1423-33. doi: 10.1038/sj.cdd.4401950. PubMed PMID: 16676004.

36. Martinou I, Desagher S, Eskes R, Antonsson B, Andre E, Fakan S, et al. The release of cytochrome c from mitochondria during apoptosis of NGF-deprived sympathetic neurons is a reversible event. J Cell Biol. 1999;144(5):883-9. doi: 10.1083/jcb.144.5.883. PubMed PMID: 10085288; PubMed Central PMCID: PMCPMC2148194.

37. Dickerson TJ, Suzuki E, Stanecki C, Shin HS, Qui H, Adamopoulos IE. Rheumatoid and pyrophosphate arthritis synovial fibroblasts induce osteoclastogenesis

independently of RANKL, TNF and IL-6. J Autoimmun. 2012;39(4):369-76. doi: 10.1016/j.jaut.2012.06.001. PubMed PMID: 22867712; PubMed Central PMCID: PMCPMC3593104.

38. Samavati L, Lee I, Mathes I, Lottspeich F, Huttemann M. Tumor necrosis factor alpha inhibits oxidative phosphorylation through tyrosine phosphorylation at subunit I of cytochrome c oxidase. J Biol Chem. 2008;283(30):21134-44. doi: 10.1074/jbc.M801954200. PubMed PMID: 18534980; PubMed Central PMCID: PMCPMC3258931.

39. Halliwell B. Oxidative stress and neurodegeneration: where are we now? J Neurochem. 2006;97(6):1634-58. doi: 10.1111/j.1471-4159.2006.03907.x. PubMed PMID: 16805774.

40. Kaur H, Halliwell B. Evidence for nitric oxide-mediated oxidative damage in chronic inflammation. Nitrotyrosine in serum and synovial fluid from rheumatoid patients. FEBS Lett. 1994;350(1):9-12. doi: 10.1016/0014-5793(94)00722-5. PubMed PMID: 8062931.

41. Misko TP, Radabaugh MR, Highkin M, Abrams M, Friese O, Gallavan R, et al. Characterization of nitrotyrosine as a biomarker for arthritis and joint injury. Osteoarthritis Cartilage. 2013;21(1):151-6. doi: 10.1016/j.joca.2012.09.005. PubMed PMID: 23025928.

42. Strzepa A, Pritchard KA, Dittel BN. Myeloperoxidase: A new player in autoimmunity. Cell Immunol. 2017;317:1-8. doi: 10.1016/j.cellimm.2017.05.002. PubMed PMID: 28511921; PubMed Central PMCID: PMCPMC5665680.

Figure 1

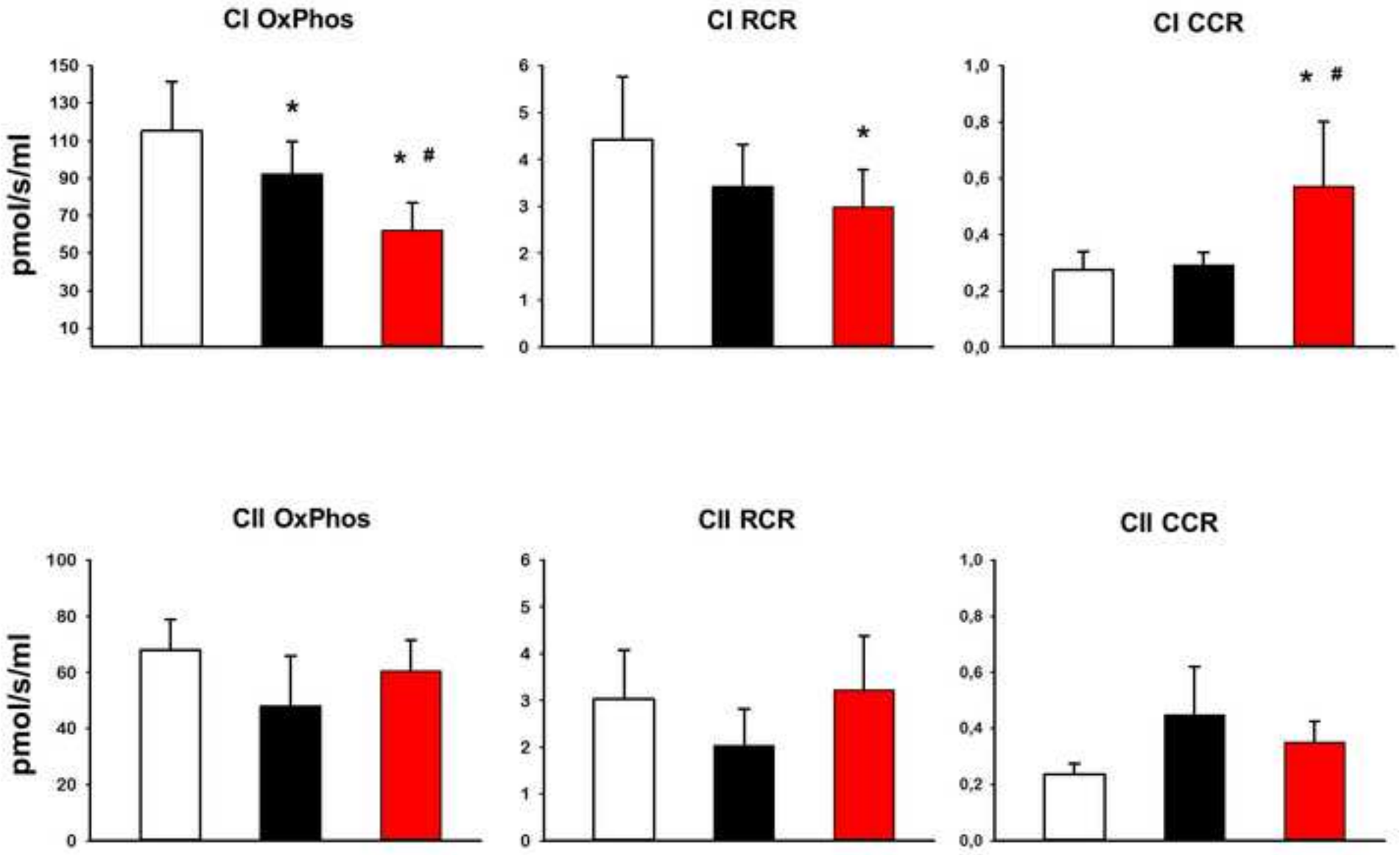

Figure 2

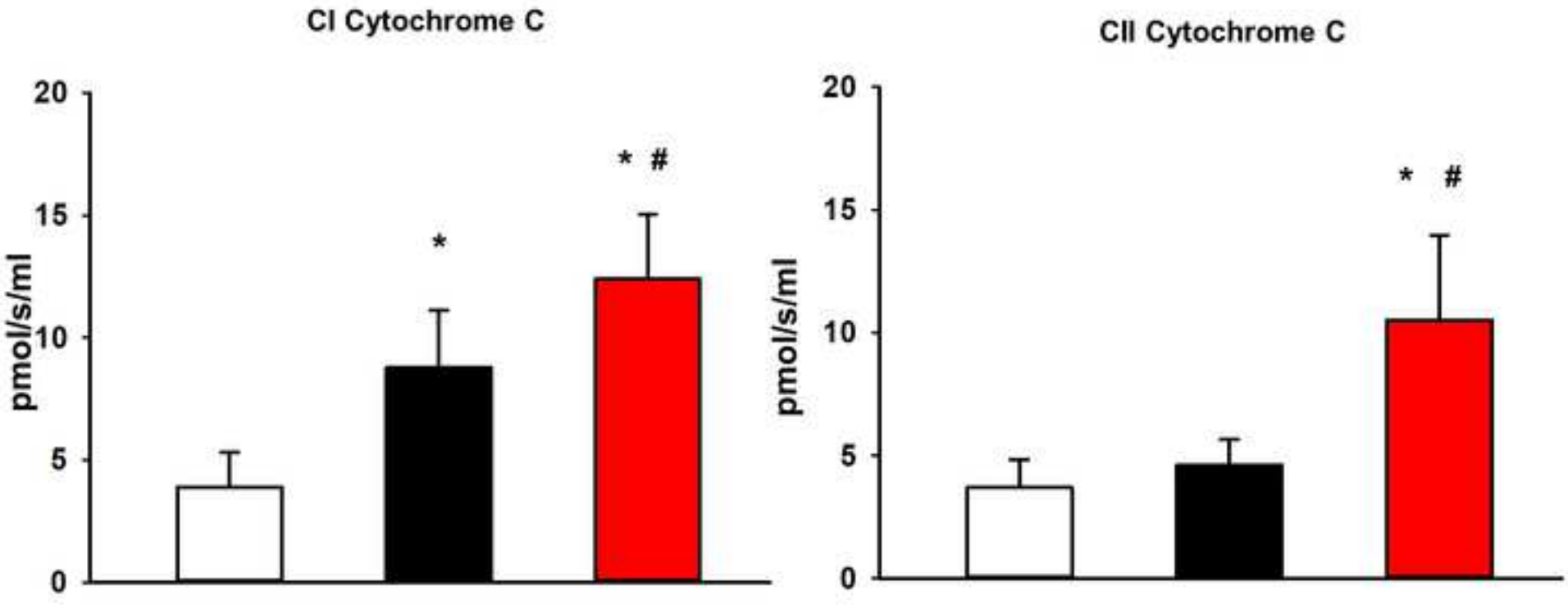

Figure 3

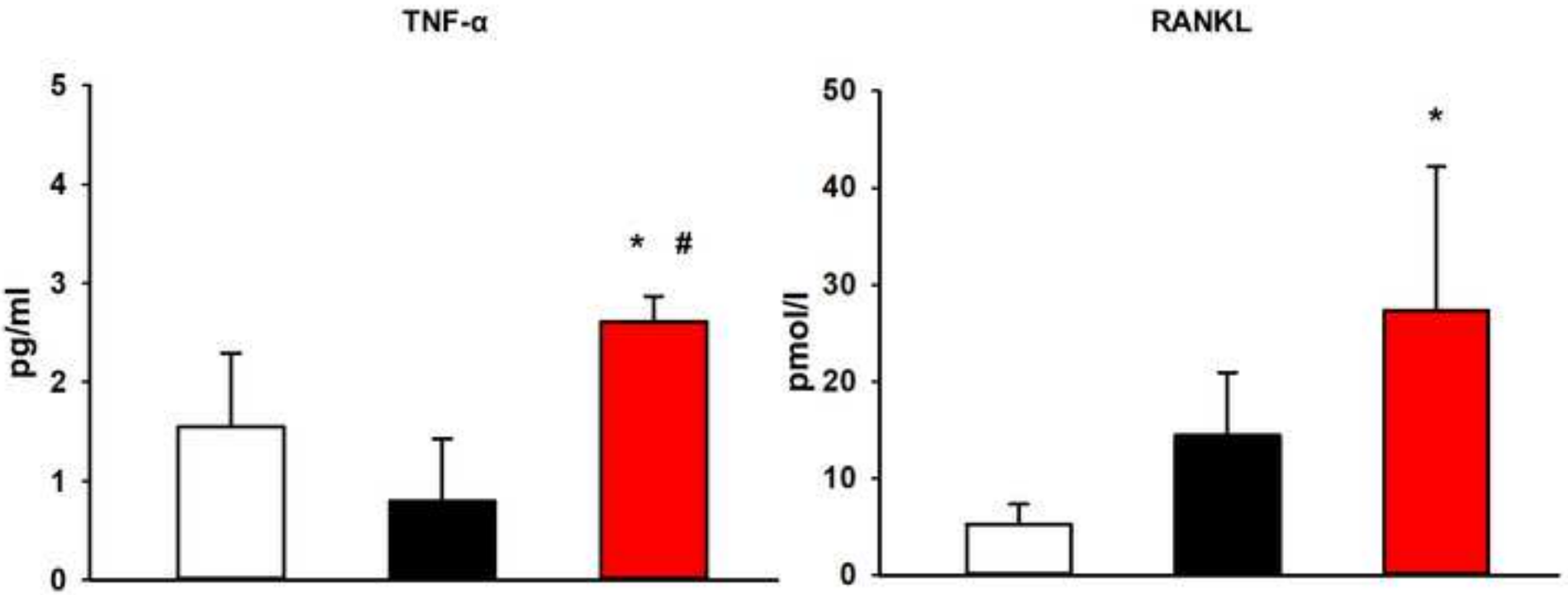

Figure 4

Click here to access/download;Figure;Fig4.tif

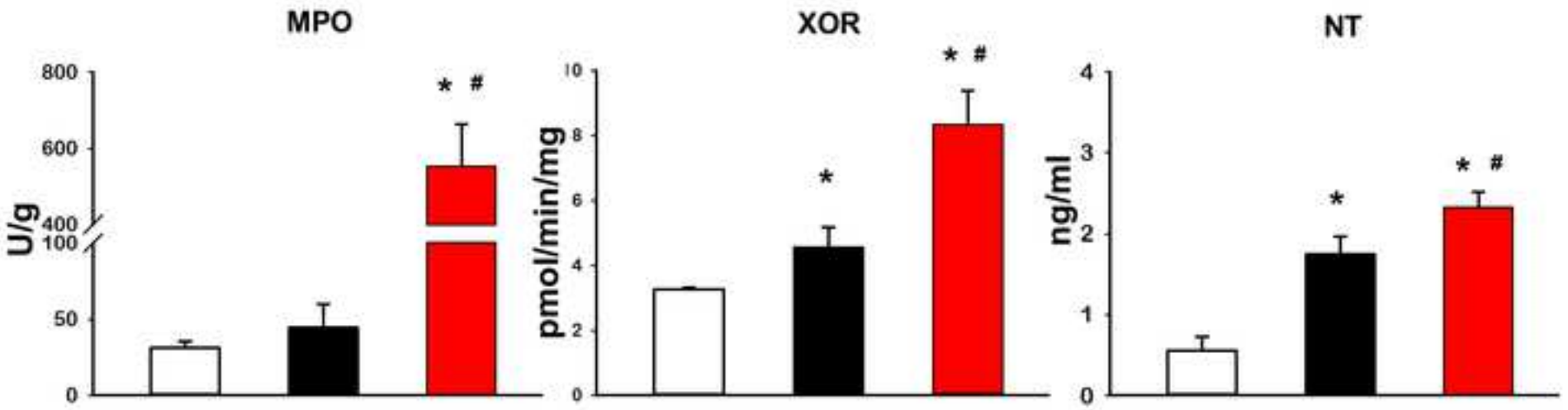

Figure 5

Click here to access/download;Figure;Fig5.tif